Investigating Small Amine Molecules as Ice Recrystallization Inhibitors

Joseph Janabi

Thesis submitted to the Faculty of Graduate and Postdoctoral Studies
In partial fulfillment of the requirements for the M.Sc. degree in Chemistry

Department of Chemistry
Faculty of Science
University of Ottawa

Candidate

_____

Joseph Janabi

Abstract

Cryopreservation is a technique used to store cells and tissues for long time. It requires the addition of a cryoprotectant, which prevents damage to cells caused by the formation of large ice crystals. Few compounds have been classified as cryprotectants, and some of them are very toxic like DMSO. Our lab is interested in the synthesis of small, non-toxic cryoprotectants that possess ice recrystallization inhibition (IRI) activity. Much attention has been drawn towards small molecules that contain an amine group because they have some activity towards inhibiting ice recrystallization. Herein we have examined few monoamine and diamine molecules as well as PAMAM dendrimer for IRI activity. Some of the small molecules tested contain an aryl ring, and we found that changing the position of groups around the ring can have some impact in the IRI activity. We have also found that increasing the number of amines in a molecule can have little effect of the IRI activity. It is hoped that these findings can open new doors for further investigation in small amino molecules and the development of novel cryoprotectants.

Corticosteroids were first identified and isolated from both teleost and elasmobranch fish. Corticosterone and cortisol were measurable in the plasma of elasmobranchs and 1α-hydroxycorticosterone (1α-OH-B) was the dominant corticosteroid produced by the internal tissue. Limited amount of 1α-OH-B was synthesized because available supplies were exhausted in the early 1990s. Synthetic 1α-OH-B was used in steroid receptor studies to examine the evolution of the corticosteroid receptor system and measure stress levels.

Acknowledgement

Firstly, all my thanks to my parents who stood by my side every step of the way during this degree, while I come over all obstacles and challenges. It is them who helped me through the rough times and guided me to the righteous path while all others disbelieved in me. Thus, I dedicate this work to them.

I would like to thank the Durst lab for their help especially Ousama who provided me with great tips and helped me to succeed. Many thanks to my close friends who believed that I had what it take to come through this stressful period of my life.

"But perhaps you hate a thing and it is good for you; and perhaps you love a thing and it is bad for you. And God Knows, while you know not."

Quran, Ch. 2 v. 216

Table of Contents

ABSTRACT II
ACKNOWLEDGEMENT III
LIST OF FIGURES VI
LIST OF GRAPHS VIII
LIST OF SCHEMES IX
LIST OF TABLES IX
LIST OF ABBREVIATIONS X

CHAPTER 1: ICE RECRYSTALLIZATION INHIBITION AND THE POTENTIAL APPLICATIONS IN CRYOPRESERVATION 1

1.1 INTRODUCTION 1
1.2 RECRYSTALLIZATION IN ICE 2
1.2.1 STRUCTURE OF ICE CRYSTALS 2
1.2.2 MECHANISM OF ICE RECRYSTALLIZATION 3
1.3 BIOLOGICAL ANTIFREEZES AS ICE RECRYSTALLIZATION INHIBITORS 5
1.3.1 STRUCTURE OF BIOLOGICAL ANTIFREEZE 5
1.3.2 THERMAL HYSTERESIS – MECHANISM OF ACTION 7
1.4 INHIBITORS OF ICE RECRYSTALLIZATION 9
1.4.1 SMALL CARBOHYDRATES MOLECULES AS ICE RECRYSTALLIZATION INHIBITORS 10
1.4.3 PEPTIDES AND GLYCOPEPTIDES ANALOGUES AS ICE RECRYSTALLIZATION INHIBITORS 16
1.4.2 SYNTHETIC POLYMERS AS ICE RECRYSTALLIZATION INHIBITORS 19
1.5 CONCLUSION 20
REFERENCES 22

CHAPTER 2: GOALS AND OBJECTIVES 30

2.1 INTRODUCTION 30
2.2 OBJECTIVE – 1: EXAMINING OTHER SMALL AMINES MOLECULES FOR IRI ACTIVITY 32
2.3 OBJECTIVE – 2: POLY(AMIDOAMINE) (PAMAM) AND IRI ACTIVITY 33
REFERENCES 36

CHAPTER 3: RESULTS AND DISCUSSION 40

3.1 IRI ACTIVITY OF AMINE DERIVATIVES 40
3.2 THE EFFECT OF INCREASING HYDROPHOBIC CHARACTER ON THE IRI ACTIVITY 41
3.2.1 FLUORINATED MOLECULES HYDROPHOBICITY AND IRI ACTIVITY 42
3.2.2 EFFECT OF AROMATIZATION ON IRI ACTIVITY 42
3.2.3 IRI ACTIVITY OF AMINOCYCLOHEXANE AND THEIR DERIVATIVES 45
3.2.4 IRI ACTIVITY OF AROMATIC AMINES. 47
3.3 SYNTHESIS OF DENDRIMERS AND ASSESSMENT OF THEIR ABILITY TO INHIBIT ICE RECRYSTALLIZATION 50
3.3.1 SYNTHESIS OF PAMAM DENDRIMER 50
3.3.2 COUPLING OF PAMAM WITH OGG 53
REFERENCES 56

CHAPTER 4: EXPERIMENTAL PROCEDURES 59

4.1 ICE RECRYSTALLIZATION INHIBITION (IRI) ASSAY: 59
4.2 GENERAL EXPERIMENTAL CONDITIONS (SYNTHETIC CHEMISTRY) 63
4.3 SYNTHESIS OF PAMAM DENDRIMER COMPOUNDS 64
4.3.1 SYNTHESIS OF MULTIESTER (G-0.5) (**75**) 64
4.3.2 SYNTHESIS OF GENERATION 0 (G0) (**76**) 65
4.3.3 SYNTHESIS OF GLYCOSIDATED ORNITHINE 65
4.3.4 COUPLING OF PAMAM WITH GLYCOSIDATED ORNITHINE 68
4.3.5 COUPLING OF PAMAM WITH GLUCONOLACTONE 68
4.3 GENERAL SYNTHESIS PROCEDURES FOR SMALL MOLECULES 68
CONCLUSIONS 72
REFERENCES 73

CHAPTER 5: 1A-HYDROXYCORTICOSTERONE (1A-OH-B) 74

5.1 INTRODUCTION 74
5.2 SYNTHESIS OF 1A-HYDROXYCORTICOSTERONE (1) 75
5.2.1 THE KIMES SYNTHESIS OF 1A-HYDROXYCORTICOSTERONE (1A-OH-B)[15,16] 76
5.3 POTENTIAL ALTERNATIVE METHODS FOR RING A DIENONE 78
5.4 OTHER POSSIBLE METHODS FOR GENERATING THE 1,2-A-EPOXIDE 79
5.4.1 DIOXIRANE REACTION WITH STEROIDS 79
5.4.2 EPOXIDATION USING DBU AND T-BUO$_2$H 80
5.5 THE AUTHORS WORK FOR THIS PROJECT 81
REFERENCES 83
APPENDIX: ^{1}H AND ^{13}C NMR SPECTRA 85

List of Figures

Figure 1.1 Representation of the hexagonal ice structure showing the a_1, a_2, a_3 and c axes and the basal, pyramidal and prism planes……..3

Figure 1.2 A liquid-layer (shaded) in a curved boundary between two ice grains. Large grains with concave boundaries (grain 2) grow larger while small grains with convex boundaries (grain 1) decrease in size to reduce the overall degree of grain boundary curvature. Arrows indicate the direction of boundary migration…….4

Figure 1.3 Atlantic Cod (Gadus morhua) (A) and Antarctic Notothenioid (Pagothenia borchgrevinki) (B)……...5

Figure 1.4 (A) Ice crystal in the presence of AFGP-8. The binding of AFGP to the surface of ice crystal changes the structure to hexagonal bipyramidal. (B) Formation of Hexagonal bipyramidal crystals by inhibition of growth on the prism faces due to adsorption of BAs……7

Figure 1.5 Activity of TH and ice growth inhibition. (A) BAs depression of freezing point of ice crystals relative to melting point results in TH gap. (B) Step pinning model. (C) Mattress model……..8

Figure 1.6 Annealed ice grains obtained from a compound that can inhibit ice recrystallization and able to maintain small ice crystals within a frozen solution…….9

Figure 1.7 Schematic representation of the ice water interface and the effect of carbohydrates on ice recrystallization……16

Figure 1.8 AFGP-8 (**1**) and first generation C-Linked AFGP analogue (monomer tripeptide)……...17

Figure 1.9 First-generation C-linked AFGP analogue $[C\text{-}(KGG)\text{-}Gal]_n$……...17

Figure 1.10 Second generation C-AFGP-analogues $[C\text{-}(OGG)\text{-}Gal]_n$ (**5**) and $[C\text{-}(SGG)\text{-}Gal]_n$ (**6**)…….18

Figure 1.11 Structures of synthetic polymers assessed for IRI activity……20

Figure 2.1 Other galactose regioisomers with either an azide or amine group…….32

Figure 2.2 1,4-cyclohexanediamine (**19**), 1,3-cyclohexanediamine (**20**), and 1,2-cyclohexanediamine (**21**). Cis-, trans-, and cis/trans mixtures have been tested for IRI activities…….33

Figure 2.3 Schematic diagram of a poly(amidoamine) dendrimer. This is a second-generation dendrimer…….34

Figure 3.1 Structure of anti-INA, dialkyldimethyl ammonium salts……40

Figure 3.2 Structure of anti-INA, Lysine-based cationic surfactants……...41

Figure 3.3 Fluorinated C-AFGP analogue (31) and galactose analogue (32)……..42

Figure 3.4 Amino cyclohexane structures tested for IRI activity…….46

Figure 3.5 Structure of trans-1,4-dibenzoylaminocyclohexane……46

Figure 3.6 Structures of different aromatic molecules with different groups (**66-74**)…..48

Figure 3.7 General structure of AFGPs.……53

Figure 3.8 C-linked AFGP analogue, OGG-Gal……54

List of Graphs

Graph 1.1 IRI activity of monosaccharides (blue) and disaccharides (yellow) at 22mM concentration plotted against the hydration numbers……...……12

Graph 1.2 IRI activities of carbohydrates at 22mM as a function of hydration index (HI)…… ……...…….……...…….14

Graph 1.3 Ice Recrystallization Inhibition (IRI) activity of molecules 1, 2, 5 and 6 compared to phosphate buffered silane (PBS) …….....……..18

Graph 2.1 IRI activities of C2 galactosyl derivatives……...……31

Graph 3.1 IRI activities of cationic anti-INAs in NaCl standard solution…...……41

Graph 3.2 IRI activity of previously synthesized aryl galactosides (**33-45**). ……...43

Graph 3.3 IRI activity of previously synthesized aryl glucosides (**46-58**)……...44

Graph 3.4 IRI activities of amino cyclohexane molecules **59-64** compared with glucose and galactose……...…….……...……...47

Graph 3.5 IRI activities of compounds (**66-74**) as shown in Figure 3.6…….….48

Graph 3.6 IRI activity of EDA and the two different stages of the PAMAM dendrimer……...…….……...……...52

List of Schemes

Scheme 3.1 Synthesis of generation -0.5 (multiester) of PAMAM dendrimer……..…51

Scheme 3.2 Synthesis of generation 0 (G0) of PAMAM dendrimer……...….52

Scheme 3.3 Retrosynthetic scheme for synthesis of AFGP analogue……..54

Scheme 5.1 Synthesis of 1α-hydroxycorticosterone using Kimes Synthesis……76

Scheme 5.2 Dehydrogenation reaction to produce double bond……...77

Scheme 5.3 Epoxidationreaction…….....…….77

Scheme 5.4 Synthesis of the double bond on ring A.……...78

Scheme 5.5 Other method used to synthesis the double bond.…….....79

Scheme 5.6 Synthesis of the double bond on ring A.……....79

Scheme 5.7 Synthesis of the epoxide.…….…..80

Scheme 5.8 Other methods to synthesize the epoxide……..……....81

List of Tables

Table 1.1 Classification and structural differences between antifreeze proteins (AFPs) and antifreeze glycoproteins (AFGPs)……...…..6

Table 1.2 Molar compressibility (10^4 K_2^o (s), cm^3 mol^{-1} bar^{-1}) and hydration numbers of different monosaccharides and disaccharides. Numbers in brackets indicates errors of molar compressibility values and hydration numbers……...11

List of Abbreviations

α	alpha
β	beta
^{1}H	proton
^{13}C	carbon
3D	three-dimensional
Ac_2O	acetic anhydride
AFGP(s)	antifreeze glycoprotein(s) antifreeze protein
AFP	alanine
Ala	atmosphere
Atm	boron trifluoride diethyletherate
$BF_3 \cdot OEt_2$	broad
br	catalytic
Cat.	carboxybenzyl
Cbz	deuterated chloroform
$CDCl_3$	deuterated methanol
CD_3OD	critical micelle concentration cryoprotective
CMC	agent
CPA	doublet
d	deuterium oxide
D_2O	doublet of doublets
dd	dichloromethane
DCM	dynamic ice shaping
DIS	dimethylformamide
DMF	dimethyl sulfoxide
DMSO	doublet of triplets
dt	ethylene diamine
EDA	electron-donating group
EDG	electrospray ionization
ESI	ethyl
Et	diethyl ether
Et_2O	ethyl acetate
EtOAc	electron-withdrawing group
EWG	fetal bovine serum
FBS	generation -0.5
G-0.5	generation 0
G0	galactose
Gal	glucose
Glc	human hepatocellular carcinoma cell line
Gly	intracellular ice formation
IIF	ice nucleating agent
IR resin	ice recrystallization inhibition
IRI	kilodaltons
kDa	lysine-glycine-glycine
KGG	

LiOH	lithium hydroxide
m	multiplet
M	molar
M^+	parent molecular ion
Man	mannose
Me	methyl
MeOH	methanol
MGS	mean grain size
$MgSO_4$	magnesium sulfate
MHz	mega Hertz
mM	millimolar
MS	molecular sieves
MTT	3-(4,5-dimethylthiazol-2-yl)-2,5-diphenyltetrazolium bromide
NaCl	sodium chloride
NADH	nicotine adenine dinucleotide
NADPH	nicotine adenine dinucleotide phosphate
NHAc	N-acetyl
NMR	nuclear magnetic resonance
OGG	ornithine-glycine-glycine
OBu	butoxy
OEt	ethoxy
OMe	methoxy
OPr	propoxy
PBS	phosphate buffered saline
PEG	polyethylene glycol
ppm	parts per million
Pr	propyl
PVP	polyvinylpyrollidone
q	quartet
QLL	quasi-liquid layer
s	singlet
SAR	structure-activity relationship
Ser	serine
SGG	serine-glycine-glycine
$SOCl_2$	thionyl chloride[SEP]t triplet
TAA	threonine-alanine-alanine
Tal	talose
TFA	trifluoroacetic acid
TH	thermal hysteresis
THF	tetrahydrofuran
Thr	threonine

Chapter 1: Ice Recrystallization Inhibition and the Potential Applications in Cryopreservation

1.1 Introduction

Cryopreservation is a technique that allows cells and tissues to be stored for long periods of time at very low temperatures (-78°C to -196°C).[1] No biochemical activities occur at these low temperatures and the degradation of cells is slowed significantly. The first reported use of cryopreservation was in 1949,[2] and since then, it has been used in many different areas, like clinical and environmental research, agriculture and food industry.[3-7]

During cryopreservation and in the post-thawing process ice crystals begin to form and as they grow larger they start to damage cells and tissues. This greatly limits the potential of cryopreservation. The addition of a cryoprotectant is required to mitigate damage associated with this process by limiting large ice crystals formation.[1,8] Some of the common cryoprotectants are dimethyl sulfoxide (DMSO) and glycerol which act as cell penetrating agents. Others such as salts, sugars and polymers, such as the natural antifreeze compounds, can also be used as cryoprotectants; these are not cell penetrating agents.[9,10] Unfortunately, most of these cryoprotectants have significant toxicity that causes decrease in functionality and viability of cells, which can be very harmful to treated patients.

A potential solution for this issue is the development of cryoprotectants that are non-toxic to cells and are capable of inhibiting ice crystals that damage cells and tissues. Some studies have looked at the naturally occurring biological antifreezes that protect organisms that live in sub-zero environments.[11] Using these molecules as models has allowed scientists to make considerable progress towards understanding and reproducing the molecular process by which these natural cryoprotectants work.[12]

1.2 Recrystallization in Ice

Ice recrystallization is defined as the growth of large crystals at the expense of small ones. This process is driven thermodynamically which results in an overall reduction in the free energy of the system. Ice recrystallization has a direct impact on many areas such as cryo-medicine (cells, tissues, etc.) and food preservation; yet, it has been less studied than the process of recrystallization in areas like metallurgy and geology.[12] In medicine, freezing biological organs, stem cells and red blood cells is very important process that helps preserve them. However, ice recrystallization remains a problem because it causes cellular damage and cell death.[13,14] One of the ways to overcome such a problem is to design inhibitors of ice recrystallization. Many compounds have been discovered including some naturally occurring biological antifreeze that are able to inhibit ice recrystallization. Also, to design new ice recrystallization inhibitors, an understanding of the structure of ice polycrystalline and the mechanism of ice recrystallization is required.

Freezing food is a process that helps decrease the rate of deterioration. In the past few decades freezing and storage process have been improved for variety of products food giving it a finite shelf life.[15,16] On the other hand, changing texture, taste and quality of frozen food product are a direct result on the ice recrystallization process.

1.2.1 Structure of Ice Crystals

Ice has many polymorphic forms. Water molecules in ice are dependent on pressure and temperature, which makes it possess different arrangements within three-dimensional space. Below 0°C and at atmospheric pressure, ice tends to form in hexagonal crystal shape. This is due to two hydrogen atoms hydrogen bonded to a single oxygen atom.[17,18] The hexagonal ice structure is characterized by four axes, a_1, a_2, a_3 and c, and the surface of the

hexagonal unit has eight faces. Two of the faces are normal to the *c*-axis and are the basal faces, and the remaining six are prism faces, Figure 1.1.[17-20]

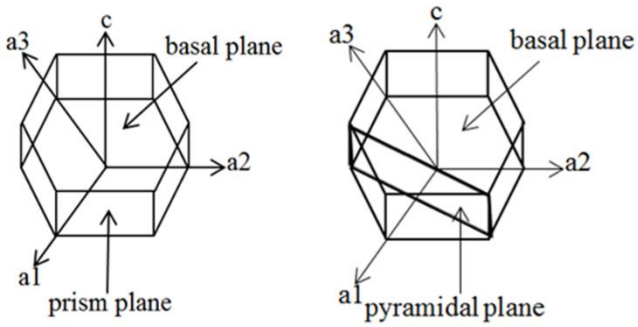

Figure 1.1 Representation of the hexagonal ice structure showing the a_1, a_2, a_3 and c axes and the basal, pyramidal and prism planes.

The arrangement of intermolecular hydrogen bonds has an influence on the properties and phases of ice. At temperature of 0 °C and atmospheric pressure, ice grows most rapidly along the *a*-axis to give hexagonal shaped crystals which grow as sheets.[21,23,25] If the ice is in an aqueous solution, the transition of the interface between the ice lattice and bulk water does not occur rapidly. According to some studies a semi-ordered layer (quasi liquid layer or QLL) exists between the highly-ordered ice lattice and the less ordered bulk water surrounding ice crystals.[24,26] Michael Faraday proposed 150 years ago that a thin liquid layer covers the surface of ice when near the melting temperature. Fletcher was the first to propose a model for the existence of the QLL in 1962, which was subsequently revised in 1968.[26,27] The thickness of interface region between ice lattice and bulk water is approximately 10-15 Å thick, but this has been shown to be temperature dependent.[28-30] Studies have suggested that the QLL is thicker on the basal and prism faces than on the pyramidal and secondary prism planes.[24]

1.2.2 Mechanism of Ice Recrystallization

The recrystallization of ice in polycrystalline aqueous solutions is believed to occur in

two ways, either through grain boundary migration or Ostwald ripening. The grain boundary migration is where large ice grains grow larger at the expense of small ice grains. Grain boundary migration occurs as individual molecules transfer from unfavorably oriented ice grains to favorably oriented ice grains. These boundaries tend to be curved and the degree of curvature is proportional to the size of the grain. Boundaries of small ice crystals have a higher degree of curvature making them more convex, and thus have a higher amount of surface energy. Large ice crystals have more concave grain boundaries and have a lower amount of surface energy. Grain boundaries migrate towards their center of curvature to reduce the overall degree of curvature, resulting in ice grains with concave boundaries, growing larger while those with convex boundaries decrease in size (Figure 1.2).[31,32] The driving force of grain boundary migration in ice arises from a reduction in grain boundary curvature, which results in an overall reduction in the energy of the system.

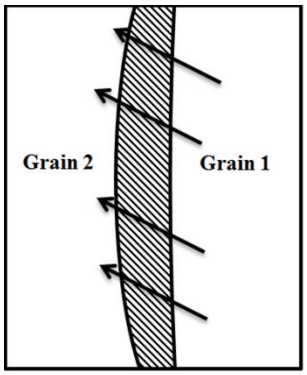

Figure 1.2 A liquid-layer (shaded) in a curved boundary between two ice grains. Large grains with concave boundaries (grain 2) grow larger while small grains with convex boundaries (grain 1) decrease in size to reduce the overall degree of grain boundary curvature. Arrows indicate the direction of boundary migration.

1.3 Biological Antifreezes as Ice Recrystallization Inhibitors

During late 1950's and early 1960's Scholander et al. have observed that marine teleost fish, Atlantic Cod (Gadus morhua) (A) and Antarctic Notothenioid (Pagothenia borchgrevinki) Figure 1.3, did not freeze during winter when the temperature of the water was -1.9°C, over one degree lower than the freezing point of blood serum.[33,34] Shortly after this observation, DeVries and Wohlschlag explained the reason for the fish survival was due to the presence of a biological antifreezes (BAs), consisting of antifreeze proteins (AFPs) and antifreeze glycoproteins (AFGPs). BAs were the first compounds to be discovered with the ability to inhibit ice recrystallization.[35-38] Also they have attracted considerable interests in both scientific and industrial communities because of their ability to prevent cryo-injury when organisms are exposed to cold temperatures.[39-41] This class of compounds is the foundation for all known ice recrystallization inhibitors even though they have different structures which makes it difficult to understand how they exhibit these properties.[42-44] BAs also exhibit thermal hysteresis (TH) activity (described below) as a result of their ability to irreversibly bind to the surface of ice crystals.[45-49]

Figure 1.3 Atlantic Cod (*Gadus morhua*) (A) and Antarctic Notothenioid (*Pagothenia borchgrevinki*) (B).

1.3.1 Structure of Biological Antifreeze

Five classes of biological antifreezes found in fish that have been identified. Four of them are of antifreeze proteins (AFPs), types I, II, III, and IV; the fifth class is of antifreeze

glycoproteins (AFGPs).[50,51] The four types of AFPs share similar functions but they are completely different in their secondary structures, which can be –helices, -rolls , random coils and globular structures (Table 1.1). AFGPs are comprised of a tripeptide repeat of $(Thr\text{-}Ala\text{-}Ala)_n$, where the secondary hydroxyl group of threpnine is glycosylated with the disaccharide β-D-galactosyl-(1-3)-α-*N*-acetyl-D- galactosamine (Table 1.1).[52-60] This has made structure-function studies of AFGPs more attractive than AFPs. The sequence of the peptide is highly conserved and only minor amino acid variations have been observed between AFGPs of different species. For example, in some species the second alanine of the sequence Thr-Ala-Ala repeat has been replaced with proline, and other species the threonine is replaced with an arginine.[61,62]

Table 1.1 Classification and structural differences between antifreeze proteins (AFPs) and antifreeze glycoproteins (AFGPs).

Characteristic	AFGP	Type I AFP	Type II AFP	Type III AFP	Type IV AFP
Mass (kDa)	2.6 – 33	3.3 – 4.5	11 – 24	6.5	12
Key Properties	AAT repeat; disaccharide	Alanine-rich α-helix	Disulfide bonded	β-sandwich	Alanine rich; helical bundle
Representative Structure	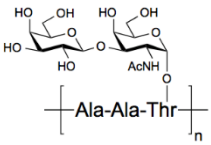		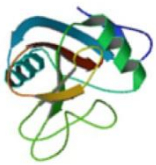		
Natural Source	Antaractic Notothenioids; northern cods	Right-eyed flounders; sculpins	Sea raven; smelt; herring	Ocean pout; wolfish; eel pout	Longhorn sculpin

AFGPs vary substantially in molecular weight based on the number of repeating glycopeptide units and have been classified into eight subtypes according to their weight.[63] AFGPs 1-5 are large and they contain up to 50 units of (Thr-Ala-Ala) with molecular weights of 20-30 kDa. On the other hand, AFGPs 6-8 are small and contain as little as four

repeating units of (Thr-Ala-Ala). Generally, it is now accepted that AFPs and AFGPs inhibits ice crystal formation by binding to specific faces of a growing ice lattice.[64,65]

1.3.2 Thermal Hysteresis – Mechanism of Action

Thermal Hysteresis (TH) is the depression of the freezing point of a solution relative to the melting point.[66] This is the result of binding BA to the surface of a seeded ice crystal.[67,68] This binding facilitates a localized freezing point depression and induces change in the ice crystal habit, which is referred to as dynamic ice shaping (DIS), Figure 1.4A.

The mechanism of TH involves an irreversible adsorption-inhibition process, where the BAs irreversibly bind to specific surface of the growing ice crystal.[67-71] The growth of ice crystals is along the c-axis when the temperature decreases below the hysteresis freezing point, which gives the characteristics of a hexagonal bipyramidal shape (Figure 1.4B).[69,72]

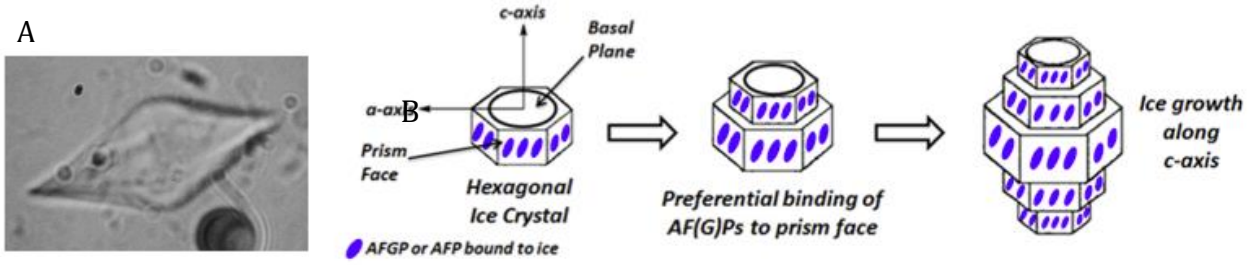

Figure 1.4 (A) Ice crystal in the presence of AFGP-8. The binding of AFGP to the surface of ice crystal changes the structure to hexagonal bipyramidal. (B) Formation of Hexagonal bipyramidal crystals by inhibition of growth on the prism faces due to adsorption of BAs.

When BAs bind to the surface of ice crystals it induces a localized freezing point depression. A study by Wilson shows that this occurs via the Kelvin (or Gibbs-Thomson) Effect.[71] Because BAs inhibits the growth of the crystal where it binds, the crystal will grow between adjacent BA molecules and this causes curved ice surfaces (Figure 1.5). This

will make water molecules unattractive to each other due to the higher energy, and hence localized freezing point depression is observed. On the other hand, the melting process is not affected by this mechanism resulting in a thermal hysteresis gap (Figure 1.5A).[71,73, 74] To understand how BAs inhibit ice growth within the thermal hysteretic gap, Raymond and DeVries have proposed a model to describe the mechanism. This model is known as the step-pinning model, where the growth of a step is inhibited by the BAs, which has pinned ice growth across the ice surface.[69]

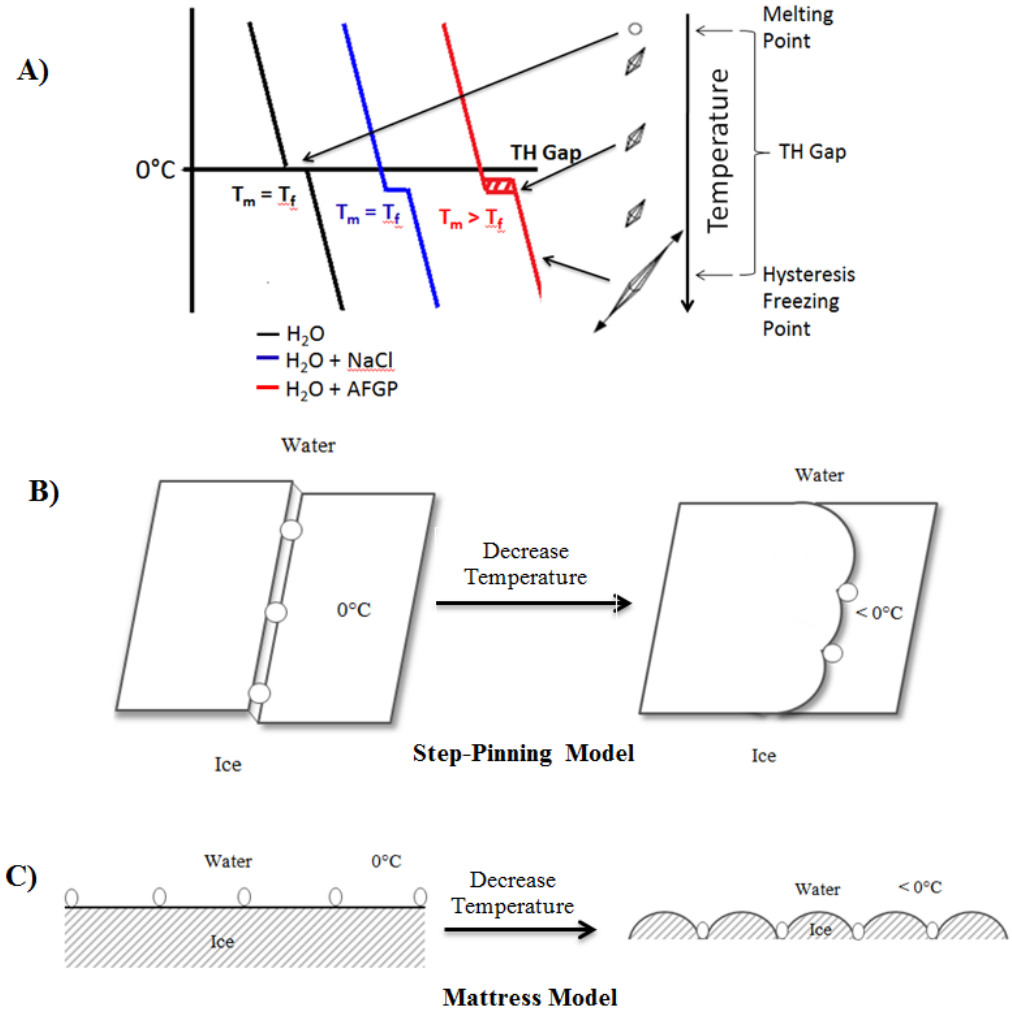

Figure 1.5 Activity of TH and ice growth inhibition. (A) BAs depression of freezing point of ice crystals relative to melting point results in TH gap. (B) Step pinning model. (C) Mattress model.

This model assumes that the growth of an ice crystal occurs in steps across the plane that the BA is adsorbed (Figure 1.5B). Knight and DeVries have proposed a second model known as the mattress model and it is a three-dimensional model (Figure 1.5C). In this model, the adsorbed BA molecules exhibit inhibition by pinning ice growth perpendicular to the ice surface.[67]

1.4 Inhibitors of Ice Recrystallization

As mentioned before, ice recrystallization is defined as the growth of large crystals at the expense of small ones. AFPs and AFGPs are capable of inhibiting the recrystallization process and limiting the size of the ice crystals (Figure 1.6), which in turn will reduce damage to cells and tissues.

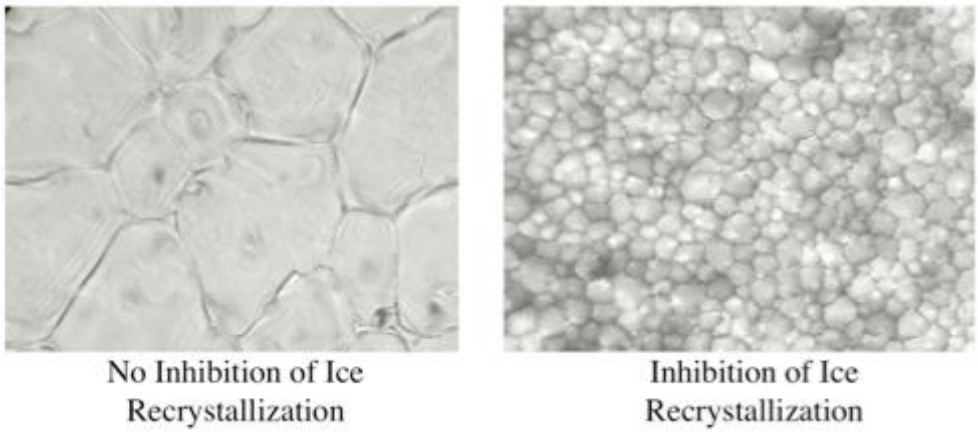

Figure 1.6 Annealed ice grains obtained from a compound that can inhibit ice recrystallization and able to maintain small ice crystals within a frozen solution.

Ice recrystallization inhibition (IRI) is now considered one of the important properties of compounds used in the cryopreservation of biological samples. IRI has been used to explore and develop alternative cryoprotectants.[75-77] In the past few decades, TH was often the only antifreeze activity assessed and correlated to structural modifications. In recent years considerable efforts has been made to discover novel ice recrystallization inhibitors.

However, the mechanism of ice recrystallization inhibition is yet to be understood, as well as the important structural features possessed by compounds that are capable of inhibiting recrystallization of ice. The majority of the work done towards ice recrystallization inhibitors is based on the synthetic structural analogues of AFGPs. Most of these analogues have been IRI inactive and some have shown activity of both TH and IRI.[78-85] Other AFGPs analogues with dramatic structural modifications have been discovered to have potent IRI activity but no TH activity.[86,87] Thus, such compounds are considered ideal for applications as novel cryoprotectants because they do not exhibit the undesirable properties of TH. This also disproved the initial belief that IRI and TH activities were linked together and opened many doors for further investigations.

1.4.1 Small Carbohydrates Molecules as Ice Recrystallization Inhibitors

Throughout the past decades, the discovery of new IRI compounds increased and grabbed the attentions of much research. The first main molecules that exhibited IRI activity were AFPs and AFGPs found in fish. The synthesis of such compounds is complex and their synthesis is very costly and time consuming. Therefore, much attention was directed toward the synthesis of simple small molecules that have the capacity to inhibit ice recrystallization. Such compounds, because of their ease of preparation, are potentially well suited for many medical, commercial and industrial applications.

The first action taken towards this idea was to investigate simple and commercially available mono- and disaccharides. This was studied by examining the correlation between IRI and carbohydrate hydration,[88] where an observation was made that a more hydrated carbohydrate moiety contributed towards higher IRI activity of the C-AFGP analogue

(OGG-Gal, **5**).[87] This observation led to a study where four monosaccharides and five disaccharides with known hydration parameters were assessed for their ability to inhibit

Table 1.2 Molar compressibility (10^4 K_2^o (s), cm^3mol^{-1} bar^{-1}) and hydration numbers of different monosaccharides and disaccharides. Numbers in brackets indicates errors of molar compressibility values and hydration numbers.[88,89]

Carbohydrate	Molar Compressibility ($K_2°(s)x10^4$,cm^3 mol^{-1} bar^{-1})	Hydration Number	Carbohydrate	Molar Compressibility ($K_2°(s)x10^4$,cm^3 mol^{-1} bar^{-1})	Hydration Number
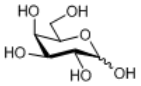 D-Galactose	-20.8 (0.5) -20.4 (0.4)	8.7 (0.2)	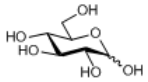 D-Glucose	-17.6 (0.3)	8.4 (0.2)
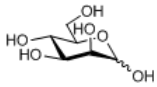 D-Mannose	-16.0 (0.5)	8.1 (0.2)	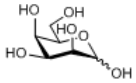 D-Talose	-11.9 (0.3)	7.7 (0.2)
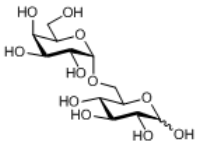 Melibiose	-31.2 (1.0)	15.5 (0.3)	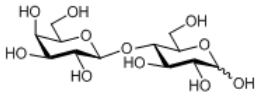 Lactose	-31.1 (0.2) -30.4 (1.0)	15.3 (0.3)
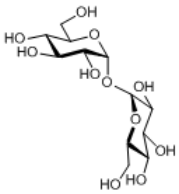 Trehalose	-30.2 (0.3)	15.3 (0.3)	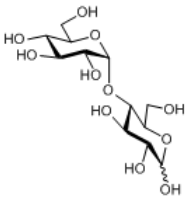 Maltose	-23.7 (1.0)	14.5 (0.3)
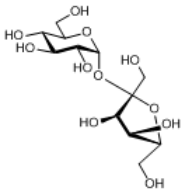 Sucrose	-17.8 (0.5)	13.9 (0.3)			

ice recrystallization (Table 1.2).[89-91] The four different monosaccharides where assessed at a concentration of 22 mM. Amongst the monosaccharides, D-galactose had the highest IRI activity, D-glucose and D-mannose had weak activity and the fourth monosaccharide, D-talose, was not active.[88] These results showed a strong linear correlation between the

hydration number of the monosaccharides and their respective IRI activity, where monosaccharides with larger hydration numbers are more IRI active.

The disaccharides also show a slightly linear correlation for their hydration number to IRI activity. Melibiose exhibited moderate IRI activity, while lactose and trehalose showed weak activity and maltose and sucrose were inactive (Graph 1.1).

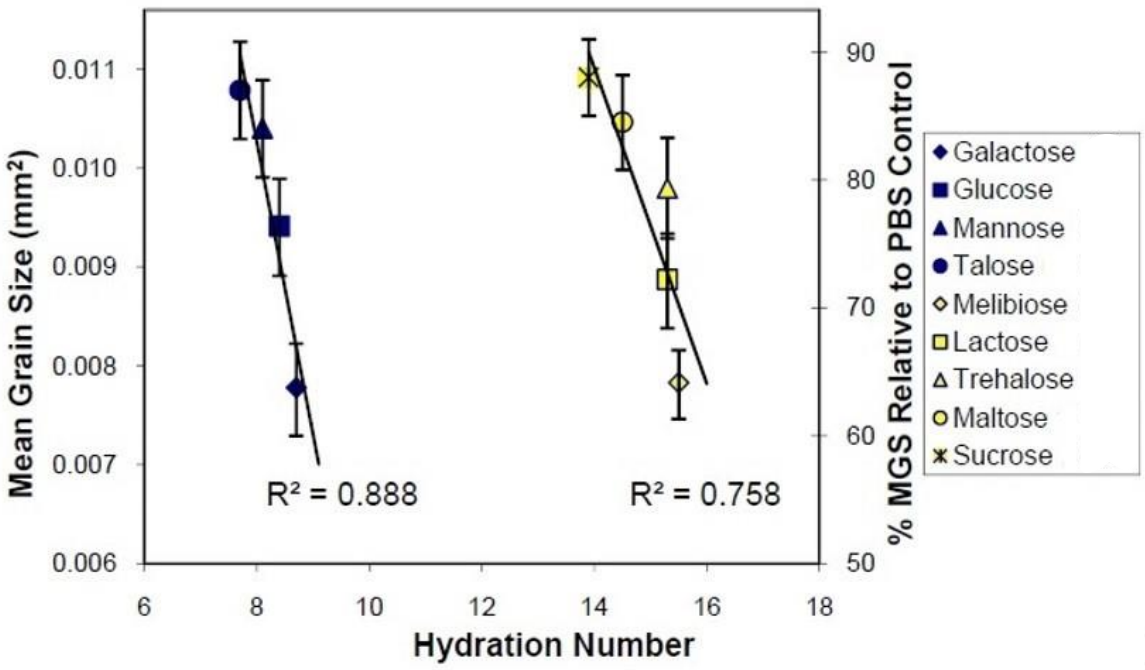

Graph 1.1 IRI activity of monosaccharides (blue) and disaccharides (yellow) at 22mM concentration plotted against the hydration numbers.[88,89,92]

The hydration number of a compound represents the number of water molecules that are tightly bound to it in the first hydration shell.[89] This number is different from the partial molar compressibility values, which take into account the first two hydration shells surrounding the molecule of interest.[88] Thus, hydration numbers are viewed as a the number of water molecules interacting with the solute in its immediate vicinity.[8,89] In the 1990's a study by Galema et al. was done on the key parameters that were thought to dictate hydration characteristics which were correlated to carbohydrate stereochemistry. The

partial molar volumes, isentropic partial molar compressibility and hydration numbers were determined using kinetic experiments and density ultrasound measurements. These measurements were done on different commercially available mono- and disaccharides.[89-91] Hydration numbers are calculated using isentropic coefficients of compressibility and they predict the number of water molecules that are hydrogen bonded to a carbohydrate molecule. The isentropic partial molar compressibility and partial molar volume values of the carbohydrates quantify their "compatibility" with the three-dimensional hydrogen-bond network of bulk-water as they are related to the size or volume the carbohydrate occupies upon hydration by water. In the Galema et al. study, it was also observed that the compatibility of the carbohydrate with the three-dimensional hydrogen bond network of bulk water was proportional to the configuration of C2 and C4 carbons of the carbohydrate molecule. An axial hydroxyl groups on C2 and C4, such as D-talose, had a higher isentropic molar compressibility value and lower hydrogen number. This also fits well into the three-dimensional hydrogen bonded network of bulk water. On the other hand, a molecule with axial hydroxyl group on C4 and equatorial hydroxyl group on C2, such as D-galactose, had lower isentropic molar compressibility value and higher hydration number. This did not fit well into the three-dimensional hydrogen bonded network of bulk water. Therefore, D-galactose was the least compatible and caused a greater distribution on the hydrogen bonded network of bulk water, whereas D-talose was the most compatible and caused least distribution on the hydrogen bonded network of bulk water. Other carbohydrates such as D-glucose and D-mannose, with an equatorial hydroxyl group on C4 and an equatorial or axial hydroxyl group on C2, respectively, had moderate fit and caused moderate distribution of the three-dimensional hydrogen bonded network of bulk water.

The disaccharides also showed a strong linear correlation of their IRI activity to their hydration numbers (Table 1.2).[88] It should be noted that the hydration numbers for disaccharides relative to monosaccharides increased significantly but that did not increase the in IRI activity (Graph 1.1). The difference in hydration number is due to the difference in total steric volume between the monosaccharides and disaccharides. Dividing the carbohydrate hydration number by their partial molar volumes will give an indication of the degree of hydration per molar volume of carbohydrate. This value was referred to as the hydration index (HI) and it provided the degree of hydration of the substrate as a function of its size or volume. The hydration index is useful in justifying why highly hydrated monosaccharides exhibited similar IRI activity as highly hydrated disaccharides at 22 mM (Graph 1.2).[88] However, at higher carbohydrate concentrations, such as 220 mM, the disaccharides were twice as IRI active as the monosaccharides.[93]

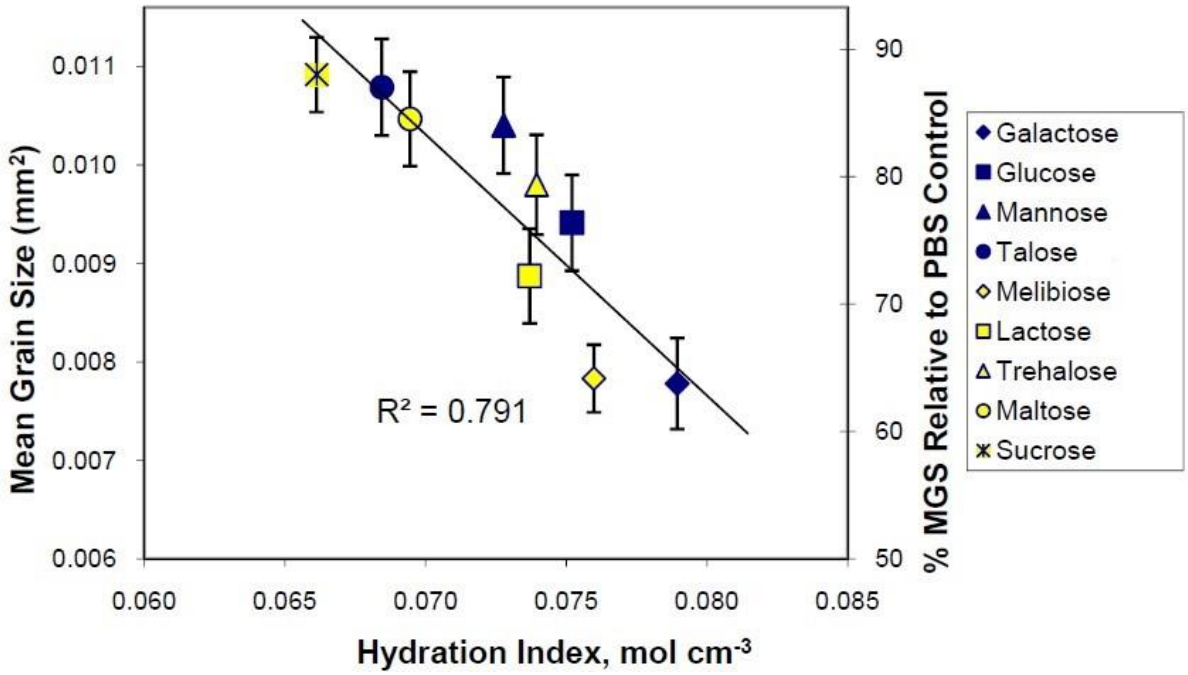

Graph 1.2 IRI activities of carbohydrates at 22mM as a function of hydration index (HI).

The discovery of the connection between hydration and IRI activity in carbohydrates produced several clues for the mechanism by which these compounds inhibit ice recrystallization. When aqueous solutions are cooled below their freezing point, the formation of hydrogen bonds between water molecules becomes less reversible.[94] This leads to an arrangement of water molecules to an ordered ice lattice. This creates a semi-ordered quasi-liquid layer (QLL) that exists between the highly-ordered ice lattice and bulk water, which leads for ice recrystallization to occur by transferring bulk water molecules to the QLL, then from the QLL to the growing ice lattice.[95,96] Since small molecule inhibitors of ice recrystallization generally do not possess TH activity, it is believed that they do not bind to ice as the compounds that possess TH do. So, instead they interact with water molecules in the QLL.[97] It was suggested that carbohydrate molecules are concentrated at the bulk water QLL interface (Figure 1.7), and if these molecules have a poor fit into the bulk water they will cause a great disturbance to its three-dimensional hydrogen bonded network, which will increase the energy associated with the transfer of bulk water to the QLL. This leads to the hypothesis that the inhibition of ice recrystallization occurs at the bulk water QLL interface due to more highly hydrated carbohydrates. Less hydrated carbohydrates fit well into bulk water and causes less disturbance to the pre-ordering of bulk water which will not inhibit ice recrystallization.

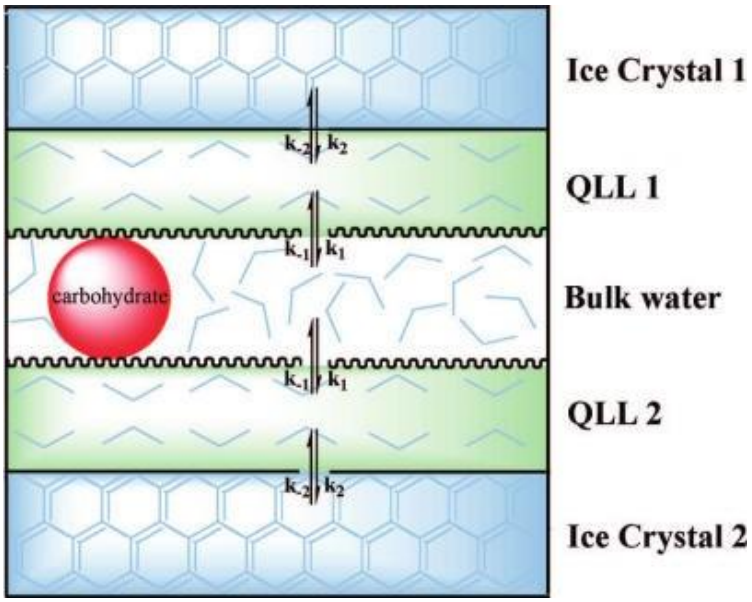

Figure 1.7 Schematic representation of the ice water interface and the effect of carbohydrates on ice recrystallization.

1.4.3 Peptides and Glycopeptides Analogues as Ice Recrystallization Inhibitors

Carbon-linked (C-linked) AFGP analogues were the first novel compounds to be reported by our group. These compounds do not have the O-glycosidic linkage that is found in AFGP, which can be hydrolyzed by acidic or basic conditions. In 2003, the Ben group reported the first set of compounds of C-linked AFGP, which were lysine-based.[98] Several strategic structural modifications have been made to AFGP analogue C-(KGG)-gal (**1**) in order to simplify the synthesis (Figure 1.8). Such modifications like the β-D- galactosyl-(1,3)-α-D-N-acetylgalactosamine disaccharide was replaced with one D-galactose molecule. Also, the Thr-Ala-Ala peptide unit was replaced with a Lys-Gly-Gly sequence.[99] The reason for lysine to be chosen is because it is similar in length to arginine. Arginine sometimes replaces threonine in smaller native AFGPs. The alanines were replaced by glycine to eliminate any possible formation of stereoisomers during the synthesis of the peptide unit.

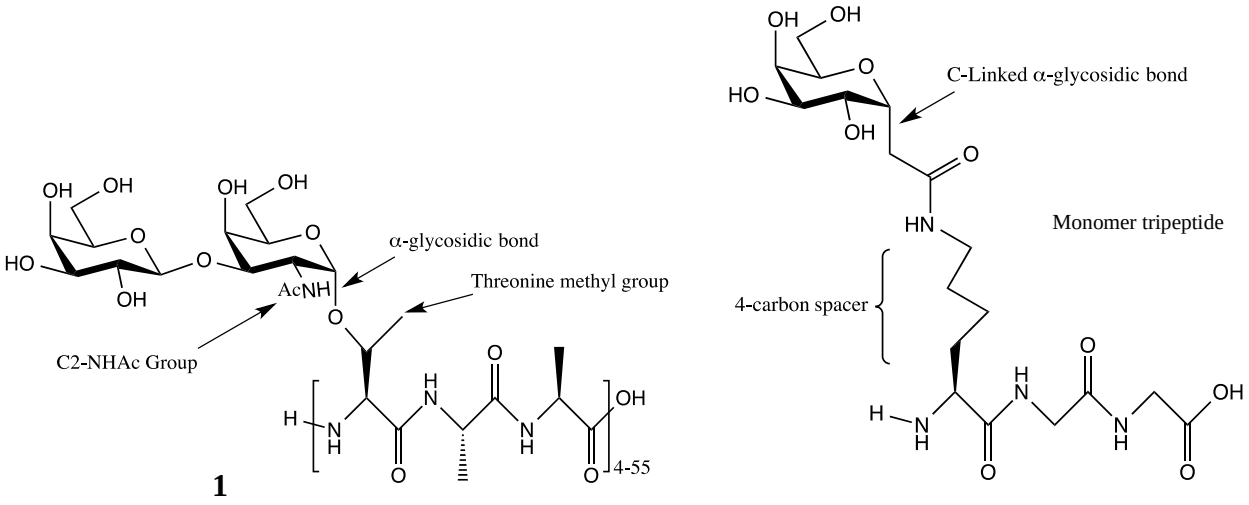

Figure 1.8 AFGP-8 (**1**) and first-generation C-Linked AFGP analogue (monomer tripeptide).

The monomer tripeptide unit (**1**) and the analogue with three repeating tripeptide units (**2**, n = 3) did not exhibit IRI activity. Yet, other analogues with six and nine repeating tripeptide units (**3,** n = 6, and **4,** n = 9) were moderately IRI active. The derivatives (**3** and **4**), Figure 1.9, were also assessed for TH activity and both exhibited a small TH gap of 0.06 °C and induced the formation of hexagonal shaped ice crystals.[98]

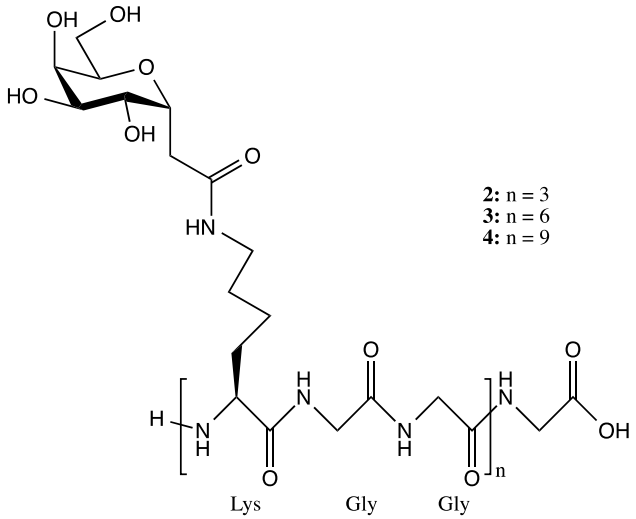

Figure 1.9 First-generation C-linked AFGP analogue $[C\text{-}(KGG)\text{-}Gal]_n$.

The second-generation analogues (**5**) and (**6**), Figure 1.10, displayed potent antifreeze activity compared to AFGP 8 (Graph 1.3) but did not show any TH activity. [100,101] On the other hand, both compounds show very little dynamic ice shaping (DIS) activity, which is very desirable property for cryopreservation. Cytotoxicity of the second-generation analogues was also assessed. It was found that [C-(OGG)-Gal]$_4$ (**3**) is non-toxic to cell lines at concentrations from 0.63 mg/mL to 2.0 mg/mL.

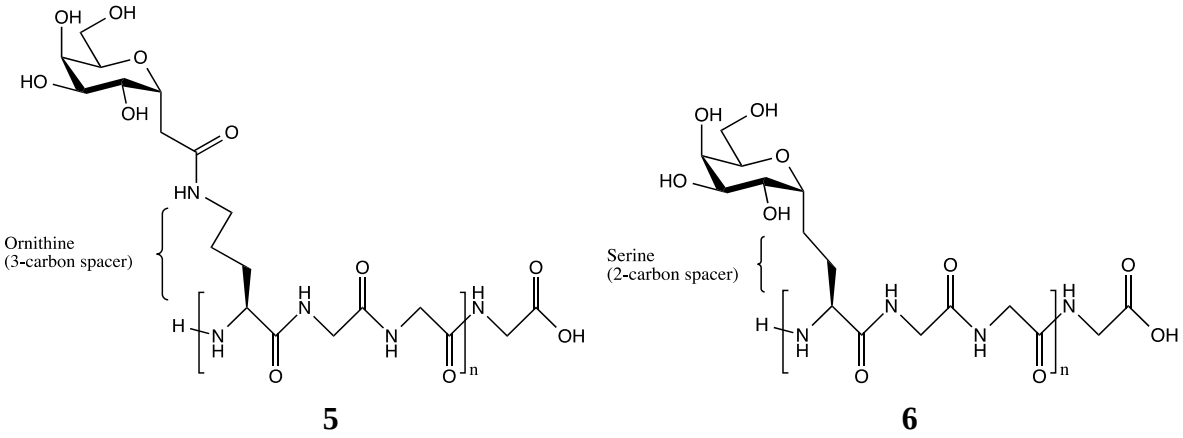

5 **6**

Figure 1.10 Second generation C-AFGP-analogues [C-(OGG)-Gal]$_n$ (**5**) and [C-(SGG)-Gal]$_n$ (**6**).[100,101]

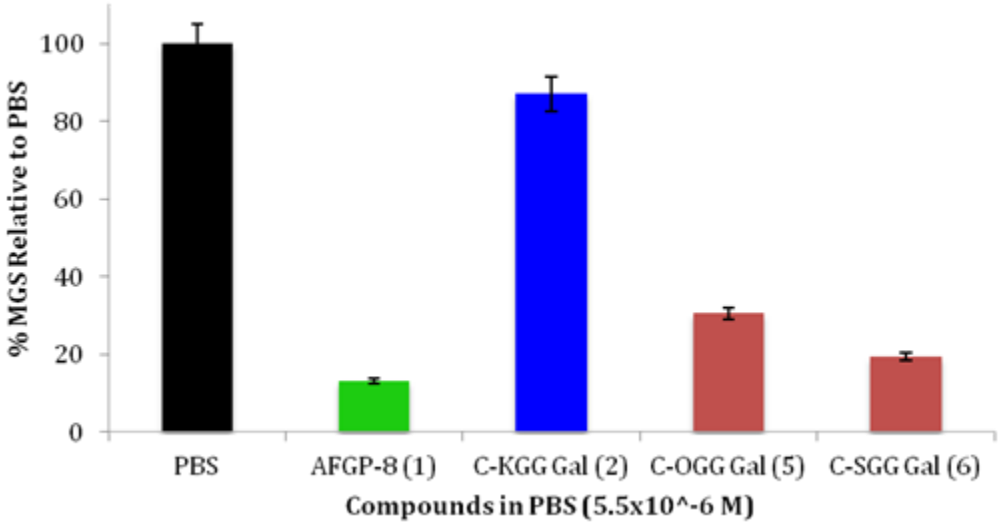

Graph 1.3 Ice Recrystallization Inhibition (IRI) activity of molecules 1, 2, 5 and 6 compared to phosphate buffered silane (PBS).

1.4.2 Synthetic polymers as Ice Recrystallization Inhibitors

Knight et al. were the first group to discover the inhibition of ice recrystallization by synthetic polymers in 1995.[102] In this discovery it was found that poly-L-histidine, poly-L-hydroxyproline and polyvinyl alcohol (PVA) exhibited IRI activity at concentrations less than 1 mg/mL in pure water, but poly-L-aspartic acid, poly-L-asparagine, polyacrylic acid and polyvinylpyrrolidone were not active. [102]

Some polymers such as PVA show mass dependency in terms of their IRI activity. A study in 2003 by Inada et al. shows an increase in RI with increasing molecular mass.[103] Polymers with an average molecular weight of 90,000 g/mol were found to have similar activity to AFP type I at same concentrations. By comparing the two compounds, the quantity of PVA required is much higher than AFP-I. A re-examination of the molecular weight by Gobson et al. was done in 2009 showing that PVA with an average molecular weight of 115, 500 g/mol has a potent IRI activity at a concentration of 5 mg/mL.[104] They have suggested that the ability of PVA to inhibit ice recrystallization is attributed to its ability to interact with the ice crystal lattice.

Polymers other than PVA have been investigated for their ability to inhibit ice recrystallization.[105] Gibson et al. have reported several IRI activities of various polymers, Figure 1.11.[105] Some of these polymers have low IRI activity such as polyacrylic acid (1 mmol/L – 8 mmol/L) (PAA, **7**), polyethylene glycol (0.5 mmol/L – 4 mmol/L) (PEG, **9**), poly-L-Lysine (0.5 mmol/L – 4 mmol/L) (**10**) and poly-L- glutamic acid (1 mmol/L – 6 mmol/L) (**11**), and their activity did not increase by increasing the concentration. Poly-L-hydroxyproline (3.5 mmol/L – 7 mmol/L) (**12**) exhibited IRI activity but this activity was dependent on its concentration. Two structures that are derived from vinyl-glycopolymers

were assessed for their ability to inhibit ice recrystallization (**13** and **14**, Figure 1.11), and found that the highest molecular weight glycopolymer with a glucose residue (**13)**, at ~105000 g/mol exhibited a moderate IRI activity. However, incorporating a different carbohydrate residue (ie: galactose) (**14**) failed to increase IRI activity. [104,105]

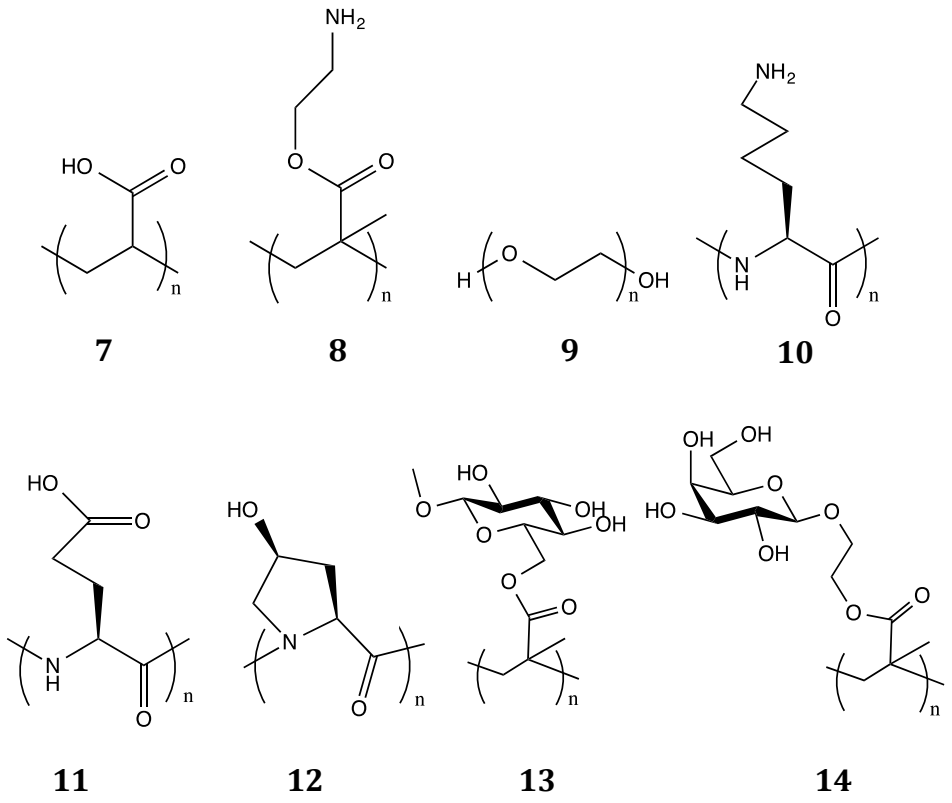

Figure 1.11 Structures of synthetic polymers assessed for IRI activity.

1.5 Conclusion

Cryopreservation is a process used to store cells and tissues for long period of time under very low temperatures. During this process, ice crystals grow large in size and damage the stored cell. Thus, cryoprotectants are required to prevent the damage to the cells. Cryoprotectants are small molecules that inhibit the growth of ice crystals during

cryopreservation. Current cryoprotetants are not suitable due to their toxicity, and further research is required to establish suitable ones that can be used to preserve cells and tissues.

References

1. Mazur, P., Cryobiology: the freezing of biological systems. Science, **1970**, 168, 939-949.

2. Polge, C.; Smith, A.V.; Parkes, A.S., Revival of Spermatozoa after Vitrification and Dehydration at Low Temperatures. Nature **1949**, 164, 666.

3. Gosden, R. G.; Picton, H. M.; Nugent, D.; Rutherford, A. J., Cancer patients, gametes, gonadal tissue, and the UK legal status. Human Fertility **1992**, 2, 107-114.

4. Loken, S. D.; Demetrick, D. J., A novel method for freezing and storing research tissue bank specimens. Human Pathology **2005**, 36, 977-980.

5. Can, A.; Karahuseyinoglu, S., Concise review: human umbilical cord stroma with regard to the source of fetus-derived stem cells. Stem Cells **2007**, 25, 2886-2895.

6. Wallis, J. G.; Wang, H.; Guerra, D. J., Expression of a synthetic antifreeze protein in potato reduces electrolyte release at freezing temperatures. Plant Mol. Biol. **1997**, 35, 323-354

7. Griffith, M.; Ewart, K. V., Antifreeze proteins and their potential use in frozen foods. Biotech. Adv. **1995**, 13, 375-403.

8. Lovelock, J. E., The mechanism of the protective action of glycerol against haemolysis by freezing and thawing. Biochim. Biophys. Acta. **1953**, 11, 28.

9. McGann, L. E., Differing Actions of Penetrating and Nonpenetrating Cryoprotective Agents. Cryobiology **1978**, 15, 382-390.

10. Doebbler, G. F.; Rinfret, A. P., The influence of protective compounds and cooling and warming conditions on hemolysis of erythrocytes by freezing and thawing. Biochim. Biophys. Acta **1962**, 58, 449-458.

11. Davies, P. L.; Hew, C. L., Biochemistry of fish antifreeze proteins., FASEB J. **1990**, 4, 2460- 2468.

12. Capicciotti, C. J.; Doshi, M.; Ben, R. N., Ice Recrystallization Inhibitors: From Biological Antifreezes to Small Molecules. Recent Developments in the Study of Recrystallization, Peter Wilson (Ed.), Intech **2013**, 177-224.

13. Baust, J.M.; Van Buskirk, R.; Baust, J.G., Cell viability improves following inhibition of cryopreservation-induced apoptosis. In Vitro Cell. Dev. Biol. Anim. **2000**, 36, 262-270.

14. Baust, J.M. Molecular Mechanisms of Cellular Demise Associated with Cryopreservation Failure. Cell Preserv. Technol. **2002**, 1, 17-31.

15. Goff, H.D. Measuring and interpreting the glass transition in frozen foods and mode1 systems. Food Res. Int. **1994**, 27, 187-189.

16. Venketesh, S.; Dayananda, C. Crit. Rev. Properties, potentials, and prospects of antifreeze proteins. Biotechnol. **2008**, 28, 57-82.

17. Fletcher, N.H. Chapter 2 - Structure and Energry of Ordinary Ice. In: editor. The Chemical Physics of Ice (1st ed.). London: Cambridge University Press; **1970**. p 23-48.

18. DeVries, A.L. and Lin, Y., Biochimica et Biophysica Acta (BBA) - Protein Structure **1977**; 495(2) 388-392.

19. Harding, M.M., Ward, L.G., and Haymet, A.D.J. Type I 'antifreeze' proteins. European Journal of Biochemistry **1999**; 264(3) 653-665.

20. Hayward, J.A. and Haymet, A.D.J. The ice/water interface: Molecular dynamics simulations of the basal, prism, {201}, and {20} interfaces of ice Ih. The Journal of Chemical Physics **2001**; 114(8) 3713-3726.

21. Fletcher, N.H. Chapter 2 - Structure and Energry of Ordinary Ice. In: editor. The Chemical Physics of Ice (1st ed.). London: Cambridge University Press; **1970**. p 23-48.

22. DeVries, A.L. and Lin, Y., Biochimica et Biophysica Acta (BBA) - Protein Structure **1977**; 495(2) 388-392.

23. Harding, M.M., Ward, L.G., and Haymet, A.D.J. Type I 'antifreeze' proteins. European Journal of Biochemistry **1999**; 264(3) 653-665.

24. Hayward, J.A. and Haymet, A.D.J. The ice/water interface: Molecular dynamics simulations of the basal, prism, {201}, and {20} interfaces of ice Ih. The Journal of Chemical Physics **2001**; 114(8) 3713-3726.

25. Fletcher, N.H. Chapter 2 - Structure and Energry of Ordinary Ice. In: editor. The Chemical Physics of Ice (1st ed.). London: Cambridge University Press; 1970. p 23-48.

26. Harding, M.M., Anderberg, P.I., and Haymet, A.D.J., 'Antifreeze' glycoproteins from polar fish. European Journal of Biochemistry **2003**; 270(7) 1381-1392.

27. Fletcher, N.H., Surface Structure of Water and Ice. Philosophical Magazine **1962**; 7(74) 255-269.

28. Fletcher, N.H., A Revised Model. Surface Structure of Water and Ice. Philosophical Magazine **1968**; 18(156) 1287-1300.

29. Karim, O.A. and Haymet, A.D.J., The ice/water interface. Chemical Physics Letters **1987**; 138(6) 531-534.

30. Karim, O.A. and Haymet, A.D.J., The ice/water interface: A molecular dynamics simulation using the simple point charge model. Journal of Chemical Physics **1988**; 89(11) 6889-6896.

31. Karim, O.A., Kay, P.A., and Haymet, A.D.J., Antifreeze Proteins at the Ice/Water Interface: Three Calculated Discriminating Properties for Orientation of Type I Proteins. The Journal of Chemi- cal Physics **1990**; 92(7) 4634-4635.

32. Alley, R.B., Perepezko, J.H., and Bentley, C.R., Grain growth in polar ice: I. Theory. Journal of Glaciology **1986**; 32(112) 415-424.

33. Alley, R.B., Perepezko, J.H., and Bentley, C.R., Grain growth in polar ice: II. Application. Journal of Glaciology **1986**; 32(112) 425-433.

34. Scholander, P.F.; van Dam, L.; Kanwisher, J.W.; Hammel, H.T.; Gordon, M.S. Supercooling and osmoregulation in arctic fish. J. Cell. Compar. Physiol. **1957**, *49*, 5-24.

35. Gordon, M.S.; Amdur, B.H.; Scholander, P.F. Freezing resistance in some northern fishes. *Biol. Bull.* **1962**, *122*, 52-62.

36. Garner, J.; Harding, M.M. Design and synthesis of antifreeze glycoproteins and mimics. *ChemBioChem.* **2010**, *11*, 2489-2498.

37. Peltier, R.; Brimble, M.A.; Wojnar, J.M.; Williams, D.E.; Evans, C.W.; DeVries, A.L. Synthesis and antifreeze activity of fish antifreeze glycoproteins and their analogues *Chem. Sci.* **2010**, *1*, 538-551.

38. Gibson, M.I.; Barker, C.A.; Spain, S.G.; Albertin, L.; Cameron, N.R. Inhibition of Ice Crystal Growth by Synthetic Glycopolymers: Implications for the Rational Design of Antifreeze Glycoprotein Mimics. *Biomacromolecules.* **2009**, *10*, 328-333.

39. Capicciotti, C.J.; Doshi, M.; Ben, R.N. Ice Recrystallization Inhibitors: From Biological Antifreezes to Small Molecules. In: P. Wilson, editor. Recent Developments in the Study of Recrystallization ed.). New York: InTech; **2013**. p 177-224.

40. DeVries, A.L.; Wohlschlag, D.E. Freezing Resistance in Some Antarctic Fishes. *Science.* **1969**, *163*, 1073-1075

41. DeVries, A.L.; Komatsu, S.K.; Feeney, R.E. Chemical and physical properties of freezing point-depressing glycoproteins from Antarctic fishes. *J. Biol. Chem.* **1970**, *245*, 2901-2908.

42. DeVries, A.L. Glycoproteins as biological antifreeze agents in antarctic fishes. *Science.* **1971**, *172*, 1152-1155.

43. Liu, S.; Ben, R.N. C-Linked Galactosyl Serine AFGP Analogues as Potent Recrystallization Inhibitors. *Org. Lett.* **2005**, *7*, 2385-2388.

44. Czechura, P.; Tam, R.Y.; Dimitrijevic, E.; Murphy, A.V.; Ben, R.N. The Importance of Hydration for Inhibiting Ice Recrystallization with C-Linked Antifreeze Glycoproteins. *J. Am. Chem. Soc.* **2008**, *130*, 2928-2929.

45. Capicciotti, C.J.; Leclère, M.; Perras, F.A.; Bryce, D.L.; Paulin, H.; Harden, J.; Liu, Y.; Ben, R.N. Potent inhibition of ice recrystallization by low molecular weight carbohydrate-based surfactants and hydrogelators. *Chem. Sci.* **2012**, *3*, 1408-1416.

46. Raymond, J.A.; DeVries, A.L. Adsorption inhibition as a mechanism of freezing resistance in polar fishes. *Proc. Natl. Acad. Sci. U.S.A.* **1977**, *74*, 2589-2593.

47. Knight, C.A.; DeVries, A.L. Effects of a polymeric, nonequilibrium "antifreeze" upon ice growth from water. *J. Cryst. Growth.* **1994**, *143*, 301-310.

48. Wilson, P.W. Antifreeze proteins: an unusual receptor–ligand interaction. *Cryoletters.* **1993**, *14*, 31-36.

49. Knight, C.A.; Cheng, C.C.; DeVries, A.L. Adsorption of alpha-helical antifreeze peptides on specific ice crystal surface planes. *Biophys. J.* **1991**, *59*, 409-418.

50. Knight, C.A.; Driggers, E.; DeVries, A.L. Adsorption to ice of fish antifreeze glycopeptides 7 and 8. *Biophys. J.* **1993**, *64*, 252-259.

51. Davies, P. L.; Sykes, B. D., Ice-binding surface of fish type III antifreeze. Curr. Opin. Struct. Biol. **1997**, 7, 828-834.

52. Harding, M. M.; Anderberg, P. I.; Haymet, A. D. J., 'Antifreeze' glycoproteins from polar fish. Eur. J. Biochem. **2003**, 270, 1381–1392.

53. Harding, M. M.; Anderberg, P. I.; Haymet, A. D. J., 'Antifreeze' glycoproteins from polar fish. Eur. J. Biochem. **2003**, 270, 1381–1392.

54. DeVries, A.L. Glycoproteins as biological antifreeze agents in antarctic fishes. *Science.* **1971**, *172*, 1152-1155.

55. Garner, J.; Harding, M.M. Design and synthesis of antifreeze glycoproteins and mimics. *ChemBioChem.* **2010**, *11*, 2489-2498.

56. Peltier, R.; Brimble, M.A.; Wojnar, J.M.; Williams, D.E.; Evans, C.W.; DeVries, A.L. Synthesis and antifreeze activity of fish antifreeze glycoproteins and their analogues *Chem. Sci.* **2010**, *1*, 538-551.

57. DeVries, A.L.; Komatsu, S.K.; Feeney, R.E. Chemical and physical properties of freezing point-depressing glycoproteins from Antarctic fishes. *J. Biol. Chem.* **1970**, *245*, 2901-2908.

58. DeVries, A.L.; Vandenheede, J.; Feeney, R.E. Evidence for a gamma-turn motif in antifreeze glycopeptides. *J. Biol. Chem.* **1971**, *246*, 305-308.

59. Feeney, R.E.; Burcham, T.S.; Yeh, Y. Antifreeze glycoproteins from polar fish blood. *Annu. Rev. Biophys. Biophys. Chem.* **1986**, *15*, 59-78.

60. Bouvet, V.; Ben, R.N. Antifreeze glycoproteins. *Cell Biochem. Biophys.* **2003**, *39*, 133-144.
61. Gibson, M.I. Slowing the growth of ice with synthetic macromolecules: beyond antifreeze(glyco) proteins. *Polym. Chem.* **2010**, *1*, 1141-1152.

62. Morris, H. R.; Thompson, M. R.; Osuga, D. T.; Ahmed, A. I.; Chan, S. M.; Vandenheede, J. R.; Feeney, R. E., Cooperative Functioning between Antifreeze Glycoproteins. J. Biol. Chem. **1978**, 253, 5155-5162.

63. Burcham, T. S.; Osuga, D. T.; Rao, B. N. N.; Bush, C. A.; Feeney, R. E., Purification and primary sequences of the major arginine-containing antifreeze glycopeptides from the fish Eleginus gracilis. J. Biol. Chem. **1986**, 261, 6384-6389.

64. Hew, C. L.; Slaughter, D.; Fletcher, G. L.; Joshi, S., Isolation and characterization of antifreeze glycoproteins from the forest fish, Microgodus tomcod. Can. J. Zool. **1981**, 60, 348-355.

65. Brown, R. A.; Yeh, Y.; Burcham, T. S. Thermal properties of water in myoglobin crystals and solutions at subzero temperatures. Biopolymers **1985**, 24, 1265-1270.

66. Kuiper, M. J.; Lankin, C.; Gauthier, S. Y.; Walker, V. K.; Davies, P. L., Purification of antifreeze proteins by adsorption to ice. Biochem. Biophys. Res. Comm. **2003**, 300, 645-648.

67. Scholander, P.F.; Maggert, J. E., Supercooling and ice propagation in blood from arctic fishes. Cryobiology **1971**, 8, 371-374.

68. Knight, C.A.; Cheng, C.C.; DeVries, A.L. Adsorption of alpha-helical antifreeze peptides on specific ice crystal surface planes. *Biophys. J.* **1991**, *59*, 409-418.

69. Knight, C.A.; Driggers, E.; DeVries, A.L. Adsorption to ice of fish antifreeze glycopeptides 7 and 8. *Biophys. J.* **1993**, *64*, 252-259.

70. Raymond, J.A.; DeVries, A.L. Adsorption inhibition as a mechanism of freezing resistance in polar fishes. *Proc. Natl. Acad. Sci. U.S.A.* **1977**, *74*, 2589-2593. 55.

71. Knight, C.A.; DeVries, A.L. Effects of a polymeric, nonequilibrium "antifreeze" upon ice growth from water. *J. Cryst. Growth.* **1994**, *143*, 301-310

72. Wilson, P.W. Explaining thermal hysteresis by the Kelvin effect. *Cryoletters.* **1993**, *14*, 31-36.

73. DeVries, A.L. The role of antifreeze glycopeptides and peptides in the freezing avoidance of antarctic fishes. *Comp. Biochem. Physiol. B: Comp. Biochem.* **1988**, *90*, 611-621.

74. Knight, C.A.; DeVries, A.L.; Oolman, L.D. Fish antifreeze protein and the freezing and

recrystallization of ice. *Nature.* **1984**, *308*, 295-296.

75. Yeh, Y.; Feeney, R.E. Antifreeze Proteins: Structures and Mechanisms of Function. *Chem. Rev.* **1996**, *96*, 601-618.

76. Chaytor, J. L. et al., Inhibiting ice recrystallization and optimization of cell viability after cryopreservation. Glycobiology **2012**, 22, 123-133.

77. Wu, L. K.; Tokarew, J. M.; Chaytor, J. L.; von Moos, E.; Li, Y. Palii, C.; Ben, R. N.; Allan, D. S., Carb. Res. **2011**, 346, 86-93.

78. Leclère, M.; Kwok, B. K.; Wu, L. K.; Allan, D. S.; Ben, R. N., C-Linked Antifreeze Glycoprotein (C-AFGP) Analogues as Novel Cryoprotectants. Bioconjugate Chem. **2011**, 22, 1804-1810.

79. Garner, J.; Harding, M.M. Design and synthesis of antifreeze glycoprotein and mimics. *ChemBioChem.* **2010**, *11*, 2489-2498.

80. Peltier, R.; Brimble, M.A.; Wojnar, J.M.; Williams, D.E.; Evans, C.W.; DeVries, A.L. ynthesis and antifreeze activity of fish antifreeze glycoproteins and their analogues. *Chem. Sci.* **2010**, *1*, 538-551.

81. Tachibana, Y.; Fletcher, G.L.; Fujitani, N.; Tsuda, S.; Monde, K.; Nishimura, S.-I. *Angew. Chem. Int. Ed.* **2004**, *43*, 856-862.

82. Miller, N.; Williams, G.M.; Brimble, M.A. *Org. Lett.* **2009**, *11*, 2409-2412.

83. 163. Peltier, R.; Evans, C.W.; DeVries, A.L.; Brimble, M.A.; Dingley, A.J.; Williams, D.E. *Cryst. Growth Des.* **2010**, *10*, 5066-5077.

84. Heggemann, C.; Budke, C.; Schomburg, B.; Majer, Z.; Wißbrock, M.; Koop, T.; Sewald, N. Ice Recrystallization Kinetics in the Presence of Synthetic Antifreeze Glycoprotein Analogues Using the Framework of LSW Theory. *Amino Acids.* **2010**, *38*, 213-222.

85. Norgren, A.S.; Budke, C.; Majer, Z.; Heggemann, C.; Koop, T.; Sewald, N. On-resin click-glycoconjugation of peptoids. *Synthesis.* **2009**, *2009*, 488-494.

86. Capicciotti, C.J.; Trant, J.F.; Leclère, M.; Ben, R.N. Synthesis of C-Linked Triazole-Containing AFGP Analogues and Their Ability to Inhibit Ice Recrystallization. *Bioconjugate Chem.* **2011**, *22*, 605-616.

87. Liu, S.; Ben, R.N. C-Linked Galactosyl Serine AFGP Analogues as Potent Recrystallization Inhibitors. *Org. Lett.* **2005**, *7*, 2385-2388.

88. 64. Czechura, P.; Tam, R.Y.; Dimitrijevic, E.; Murphy, A.V.; Ben, R.N. Antifreeze glycoprotein analogues and uses thereof. *J. Am. Chem. Soc.* **2008**, *130*, 2928-2929.

89. Tam, R.Y.; Ferreira, S.S.; Czechura, P.; Chaytor, J.L.; Ben, R.N. Hydration index--a better parameter for explaining small molecule hydration in inhibition of ice recrystallization. *J. Am. Chem. Soc.* **2008**, *130*, 17494-17501.

90. Galema, S.A.; Høiland, H. Stereochemical aspects of hydration of carbohydrates in aqueous solutions. 3. Density and ultrasound measurements. *J. Phys. Chem.* **1991**, *95*, 5321-5326.

91. Galema, S.A.; Engberts, J.B.F.N.; Hoeiland, H.; Foerland, G.M. Phase behavior of aqueous mixtures of dodecyltrimethylammonium bromide (DTAB) and sodium dodecyl sulfate (SDS). *J. Phys. Chem.* **1993**, *97*, 6885-6889.

92. Galema, S.A.; Howard, E.; Engberts, J.B.F.N.; Grigera, J.R. The effect of stereochemistry upon carbohydrate hydration. A molecular dynamics simulation of β-d-galactopyranose and (α, β)-D-talopyranose. *Carbohydr. Res.* **1994**, *265*, 215-225.

93. Høiland, H.; Hølvik, H., Experimental Study of the Hydration Properties of Homologous Disaccharides. J. Solution Chem. **1978**, 7, 587-596.

94. Chaytor, J.L.; Tokarew, J.M.; Wu, L.K.; Leclère, M.; Tam, R.Y.; Capicciotti, C.J.; Guolla, L.; von Moos, E.; Findlay, C.S.; Allan, D.S.; Ben, R.N. Inhibiting ice recrystallization and optimization of cell viability after cryopreservation. *Glycobiology.* **2012**, *22*, 123-133.

95. Malenkov, G., Liquid water and ices: understanding the structure and physical properties. J. Phys.: Condens. Matter **2009**, 21, 283101-283136.

96. Halter, P.U.; Bilgram, J.H.; Känzig, W. Properties of the solid-liquid interface layer of growing ice crystals: A Raman and Rayleigh scattering study. *J. Chem. Phys.* **1988**, *89*, 2622-2629.

97. Bilgram, J.H. The structure and properties of melt and concentrated solutions. *Prog. Cryst. Growth Charact. Mater.* **1993**, *26*, 99-119.

98. Czechura, P.; Tam, R.Y.; Dimitrijevic, E; Murphy, A.V; Ben, R. N., The Importance of Hydration for Inhibiting Ice Recrystallization with C-Linked Antifreeze Glycoproteins. J. Am. Chem. Soc., **2008**, 130 (10) 2928-2929.

99. Eniade, A.; Purushotham, M.; Ben, R.N.; Wang, J.B.; Horwath, K. Activation of Ice Recrystallization Inhibition Activity of Poly(vinyl alcohol) using a Supramolecular Trigger. *Cell Biochem. Biophys.* **2003**, *38*, 115-124.

100. Eniade A.; Hauer, L.; Ben, R.N., Synthesis of a C-linked Antifreeze Glycoprotein (AFGP) Mimic: Probes for Investigating the Mechanism of Action. Org. Lett. **1999**, 1, 1759-1762.

101. Eniade, A.; Purushotham. M.; Ben, R. N.; Wang, W.; Horwarth, K., A serendipitous

discovery of antifreeze protein-specific activity in C-linked antifreeze glycoprotein analogs. Cell Biochem. Biophys. **2003**, 38, 115-124.

102. Liu, S.; Ben, R. C-Linked Galactosyl Serine AFGP Analogues as Potent Recrystallization Inhibitors. Org. Lett. **2005**, 7, 2385-2388.

103. Knight, C.A., Single Crystals of MoS2 Several Molecular Layers Thick. Journal of Applied Physics **1966**, 37(2) 568-574.

104. Inada, T. and Lu, S.-S., Inhibition of Recrystallization of Ice Grains by Adsorption of Poly(Vinyl Alcohol) onto Ice Surfaces. Crystal Growth and Design **2003**, 3(5) 747-752.

105. Gibson, M.I., Barker, C.A., Spain, S.G., Albertin, L., and Cameron, N.R., Inhibition of ice crystal growth by synthetic glycopolymers: implications for the rational design of antifreeze glycoprotein mimics. Biomacromolecules **2009**, 10(2) 328-333.

106. Gibson, M.I., Slowing the growth of ice with synthetic macromolecules: beyond antifreeze(glyco) proteins. Polymer Chemistry **2010**, 1(8) 1141-1152.

Chapter 2: Goals and Objectives

2.1 Introduction

The toxicity of the currently available cryoprotectants limits their use for many applications especially in clinical and medical settings. Cryopreservation is the only technique available for successful long-term storage of cells and tissues.[1-13] Currently, the most commonly used cryoprotectants are DMSO and glycerol which are penetrating cryoprotectants. These two penetrating cryoprotectants, especially DMSO at the required concentration are very toxic and their toxicity has been well documented *in vitro* and in clinical settings.[14,15] The removal of these penetrating cryoprotectants can be done prior to the diffusion of the cryopreserved cells, but this process is time consuming, expensive and damaging to cells.[16,17] Because of these issues, it is required to develop and improve cryoprotectants to reduce or eliminate the use of DMSO or glycerol.

Ice recrystallization is considered a significant contributor to cell injury and death during cryopreservation.[4,9,11,18] The mechanism by which some molecules are capable of inhibiting ice recrystallization is still not clear, which makes the rational design of these ice recrystallization inhibition (IRI) molecules very difficult and time consuming. Despite the huge potential of IRI in the field of cryobiology and cryopreservation. IRI, research activity has been limited to biological antifreezes (BAs) such as antifreeze proteins (AFPs) and antifreeze glycoproteins (AFGPs).[19-24] The use of these BAs has not been very successful because these compounds have the ability to bind to ice crystals resulting in thermal hysteresis (TH) and structural changes of ice crystals.[25-28] Both TH and the change in structure of ice can cause cellular damage during cryopreservation and significantly decrease the viability of cells post thaw.

As previously mentioned, the IRI activity of certain carbohydrates is believed to be linked with their ability to interact strongly with the layer of bulk water which solvates the molecule in aqueous solution.[29,30] Therefore, the Ben group decided to alter the structure of some carbohydrates by replacing a hydroxyl group at C2 or C4 in monosaccharides by a nitrogen function such as N_3, NH_2 and NHAc. This was expected to provide some insight into the molecular properties that can be beneficial for IRI activity. Other non-carbohydrate small molecules that have amine or diamine functional groups were also investigated hoping that these might show interesting results regarding IRI-activity.

In 2009, Ferreira tested a small number of C2 functionalized galactosyl derivatives for IRI activity and compared the results with galactose itself (Graph 2.1).[31] It was observed

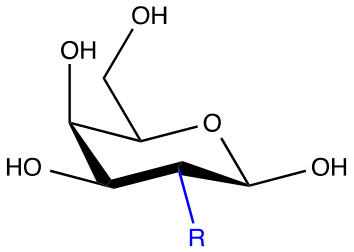

(**15**) R = N_3
(**16**) R = NH_3^+
(**17**) R = NHAc
(**18**) R = OH

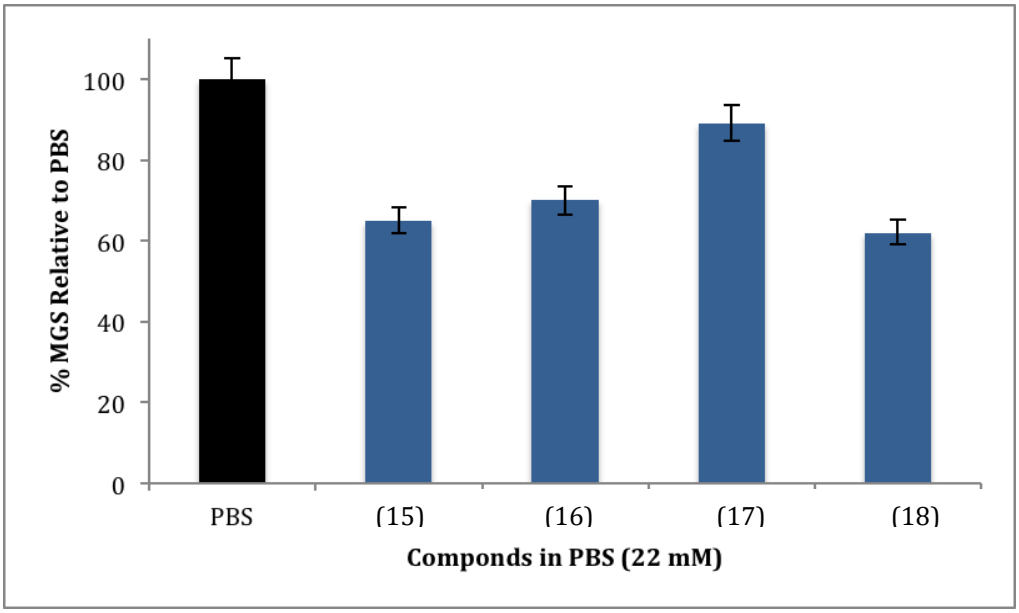

Graph 2.1 IRI activities of C2 galactosyl derivatives.[31]

that galactose gave the highest IRI activity.[18] Replacement of the hydroxyl group at C2 in

galactose by azide[15] resulted in lower IRI activity; further decreases were observed for galactosamine and *N*-acetyl-galactosamine with the latter having significantly less active IRI activity than the other derivatives.

Chaytor prepared and evaluated a similar series of galactose derivatives in which OH group at positions other than C2 were replaced by N_3 and NH_3^+ (Figure 2.1).[32] Chaytor's results paralleled those of Ferreira and it was concluded that galactose derivatives in whirl an OH group is replaced by N_3 have more potent IRI activity than the corresponding RNH_3^+ (Graph 2.1).

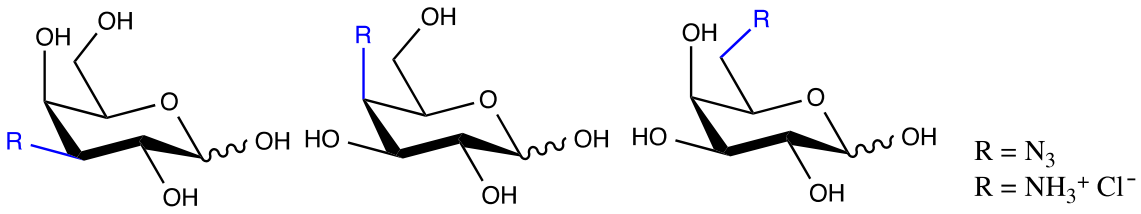

Figure 2.1 Other galactose regioisomers with either an azide or amine group.

2.2 Objective – 1: Examining other small amines molecules for IRI activity

Research in our group with amines has led to a conclusion that 1,2-cyclohexanediamine inhibits ice recrystallization. Based on that, the goal for this project was to take a step back to include cyclohexylamine as well as different cyclohexanediamine isomers, both positional and stereoisomers, and tested these for IRI activity. Keeping in mind the ultimate goal of developing cryoprotectants that are non-toxic to cells and are capable of inhibiting ice crystals that damage cells and tissues (Figure 2.2).

Tam et al. have reported that greater hydration correlates with greater IRI activity in simple carbohydrates.[33] Because amines are protonated at physiological pH, the use of the phosphate buffered saline (PBS) as a solvent will protonate amines to their respective ammonium ions (NH_3^+). Bowers et al. reported that three water molecules form hydrogen

bonds with ammonium; each water molecule will form the same hydrogen bond with one of the three-amine hydrogens in $-NH_3^+$.

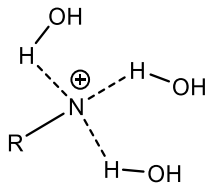

The binding energy will steadily decrease with increasing water molecules due to increasing charge delocalization, which causes the formation of new hydration shell.[34]

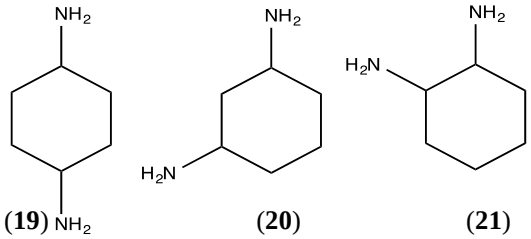

Figure 2.2 1,4-cyclohexanediamine (**19**), 1,3-cyclohexanediamine (**20**), and 1,2-cyclohexanediamine (**21**), cis-, trans-, and cis/trans mixtures have been tested for IRI activities.

2.3 Objective – 2: Poly(amidoamine) (PAMAM) and IRI activity

Poly(amidoamine) (PAMAM) dendrimers are synthetic polymers with unique structural and physical characteristics.[35] These dendrimers consist of an ethylenediamine (EDA) core, a repeating monomer unit of polyamidoamine and a terminal amino group, which can be used in the synthesis of further generations of the dendrimer or coupling to other molecules (Figure 2.3).

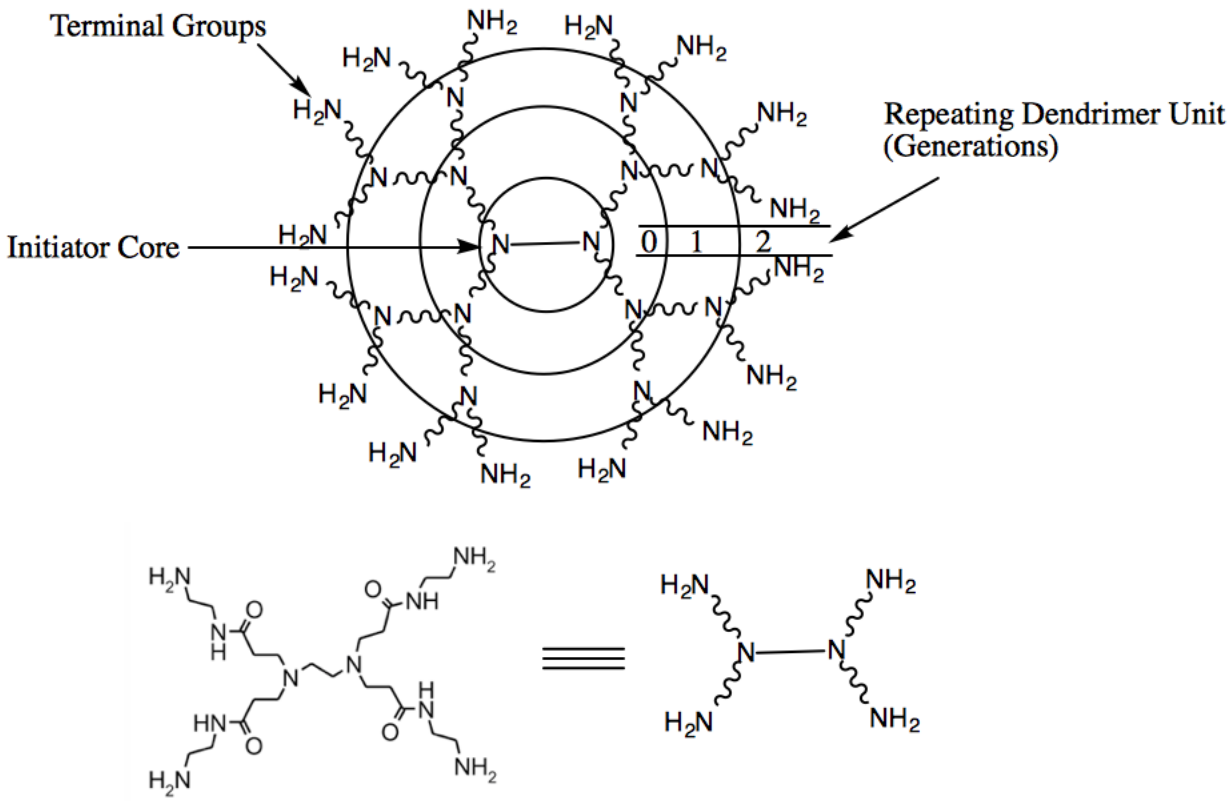

Figure 2.3 Schematic diagram of a poly(amidoamine) dendrimer. This is a second-generation dendrimer.[35]

PAMAM dendrimers (Figure 2.3) were first synthesized in 1985 by Smith et al. and since then have been studied extensively.[36] PAMAM dendrimers were the first dendrimer family to be commercialized; and it exhibits greater compatibility of surface amines and interior amide bonds than other dendrimer families.[37] Simple PAMAM dendrimers have shown penetration capability to a wide range of cell lines, and an additional targeting ligands at the terminal ends are required for the selectivity of penetration of cell types. This property of PAMAM makes them very useful compounds for drug delivery at various generations. A disadvantage is that of cell lysis and death can be caused by increasing the molecular weight of and surface charge of PAMAM dendrimer resulting in an increase of cytotoxic behavior.[38-43]

Other studies have shown that mediating the positive charge on PAMAM dendrimer surfaces decreases their cytotoxicity. This suggests a potential for DNA transfection applications.[44,45-47] Our interest in this compound is to see the effect the length of polyamine branches in the dendrimer on IRI activity.

The objective of this project was to synthesize PAMAM dendrimer and make different derivatives by coupling sugars and other molecules to the terminal ends of the dendrimer and to test all molecules for IRI activity

References

1. Baust, J.G.; Gao, D.; Baust, Cryopreservation: An emerging paradigm change. J.M. *Organogenesis.* **2009**, *5*, 90-96.

2. Bakhach, The cryopreservation of composite tissues - Principles and recent advancement on cryopreservation of different type of tissues. J. *Organogenesis.* **2009**, *5*, 119-126.

3. Scott, K.L.; Lecak. Biopreservation of red blood cells: past, present, and future. J.; Acker, J.P. *Transfus. Med. Rev.* **2005**, *19*, 127-142.
4. Fowler, A.; Toner, M. Cryo-injury and biopreservation. Ann. N.Y. Acad. Sci. **2005**, *1066*, 119-135.

5. Hunt, C.J. Cryopreservation of Human Stem Cells for Clinical Application: A Review. Transfus. Med. Hemoth. **2011**, 38, 107-123

6. Yang, H.; Acker, J.P.; Hannon, J.; Miszta-Lane, H.; Akabutu, J.J.; McGann, L.E. Damage and protection of UC blood cells during cryopreservation. *Cytotherapy.* **2001**, *3*, 377-386.

7. Kanias, T.; Acker, J.P. Biopreservation of red blood cells – the struggle with hemoglobin oxidation. *FEBS J.* **2010**, *277*, 343-356.

8. Valeri, C.R.; Ragno, G. An approach to prevent the severe adverse events associated with transfusion of FDA-approved blood products. Transfusion Apheresis Sci. **2006**, *34*, 271-287. 9.

9. Mazur, P. Freezing of living cells: mechanisms and implications. Am. J. Physiol. - Cell Physiol. **1984**, *247*, C125-C142.

10. Meryman, H.T. Cryopreservation of living cells: principles and practice. Transfusion. **2007**, *47*, 935-945.

11. Mazur, P. Life in the Frozen State - Principles of Cryobiology (Boca Baton, FL: CRC Press; **2004**.

12. Mazur, P. *Principles of cryobiology*. 2004. CRC Press LLC.

13. Holovati, J.L.; Hannon, J.L.; Gyongyossy-Issa, M.I.C.; Acker, J.P. Blood preservation workshop: new and emerging trends in research and clinical practice. *Transfus. Med. Rev.* **2009**,*23*, 25-41.

14. Berz, D.; McCormack, E.M.; Winer, E.S.; Colvin, G.A.; Quesenberry, P.J. Cryopreservation of hematopoietic stem cells. *Am. J. Hematol.* **2007**, *82*, 463-472.

15. Galmes, A.; Gutiérrez, A.; Sampol, A.; Canaro, M.; Morey, M.; Iglesias, J.; Matamoros, N.; Duran, M.A.; Novo, A.; Bea, M.D.; Galán, P.; Balansat, J.; Martínez, J.; Bargay, J.; Besalduch, J. Long-Term Hematologic Reconstitution And Clinical Evaluation Of Autologous Peripheral Blood Stem Cell Transplantation After Cryopreservation Of Cells With 5% And 10% Dimethylsulfoxide At −80°C In A Mechanical Freezer. *Haematologica.* **2007**, *92*, 986-989.

16. Hess, J.R. Red cell freezing and its impact on the supply chain. *Transfus. Med.* **2004**, *14*, 1-8.

17. Valeri, C.R.; Ragno, G.; Pivacek, L.E.; Srey, R.; Hess, J.R.; Lippert, L.E.; Mettille, F.; Fahie, R.; O'Neill, E.M.; Szymanski, I.O. A multicenter study of in vitro and in vivo values in human RBCs frozen with 40-percent (wt/vol) glycerol and stored after deglycerolization for 15 days at 4 degrees C in AS-3: assessment of RBC processing in the ACP 215. *Transfusion.* **2001**, *41*, 933-939.

18. Acker, J.P.; McGann, L.E. IInnocuous Intracellular Ice Improves Survival of Frozen Cells. *Cell Transplant.* **2002**, *11*, 563-571.

19. Garner, J.; Harding, M.M. Design and synthesis of antifreeze glycoproteins and mimics. *ChemBioChem.* **2010**, *11*, 2489-2498.

20. Harding, M.M.; Anderberg, P.I.; Haymet, A.D.J. Antifreez glucoproteins from polar fish. *Eur. J. Biochem.* **2003**, *270*, 1381-1392.

21. Harding, M.M.; Ward, L.G.; Haymet, A.D.J. Type I antifreeze proteins., structure-activity studies and mechanisms of ice growth inhibition. *Eur. J. Biochem.* **1999**, *264*, 653-665.

22. Pudney, P.D.A.; Buckley, S.L.; Sidebottom, C.M.; Twigg, S.N.; Sevilla, M.-P.; Holt, C.B.; Roper, D.; Telford, J.H.; McArthur, A.J.; Lillford, P.J. The physico-chemical characterization of a boiling stable antifreeze protein from perennial grass (*Lolium perenne*). *Arch. Biochem. Biophys.* **2003**, *410*, 238- 245.

23. Jia, Z.; Davies, P.L. Antifreeze proteins: an unusual receptor-ligand interaction. *Trends Biochem. Sci.* **2002**, *27*, 101-106.

24. Yu, S.O.; Brown, A.; Middleton, A.J.; Tomczak, M.M.; Walker, V.K.; Davies, P.L. Ice restructuring inhibition activities in antifreeze proteins with distinct differences in thermal hysteresis. *Cryobiology.* **2010**, *61*, 327-334.

25. Chao, H.; Davies, P.L.; Carpenter, J.F. Effects of antifreeze proteins on red blood cell survival during cryopreservation. *J. Exp. Biol.* **1996**, *199*, 2071-2076.

26. Wang, T.; Zhu, Q.; Yang, X.; Layne, J.R.J.; DeVries, A.L. Antifreeze

glycoproteins from antarctic notothenioid fishes fail to protect the rat cardiac explant during hypothermic and freezing preservation. *Cryobiology.* **1994**, *31*, 185-192.

27. Mugnano J.A., Wang T., Layne J.R.Jr, De Vries A.L., Lee R.E.. Antifreeze glycoproteins promote lethal intracellular freezing of rat cardiomyocytes at high subzero temperatures, Cryobiology, **1995**, 32, 556-557.

28. Rubinsky, B.; Arav, A.; DeVries, A.L. The cryoprotective effect of antifreeze glycopeptides from antarctic fishes. *Cryobiology.* **1992**, *29*, 69-79.

29. Tam R.Y.; Ferreira, S. S.; Czechura, P.; Chaytor, J. L.; Ben, R. N., Hydration index--a better parameter for explaining small molecule hydration in inhibition of ice recrystallization. J. Am. Chem. Soc. **2008**, 130, 17494–17501.

30. Czechura, P.; Tam, R.Y.; Dimitrijevic, E; Murphy, A.V; Ben, R. N., The Importance of Hydration for Inhibiting Ice Recrystallization with C-Linked Antifreeze Glycoproteins. J. Am. Chem. Soc., **2008**, 130 (10) 2928-2929.

31. Ferreira, S. S., M. Sc. Dissertation, University of Ottawa, **2009**

32. Chaytor, J. L., Ph.D. Dissertation, University of Ottawa, **2010**

33. Czechura, P.; Tam, R. Y.; Dimitrijevic, E.; Murphy, A. V.; Ben, R. N. The Importance of Hydration for Inhibiting Ice Recrystallization with C-Linked Antifreeze Glycoproteins. *Journal of American Chemical Society,* **2008,** *130,* 2928.

34. Liu, D., Wyttenbach, T., Bowers, M. T., Hydration of protonated primary amines: effects of intermolecular and intramolecular hydrogen bonds. International Journal of Mass spectrometry, **2004**, 236, 81-90.

35. Peterson, J., Allikmaa, V., Subbi, J., Pehk, T., Lopp, M., Structural deviations in poly(amidoamine) dendrimers: a MALDI-TOF MS analysis. *Eur. Plym.* **2003**, 39, 33-42.

36. Tomalia, D. A., Baker, H., Dewald, J., Hall, M., Kallos, G., Martin, S., Roeck, J., Ryder, J., Smith, P. A New Class of Polymers: Starburst-Dendritic Macromolecules. *Polymer Journal*, **1985** 17, 117–32.

37. Esfand, Roseita., Tomalia, Donald A. Poly(amidoamine) (PAMAM) dendrimers: from biomimicry to drug delivery and biomedical applications. *Drug Discovery Today* 2001, 6 (8), 427–436.

38. Fischer, D., Li, Y., Ahlemeyer, B., Krieglstein, J., Kissel, T. In vitro cytotoxicity testing of polycations: influence of polymer structure on cell viability and hemolysis. *Biomaterials* **2003**, 24 (7), 1121–31.
39. Roberts, C., Bhalgat, K., Zera, T. Preliminary biological evaluation of polyamidoamine (PAMAM) StarburstTM dendrimers. *Journal of Biomedical Materials Research* **1996**, 30 (1), 53–65.

40. Malik, N., Wiwattanapatapee, R, Klopsch, R., Lorenz, K., Frey, H. Weener, J.W., Meijer, E.W., Paulus, W., Duncan, R. Dendrimers: relationship between structure and biocompatibility in vitro, and preliminary studies on the biodistribution of 125I-labelled polyamidoamine dendrimers in vivo. *Journal of Controlled Release* **2000**, 65 (1–2): 133–48.

41. Mukherjee, S., Davoren, M., Byrne, J. In vitro mammalian cytotoxicological study of PAMAM dendrimers - towards quantitative structure activity relationships. *Toxicology in Vitro* **2010**, 24 (1), 169–77.

42. Mukherjee, P., Lyng, M., Garcia, A., Davoren, M., Byrne, J. Mechanistic studies of in vitro cytotoxicity of poly(amidoamine) dendrimers in mammalian cells. *Toxicology and Applied Pharmacology* **2010**, 248 (3): 259–68.

43. Mukherjee, P., Byrne, J. Polyamidoamine dendrimer nanoparticle cytotoxicity, oxidative stress, caspase activation and inflammatory response: Experimental observation and numerical simulation. *Nanomedicine: Nanotechnology, Biology and Medicine* **2013**, 9 (2), 202–11.

44. Haensler, J., Szoka Jr, C. Polyamidoamine cascade polymers mediate efficient transfection of cells in culture. *Bioconjugate Chemistry* **1993**, 4(5): 372–9.

45. Bielinska, A., Kukowska-Latallo, JF., Johnson, J., Tomalia, DA., Baker Jr, Regulation of in vitro gene expression using antisense oligonucleotides or antisense expression plasmids transfected using starburst PAMAM dendrimers. J. *Nucleic Acids Research* **1996**, 24 (11), 2176–82.

46. Kukowska-Latallo, J. F., Bielinska, A. U., Johnson, J., Spindler, R., Tomalia, D. A., Baker, J. R. Kukowska-Latallo, J. F., Bielinska, A. U., Johnson, J., Spindler, R., Tomalia, D. A. & Baker, J. R. Efficient transfer of genetic material into mammalian cells using starburst polyamidoamine dendrimers. Proc. Natl Acad. Sci. USA 93, 4897-4902. *Proceedings of the National Academy of Sciences* **1996**, 93 (10), 4897–902

47. Bielinska, U., Chen, C., Johnson, J., Baker Jr, R. DNA Complexing with Polyamidoamine Dendrimers: Implications for Transfection. *Bioconjugate Chemistry* **1999**, 10 (5), 843–50.

Chapter 3: Results and Discussion

3.1 IRI activity of amine derivatives

In recent years, there has been much interest in the rational design of ice recrystallization inhibitors (IRIs) that can prevent cell damage during cryopreservation.[1-3] Dimethyl sulfoxide (DMSO) and glycerol have been used as cryoprotectants since the 1950's despite their significant cytotoxicity and low cell recovery post-cryopreservation.[4-6] Naturally occurring biological anti-freezes[7-9] have also been considered as cryoprotectants along with polyvinyl alcohol (PVA),[2] polylysilanes[10] and other anti-ice nucleating agents (anti-INAs).[11,12] These compounds have yet to demonstrate the high post-thaw viabilities typical of DMSO.

Anti-INAs are compounds that have been used to protect plants from frost injury, which is caused by ice nucleation active bacteria.[13] Most anti-INAs are peptides, but small molecules such as lysine based surfactants and dialkyldimethylammonium salts have been reported as having anti-INA activity. Quaternary ammonium salts **22-24** (Figure 3.1), because they have anti-INA activity, have also been examined for their ability to inhibit ice recrystallization (Graph 3.1).[14] A 0.5 mg mL^{-1} NaCl solution was used rather than PBS solution because the compounds were more soluble in the NaCl solution. The use of 0.5 mg mL^{-1} solution is very effective in excluding false-positive recrystallization effects.[15] The 0.5 mg mL^{-1} NaCl solution has similar physiological properties as PBS.

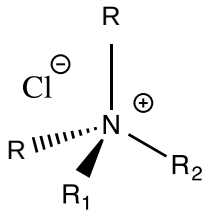

	R_1	R_2
22	Bn	$C_{16}H_{33}$
23	CH_3	$C_{10}H_{21}$
24	CH_3	$C_{16}H_{33}$

Figure 3.1 Structure of anti-INA.[14]

Lysine-based cationic surfactants **25-30** (Figure 3.2) have also been tested as anti-INAs with the potential to protect crops against cryo-injury. These molecules failed to inhibit ice nucleation.[13] The IRI activity of molecules **22-30** in 0.5% NaCl solution, as discussed previously, are listed in Graph 3.1.[14]

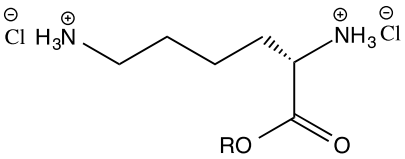

R =

(**25**) Bn n-(**28**) $C_{16}H_{33}$
(**26**) CH_3 n- (**29**) $C_{10}H_{21}$
(**27**) C_2H_5 n- (**30**) $C_{16}H_{33}$

Figure 3.2 Structure of anti-INA, Lysine-based cationic surfactants.[14]

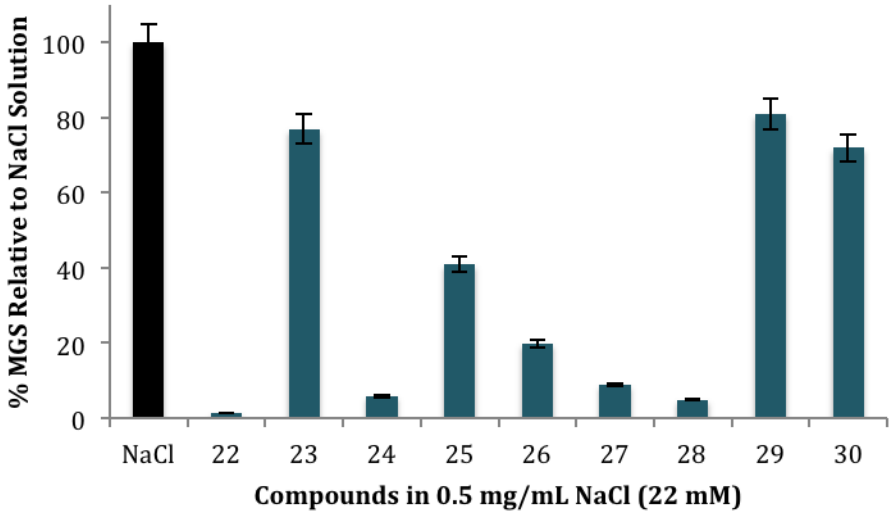

Graph 3.1 IRI activities of cationic anti-INAs in NaCl standard solution.

3.2 The effect of increasing hydrophobic character on the IRI activity

There are few studies that have been published that connect hydrophobicity to ice recrystallization inhibition (IRI). Since TH and IRI operate via separate mechanisms,[16,17] hydrophobic interactions may not necessarily be a factor for IRI activity. As such, separate studies have been performed by our laboratory to address the influence of hydrophobic moieties on IRI activity.

3.2.1 Fluorinated molecules hydrophobicity and IRI activity

The fluorinated AFGP analogue (**31**) has been synthesized by Chaytor et al. and tested its IRI activity. The IRI activity then was compared with that of $[C\text{-}(OGG)\text{-}Gal]_4$ and AFGP 8 (**1**).[18,19] Also, to examine the effect of pseudo-hydrophobic moiety of IRI ability, a fluorinated galactose derivative (**32**) was synthesized and compared to galactose (Figure 3.3). The addition of the fluorine group was found to decrease the IRI activity of the compound. This result was rationalized by the increasing hydrophobic character of the fluorinated moiety. As mentioned in previous chapters, a more potent inhibitor of ice recrystallization is the one that better disrupt the layer of bulk water surrounding the molecule.[16] Very similar to hydrocarbons, fluorine atoms have been shown to facilitate the ordering of water molecules, which will facilitate ice recrystallization by allowing the transfer of water molecules into the ice lattice.[20] This shows that the hydrophobic interactions of fluorine in the molecule have a negative effect on ice recrystallization inhibition.

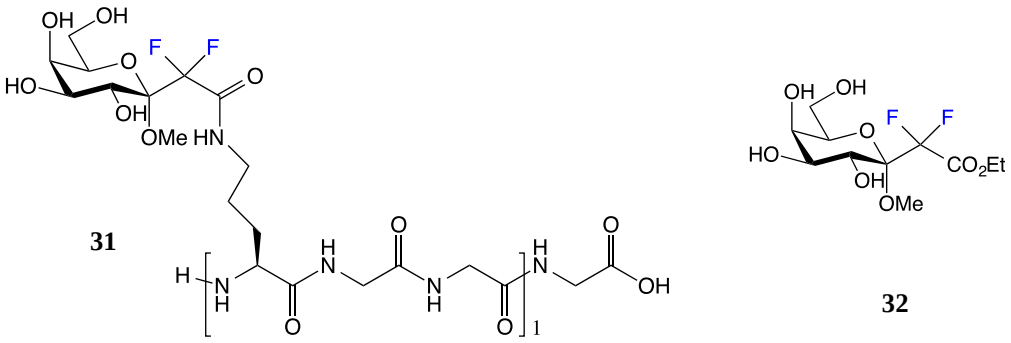

Figure 3.3 Fluorinated C-AFGP analogue (31) and galactose analogue (32).[18,19]

3.2.2 Effect of aromatization on IRI activity

It has been established that compounds with greater degree of hydration would display more potent IRI activity. This phenomenon occurs due to greater discrepancy in the three-

dimensional network of the surrounding water molecules.[21] Our laboratory has investigated the IRI activity of different O-aryl glycoside analogues and found that some of them are very potent inhibitors of ice recrystallization.[22] This has opened the door for further investigations of the relationship between IRI and the nature of the aromatic group, including substitution patterns.

Our group carried out a study to examine the effect of differentsubstituents on the aryl groups in O-aryl derivatives of galactose and glucose. The initial study was done by Trant who examined a series of para substituted aryl galactosides (**33-45**).[23] In comparison to aryl galactosides, Capicciotti and Mancini have synthesized and tested for IRI activity the corresponding aryl glucosides (**46-58**) and found that some of them are more active than their galactose-based analogues.[22]

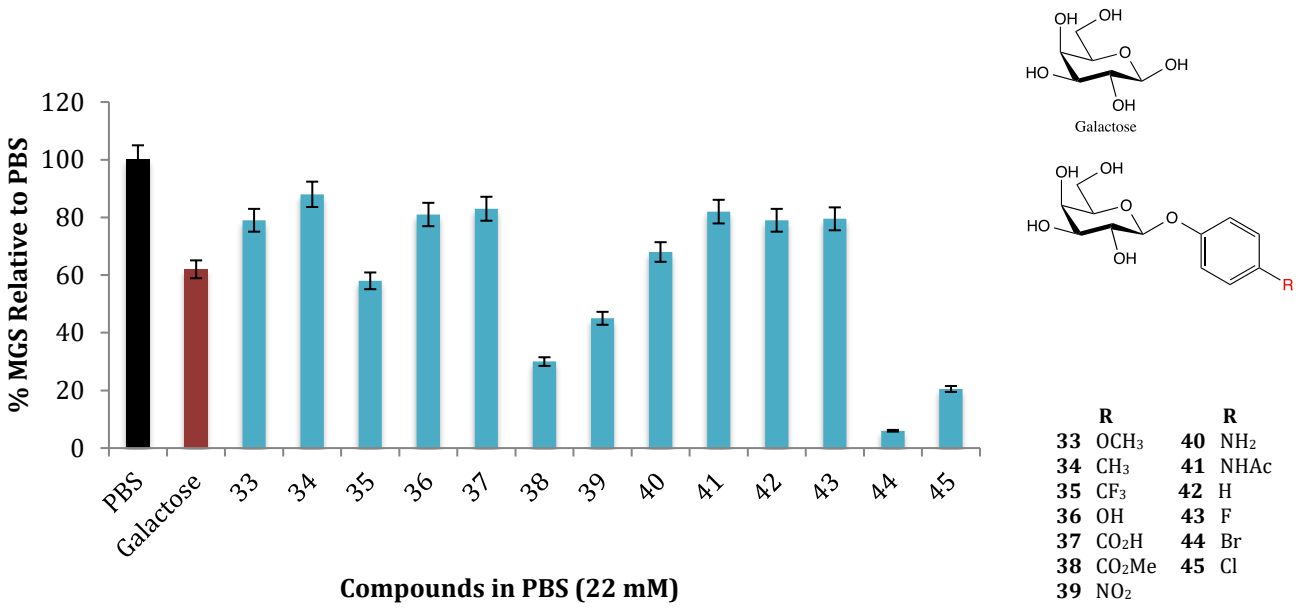

Graph 3.2 IRI activity of previously synthesized aryl galactosides (**33-45**).

It was hypothesized that hydrogen bonding ability of the anomeric oxygen with the surrounding water molecules may be one of the factors that contribute to the IRI activity of carbohydrates.[22,23] If this hypothesis was to be true, then one be expected to find electron-donating groups on the aryl ring. This is because the electron-donating group would increase the density of the anomeric oxygen allowing it to form stronger hydrogen bonds. The presence of an electron-withdrawing group on the aromatic ring will be predicted to have an opposite impact on the IRI activity.

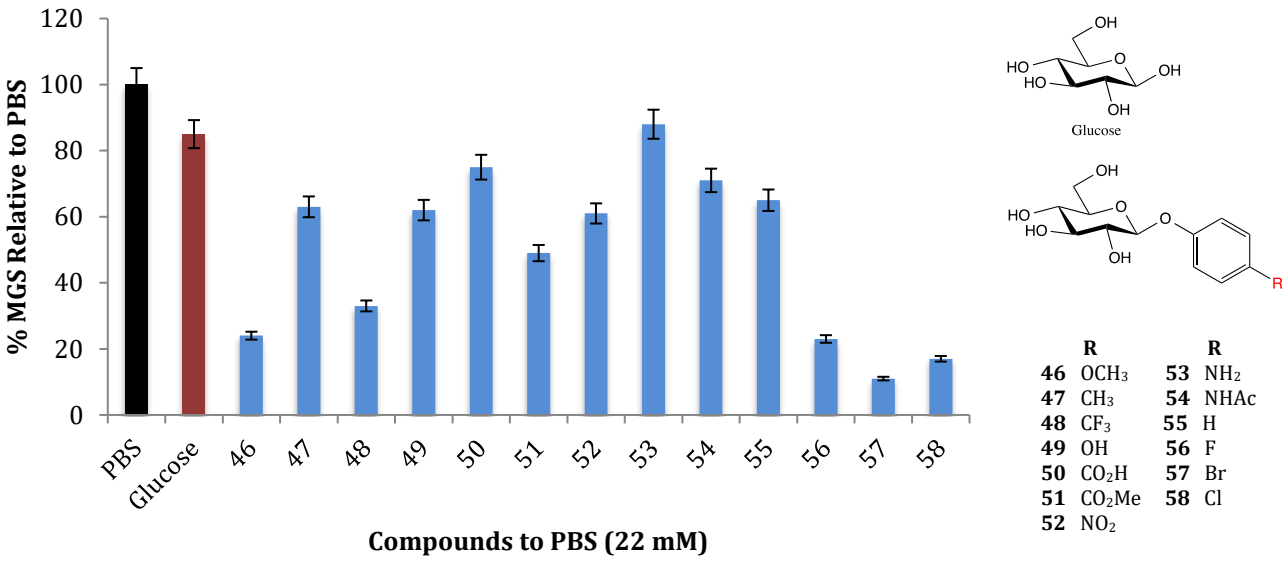

Graph 3.3 IRI activity of previously synthesized aryl glucosides (**46-58**).

The IRI activity results obtained from the Ben lab do not support the above hypothesis, and there is no clear trend when compared with the first generation of aryl glycosides synthesized. Thus, it cannot be concluded that an increase in electron density of the aryl ring at the anomeric oxygen will provide an increase in IRI activity of the aryl glycoside. Also, there is no correlation in IRI activity based only on the electronic properties of the aryl ring, since both electron-donating and electron-withdrawing groups have similar

potent IRI activities. These results and observations show that the hydrogen bonding ability of the anomeric oxygen is not an important factor for IRI activity.

These results led to further investigation for IRI activity of aryl molecules with different functional groups and amino cyclohexane molecules.

3.2.3 IRI activity of aminocyclohexane and their derivatives

The shape of the six-membered ring in cyclohexane derivatives is very similar to that of glycosides, where the only difference between them is the presence of oxygen in the ring for glycoside. I have examined several cyclohexane structures that contain one or two amino group (**59-64)** as shown in (Figure 3.4). The IRI activity results obtained from these molecules are very comparable and relative to glucose and galactose previously discussed. The chair shape of cyclohexane is identical to that of glucose and galactose, except for the oxygen atom in the six-membered ring in the two sugar molecules. The stability of the chair conformation and the electron donating/accepting groups present play an important role in giving the molecule a RI property.

The RI activity of various cyclohexyl amines is very similar independent of the location of the amine substituents on the cyclohexane ring. All of these compounds are more active in the IRI assay than glucose and galactose (Graph 3.4). The proposed reason for having better RI activity is the lower number of electronegative atoms, one or two nitrogen atoms for **59-64** vs six oxygens, one bonded to each of the five carbon atoms and one within the cycle for the carbohydrate molecules.

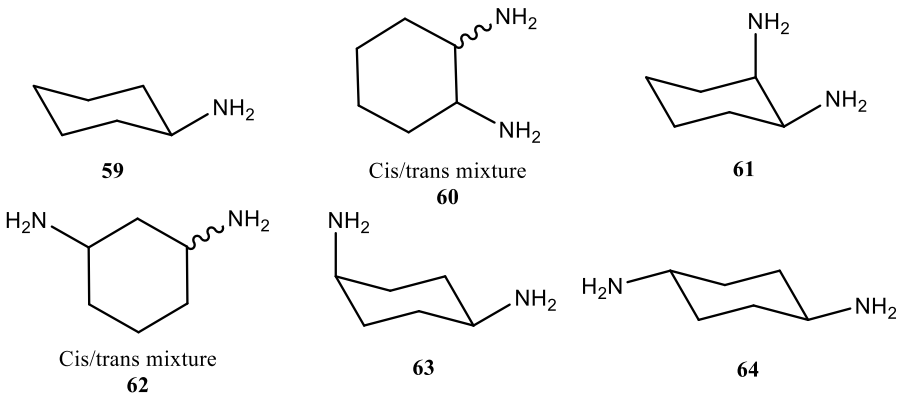

Figure 3.4 Amino cyclohexane structures tested for IRI activity.

Trans-1,4-dibenzoylaminocyclohexane (**65**) was synthesized but could not be evaluated since it was not soluble in PBS or NaCl solutions (Figure 3.5). In retrospect, we should have prepared diacetates, since such compounds might be expected to be more soluble in the PBS medium than **65**. Time constraints did not allow this to occur.

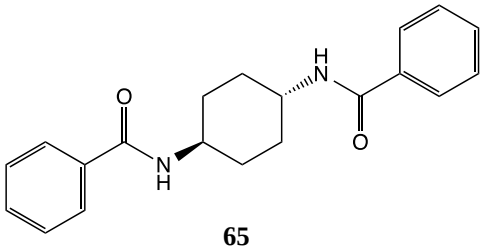

65

Figure 3.5 Structure of trans-1,4-dibenzoylaminocyclohexane

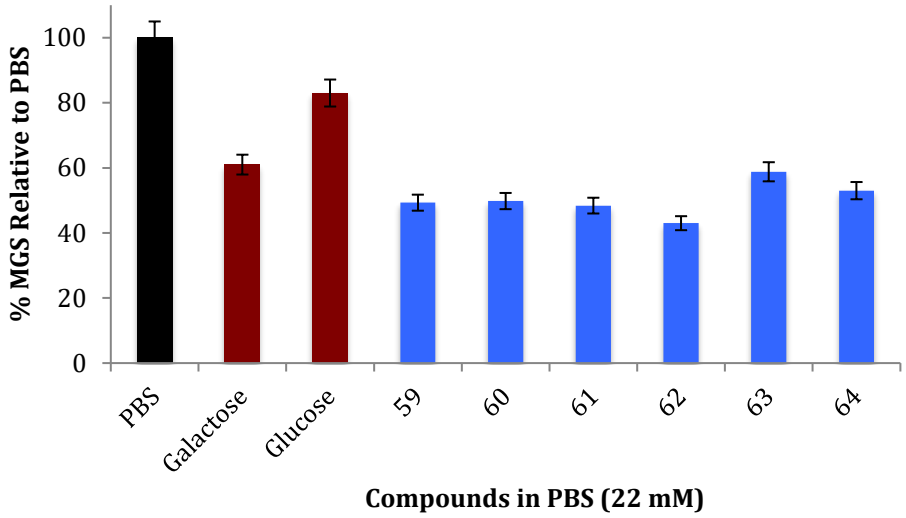

Graph 3.4 IRI activities of amino cyclohexane molecules **59-64** compared with glucose and galactose.

3.2.4 IRI activity of aromatic amines.

As was observed in previous sections, the nature of substituents on the aryl ring of aryl glycosides results in compounds with different IRI activity. There is, however, little information about the activity of aromatic molecules that are not linked to glycosides. I have examined a number of anilines, benzyl amines and aryl hydrazines compounds with a variety of substituents at different positions (*ortho*, *meta*, and *para*) for IRI activity. Some of them show very interesting results when compared to aryl glycosides structures. Testing for IRI activity was carried out on benzene derivatives carrying amine ($-NH_2$), hydrazine ($-N_2H_3$), hydroxyl (-OH), methylamine ($-NHCH_3$), methoxy ($-OCH_3$), fluorine (-F) and bromine (-Br), or a combination of these groups (**66-74**).

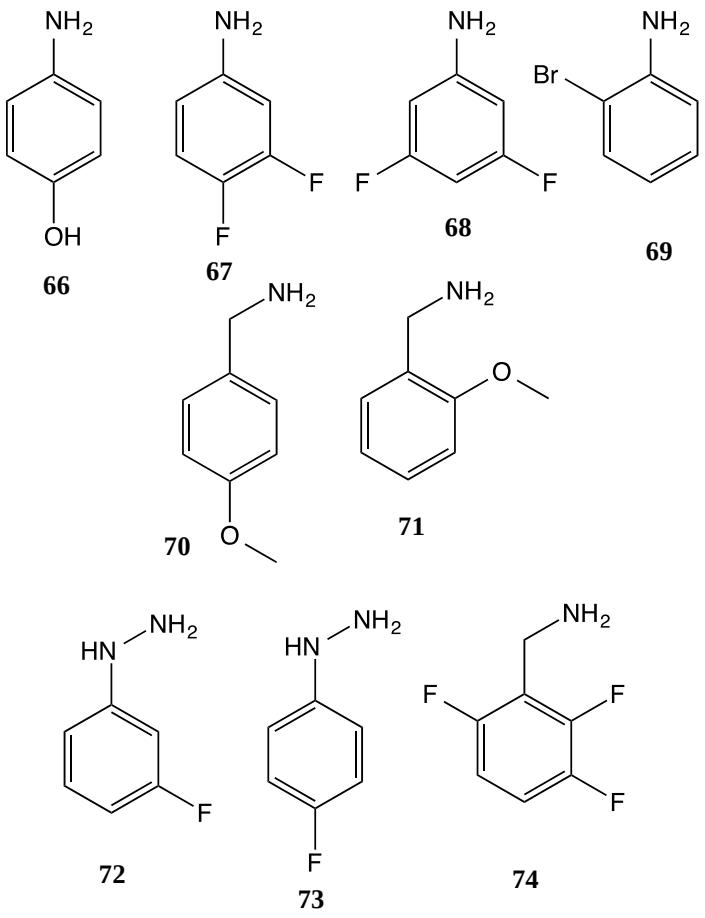

Figure 3.6 Structures of different aromatic molecules with diverse groups (**66-74**).

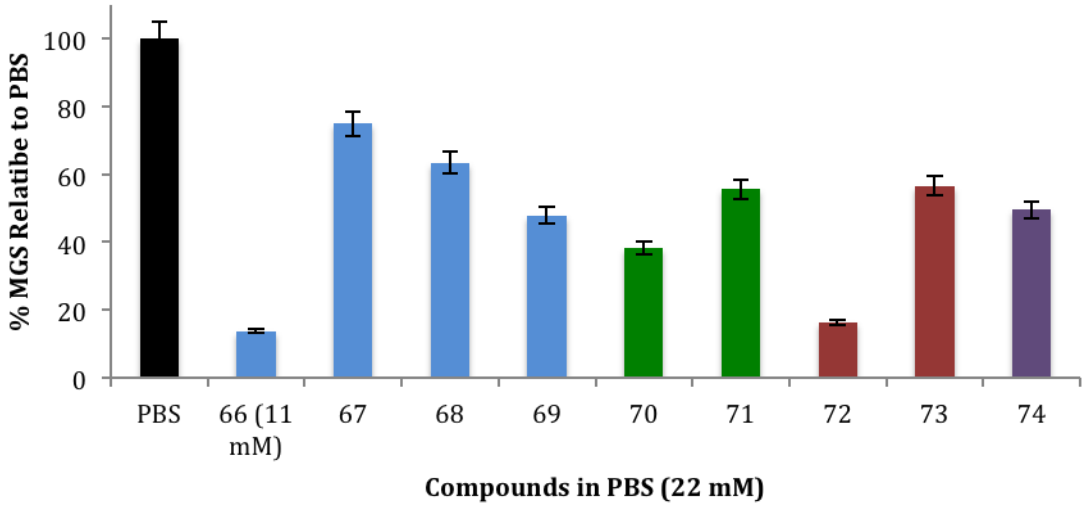

Graph 3.5 IRI activities of compounds (**66-74)** as shown in Figure 3.6.

Looking at the results above, *p*-aminophenol (**66**) has the highest IRI activity over all other compounds tested. The concentration of **66** is 11 mM rather than 22 mM because at higher concentrations the crystals of the compound in PBS were very small and could not be analyzed, but at lower concentrations it was possible to analyze the data. Replacing the alcohol group in **66** with a halogen decreased the IRI activity as shown in compounds **67-69** (Graph 3.5). A possible reason that could explain this is the ability of the hydroxyl group to donate a hydrogen bond as well as accepting them. Even though 4-aminophenol is a reasonable good IRI it would likely not be developed because it is considered a minor nephrotoxic metabolite of phenacetin and acetaminophen (paracetamol) in man. 4-Aminophenol can undergo autoxidations and metal-catalyzed and enzymatic oxidations in man to produce reactive oxygen species.

The insertion of a carbon between the amine and the aromatic ring, and replacing the hydroxyl group with a methoxy group, has a negative effect on the IRI activity as shown for compounds **70** and **71** (Figure 3.6). These changes make the molecule non-planar because the amine group and the carbon of the methoxy group are now pointing out of the plane of the molecule. Compound **72** shows surprisingly high IRI activity compared to compounds **67, 68,** and **73**. Changing the position of fluorine from *meta*- to *para*- (**73**) decreased the IRI activity; on the other hand, compound **74** has fluorine on the o*rtho*-positions and a *meta*- position, which did not affect the IRI activity a lot compared to compounds **70-72** (Figure 3.6).

Another reason for the difference in IRI activity is that aromatic amines are much less basic than aliphatic amines and as such make weaker hydrogen bonds than the aliphatic amines such as the aminocylohexanes. This will play a role in the order of water molecules

around compound, which will result in differences in IRI activity. Also, another difference is that the benzene ring is a flat π-electron system and cyclohexane is a saturated hydrocarbon existing in a chair conformation.

3.3 Synthesis of Dendrimers and Assessment of Their Ability to Inhibit Ice Recrystallization

Poly(amidoamine) (PAMAM) dendrimers are considered the first complete dendrimer family to be synthesized, characterized and commercialized. Due to these facts, they are recognized as a unique new class of synthetic nanostructures. Dendrimers allow the precise control of size, shape and placement of functional groups that is desirable for many applications.[24]

PAMAM is less toxic than other related dendrimers. It exhibits minimal cytotoxicity across multiple toxicity screens, including tests of metabolic activity, cell breakdown, and nucleus morphology. Due to the different sensitivities of the various cell lines, PAMAM toxicity can increase or decrease, yet, it remains less toxic than other dendrimer families' overall.[25]

3.3.1 Synthesis of PAMAM Dendrimer

A mixture of ethylene diamine (EDA) in methanol was cooled down to 0°C. Then methyl acrylate was added drop wise with 10% excess. After the addition of methyl acrylate, the reaction was warmed up to room temperature and stirred for six days to obtain G -0.5 (multiester). The system was under inert conditions.

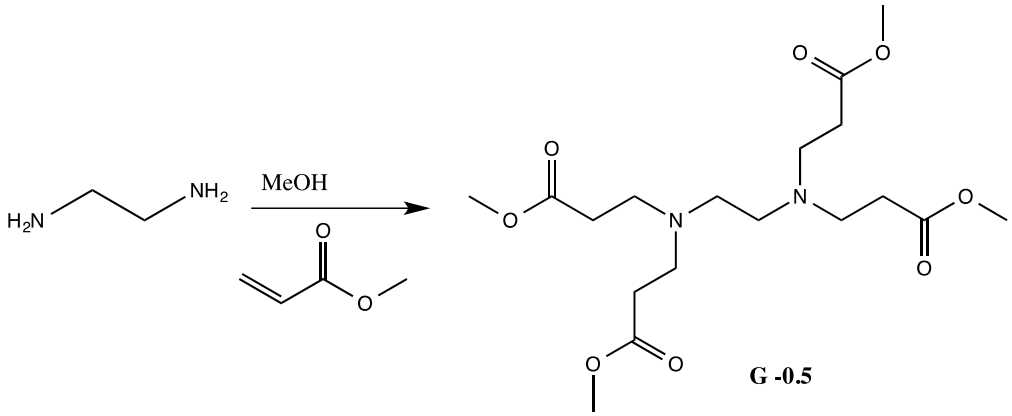

Scheme 3.1 Synthesis of generation -0.5 (multiester) of PAMAM dendrimer (**75**).

The following step is to synthesize generation 0 of PAMAM dendrimer. G -0.5 was dissolved in methanol and cooled down to -30°C under inert conditions. In a separate flask, EDA was also dissolved in methanol under inert conditions. Then the multi-ester solution was gradually added to EDA solution at a temperature below -25°C. After addition, the reaction mixture was warmed up to room temperature and left to stir for 168h to obtain generation 0 (G0) of PAMAM dendrimer. Both generations are symmetric, meaning that in NMR, the number of carbons will only be counted once. The proton NMR spectrum shows some impurities (i.e. methanol and methyl ester) that did not evaporate after leaving it for several hours under high vacuum. These impurities as evidenced by the having extra peaks in the NMR increased the weight of the final product resulting in a "yield" above 100%. Other characterizations such as MS and GC helped identify the structure of the product.

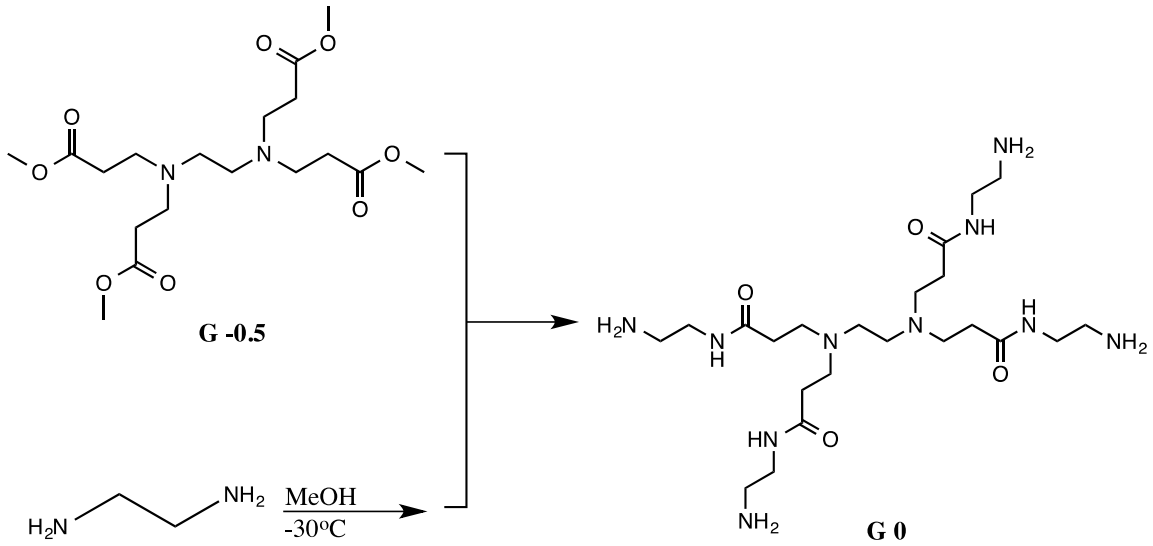

Scheme 3.2 Synthesis of generation zero (**G0**) of PAMAM dendrimer (**76**).

EDA, G -0.5 and G0 dendrimers were tested for IRI activity. The results show that by increasing the size of the dendrimer, the IRI activity increases but by a very small extent (Graph 3.6).

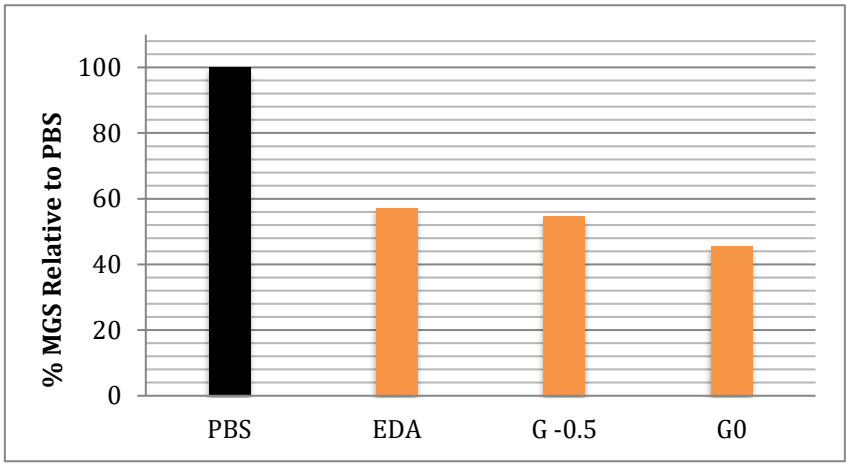

Graph 3.6 IRI activity of EDA and the two different stages of the PAMAM dendrimer.

The results are very similar to those shown previously for compounds **59-64**. The presence of one amine group will increase the IRI activity and if more amino groups are added, the results will not be changed significantly.

3.3.2 Coupling of PAMAM with OGG

One of the first antifreeze glycoprotein (AFGP) analogues reported to have IRI activity while lacking TH activity was OGG-Gal (Figure 3.8). AFGPs are found in Antarctic notothenioids and Arctic cod, as mentioned in chapter 1. There are eight classes of AFGP 1-8, based on their size (2.6 – 33.7 kDa). AFGPs consist of a tripeptide repeat of Ala-Ala-Thr, where the secondary hydroxyl group of threonine is glycosylated with a β-D-galactosyl-(1,3)-α-*N*-acetyl-D-galactosamine disaccharide.[26, 27]

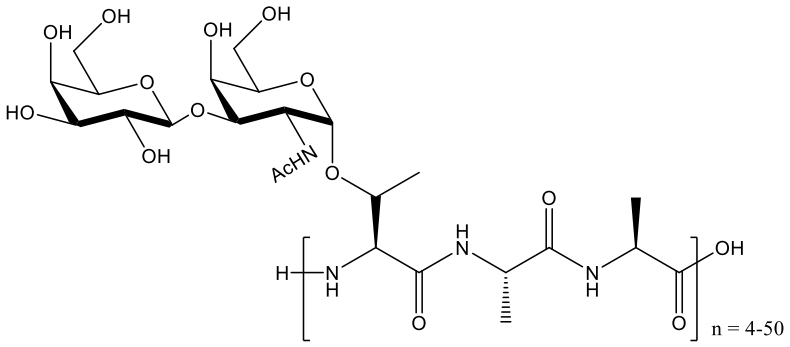

Figure 3.7 General structure of AFGPs.

OGG-Gal is a carbon-l inked (*C* linked) derivative containing a galactosyl moiety coupled to the γ-amine of ornithine in the tripeptide repeats. It possesses high IRI activity at micromolar concentrations, but unlike AFGP-8, it does not exhibit any significant TH activity (Figure 3.8).[1,2(chapter 3)] OGG-Gal is not amenable to the large-scale synthesis required to produce sufficient quantities for applications in cryopreservation, thus, it was subsequently truncated to determine the smallest possible subunit exhibiting potent IRI activity.[28]

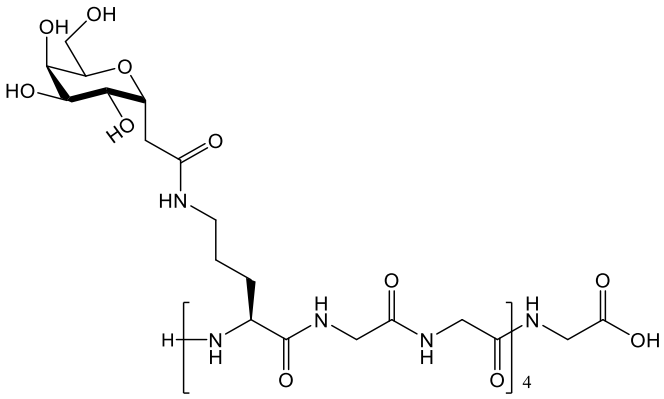

Figure 3.8 C-linked AFGP analogue, OGG-Gal

For example, the synthesis of the analogue **C-linked AFGP** involves first manipulation of the monosaccharide residue to obtain a *C*-linked carboxylic acid followed by glycosidation to the ε-amine of ornithine and subsequent solid phase peptide synthesis to obtain the final glycopeptide (Scheme 1.1).[191, 208] The glycosidated ornithine building block is obtained in yields ranging from 30-40% and the solid phase peptide synthesis provides a yield of approximately 20%. Therefore, **C-linked AFGP** is obtained in overall yields of 6-8%. Due to the low overall yield and lengthy synthesis, these molecules are not amenable for large-scale synthesis. [29-35]

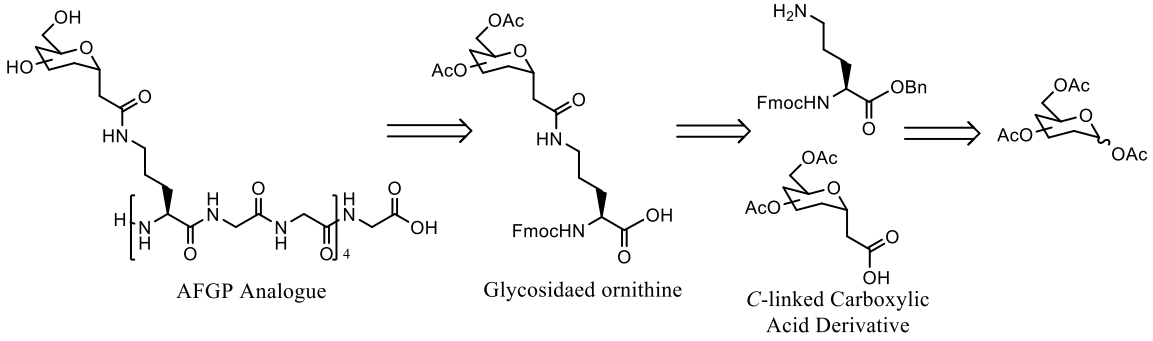

Scheme 3.3. Retrosynthetic scheme for synthesis of AFGP analogue.[29-35]

The synthesis of OGG-Gal started as shown in Scheme 3.3. Unfortunately, the work was not done due to conflicts, but during the process, synthesis of glycosidated ornithine was achieved. Also, coupling glycosidated ornithine to PAMAM dendrimer was done, but

the IRI testing was not performed. The starting material used to synthesize glycosidated ornithine are methyl-D-galactopyranoside monohydrate and Fmoc-Orn(Boc)-OH. The synthesis involved manipulation of the methyl-D-galactopyranoside monohydrate to obtain a carboxylic acid group on C-1 of the galactose molecule. Then the Fmoc-Orn(Boc)-OH was manipulated to make an ionic salt with TFA. The two compounds are then coupled together to give the final product, glycosidated ornithine.

References

1. J. G Garner and M. M. Harding, Design and Synthesis of Antifreeze Glycoproteins and Mimics. ChemBioChem, **2010**, 11, 2489. 2

2. M. I. Gibson, C. A. Barker, S. G. Spain, L. Albertin and N. R. Cameron, Inhibition of ice crystal growth by synthetic glycopolymers: implications for the rational design of antifreeze glycoprotein mimics. Biomacromolecules, **2009**, 10, 328.

3. R. Peltier, M. A. Brimble, J. M. Wojnar, D. E. Williams, C. W. Evans and A. L. DeVries, Synthesis and antifreeze activity of fish antifreeze glycoproteins and their analogues. Chem. Sci., **2010**, 1, 538.
4. G. M. Fahy, The relevance of cryoprotectant "toxicity" to cryobiology. Cryobiology, **1986**, 23, 1.

5. T. Konuma, J. Ooi, S. Takahashi, A. Tomonori, T. Tsukada, T. Kobayashi, S. Sato, S. S. K. Kato, Y. Ebihara, T. Nagamura- Inoue, K. Tsuji, A. Tojo and S. Asano, Cardiovascular toxicity of cryopreserved cord blood cell infusion. Bone Marrow Transplant., **2008**, 41, 861.

6. K. Liseth, J. F. Abrahamsen, S. Bjørsvik, K. Grøttebø and Ø. Bruserud. The viability of cryopreserved PBPC depends on the DMSO concentration and the concentration of nucleated cells in the graft. Cytotherapy, **2005**, 7, 328.

7. J. F. Carpenter and T. N. Hansen. Antifreeze protein modulates cell survival during cryopreservation: mediation through influence on ice crystal growth. Proc. Natl. Acad. Sci. U. S. A., **1992,** 89, 8953.

8. H. Chao, P.L. Daviesand J.F. Carpenter. Effects of antifreeze proteins on red blood cell survival during cryopreservation. J. Exp.Biol.,**1996**,199, 2071.

9. B. Rubinsky, A. Aravand A.L. DeVries. The Cryoprotective Effect of Antifreeze Glycopeptides from Antarctic Fishes. Cryobiology,**1992**,29,69.

10. K. Matsumura and S.-H. Hyon. Polyampholytes as low toxic efficient cryoprotective agents with antifreeze protein properties. Biomaterials, **2009**, 30, 4842.

11. T. Inada, T. Koyama, F. Goto and T. Seto. Inactivation of Ice Nucleating Activity of Silver Iodide by Antifreeze Proteins and Synthetic Polymers. J. Phys. Chem. B, **2012**, 116, 5364.

12. T. Inada, T. Koyama, F. Goto and T. Seto. Ice Nucleation in Emulsified Aqueous Solutions of Antifreeze Protein Type III and Poly(vinyl alcohol). J. Phys. Chem. B, **2011**, 115, 7914.

13. M. Watanabe, T. Makino, K. Okada, M. Hara, S. Watabe and S. Arai.

Alkylbenzyldimethylammonium salt as inhibitors for the ice nucleating activity of *Erwinia ananas*. Agric. Biol. Chem., **1988**, 52, 201.

14. A. Balcerzak, M. Febbraro, R. Ben. The importance of hydrophobic moieties in ice recrystallization inhibitors. The Royal Society of Chemistry, **2013**, 3, 3232-3236.

15. C. A. Knight, D. Wen and R. A. Laursen. Nonequilibrium antifreeze peptides and the recrystallization of ice. Cryobiology, **1995**, 32, 23.

16. Tam R.Y.; Ferreira, S. S.; Czechura, P.; Chaytor, J. L.; Ben, R. N., Hydration index--a better parameter for explaining small molecule hydration in inhibition of ice recrystallization. J. Am. Chem. Soc. **2008**, 130, 17494–17501.

17. Czechura, P.; Tam, R.Y.; Dimitrijevic, E; Murphy, A.V; Ben, R. N., The Importance of Hydration for Inhibiting Ice Recrystallization with C-Linked Antifreeze Glycoproteins. J. Am. Chem. Soc., **2008**, 130 (10) 2928-2929.

18. Chaytor, J. L.; Ben, R. N., Bioorg. Assessing the ability of a short fluorinated antifreeze glycopeptide and a fluorinated carbohydrate derivative to inhibit ice recrystallization. Med. Chem. Lett. **2010**, 20, 5251-5254.

19. Chaytor, J. L., Ph.D. Dissertation, University of Ottawa, **2010**.

20. Biffinger, J. C.; Kim, H. W.; DiMagno, S. G.; The polar hydrophobicity of fluorinated compounds. ChemBioChem **2004**, 5, 622-627.

21. Tam, R. Y.; Ferreira, S. S.; Czechura, P.; Chaytor, J. L.; Ben, R. N., Hydration index--a better parameter for explaining small molecule hydration in inhibition of ice recrystallization. J. Am. Chem. Soc. **2008**, 130, 17494-17501.

22. C. Capicciotti, Ph.D. Dissertation, University of Ottawa, **2014.**

23. Trant, J. T.; Doshi, M.; Ben, R. N., unpublished results, **2010**.

24. Esfand, R. and Tomalia, D.A. Poly(amidoamine) (PAMAM) denrimers: from biomimicity to drug delivery and biomedical applications. **2001.** 6, 8, 427-436.

25. Fischer, Dagmar; Li, Youxin; Ahlemeyer, Barbara; Krieglstein, Josef; Kissel, Thomas. "In vitro cytotoxicity testing of polycations: Influence of polymer structure on cell viability and hemolysis". **2003.** *Biomaterials*. 24 (7): 1121–31.

26. Harding, M. M.; Anderberg, P. I.; Haymet, A. D. J. *Eur. J. Biochem.* 'Antifreeze' glycoproteins from polar fish. **2003**, *270* (7), 1381.

27. Garner, J.; Harding, M. M. *ChemBioChem.* Design and Synthesis of Antifreeze Glycoproteins and Mimics. **2010**, *11* (18), 2489.

28. Trant, J. F.; Biggs, R. A.; Capicciotti, C. J.; Ben, R. N. *RSC Adv.* Developing highly active small molecule ice recrystallization inhibitors based upon C-linked antifreeze glycoprotein analogues. **2013**, *3* (48), 26005.

29. Czechura, P.; Tam, R. Y.; Dimitrijevic, E.; Murphy, A. V; Ben, R. N. The Importance of Hydration for Inhibiting Ice Recrystallization with C-Linked Antifreeze Glycoproteins. J. Am. Chem. Soc. **2008**, 130 (10), 2928.

30. Abraham, S., Keillor, K., Capicciotti, C.J., Perley-Robertson, G.E., Keillor, J.W., Ben, R. N. Quantitative Analysis of the Efficacy and Potency of Novel Small Molecule Ice Recrystallization Inhibitors. Cryst. Growth Des. **2015**, 15 (10), 5034.

31. van der Wal, S.; Capicciotti, C. J.; Rontogianni, S.; Ben, R. N.; Liskamp, R. M. Synthesis and evaluation of linear CuAAC-oligomerized antifreeze neo-glycopeptides. J. Medchemcomm. **2014**, 5 (8), 1159.

32. Capicciotti, C. J.; Trant, J. F.; Leclère, M.; Ben, R. N. Synthesis of C-linked triazole-containing AFGP analogues and their ability to inhibit ice recrystallization. Bioconjug. Chem. **2011**, 22 (4), 605.

33. Liu, S.; Ben, R. N. C-Linked Galactosyl Serine AFGP Analogues as Potent Recrystallization Inhibitors. Org. Lett. **2005**, 7 (12), 2385.

34. Leclère, M.; Kwok, B. K.; Wu, L. K.; Allan, D. S.; Ben, R. N. C-linked antifreeze glycoprotein (C-AFGP) analogues as novel cryoprotectants. Bioconjug. Chem. **2011**, 22 (9), 1804.

35. Tam, R. Y.; Ferreira, S. S.; Czechura, P.; Chaytor, J. L.; Ben, R. N. Hydration index--a better parameter for explaining small molecule hydration in inhibition of ice recrystallization. J. Am. Chem. Soc. **2008**, 130 (51), 17494.

Chapter 4: Experimental Procedures

4.1 Ice Recrystallization Inhibition (IRI) Assay:

IRI activity was assessed using the "splat cooling" method.[1,2] The analyte was dissolved in phosphate buffered silane (PBS) solution and a 10 μL drop of this solution was dropped from a height of two meters onto a polished aluminum block which was pre-cooled to approximately -78°C. The frozen droplet forms an ice wafer with a diameter of approximately to 1cm in diameter and 20 μm in thickness. The wafer is then transferred to a cryostorage unit held at -6.4°C. After 30 minutes of annealing in the cryostorage, the wafer was photographed between crossed polarizing filters using a Nikon CoolPix 5000 digital camera fitted to a microscope. A total of three ice wafers were prepared for each analyte, and for each wafer a total of three photographs were taken. From each photograph, the areas of 12 random crystals were measured using domain recognition software (DRS).[3] All data was plotted and analyzed using Microsoft Excel. The mean grain (ice crystal) size (MGS) of the sample was compared to the MGS of the control (PBS) solution for the same day of testing. The IRI activity is reported as the percentage of the sample MGS relative to the PBS control. Each sample is plotted along with its standard error of the mean. Small crystals indicate small MGS percentage, which means high IRI activity. Some of the molecules that were tested for IRI activity are listed below.

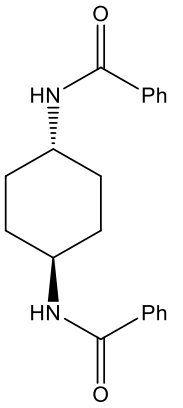

77

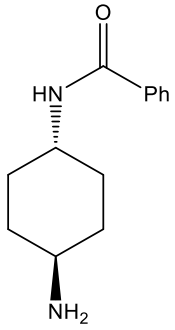

78

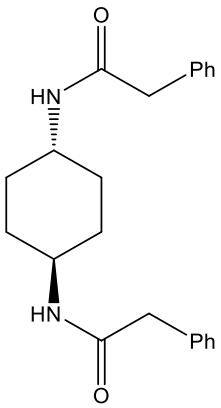

79

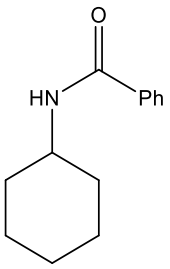

80

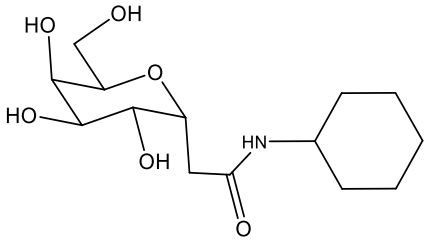

81

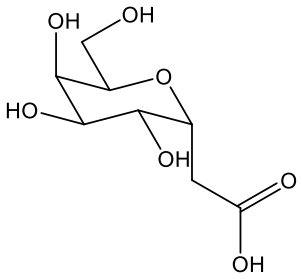

82

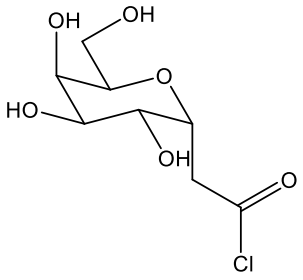

83

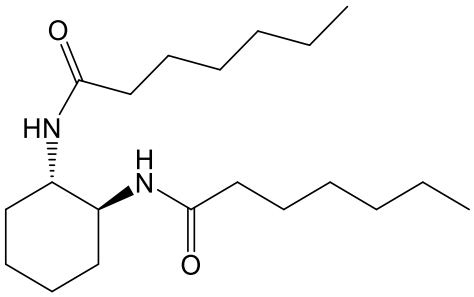

84

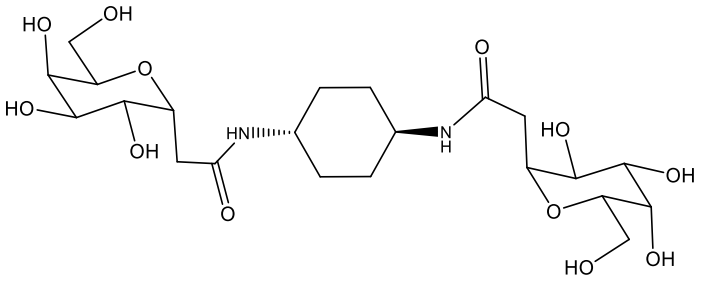

85

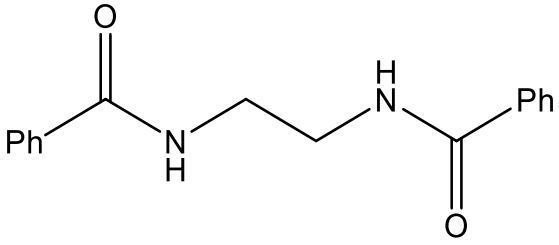

86

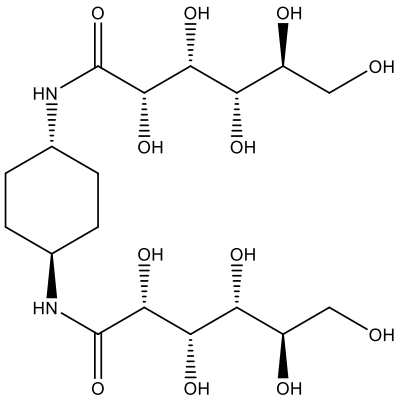

87

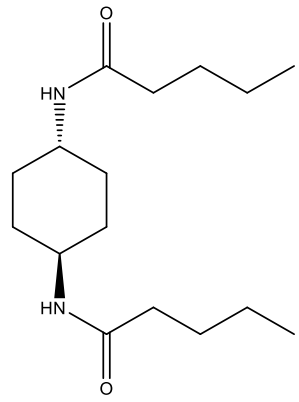

88

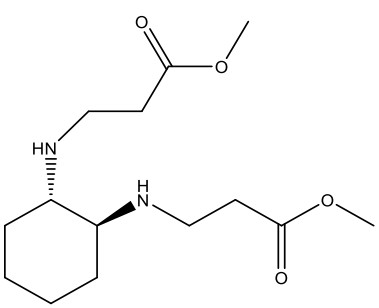

89

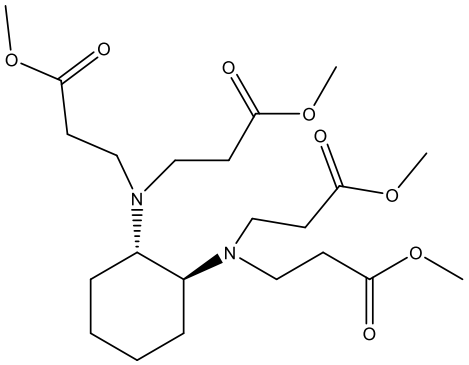

90

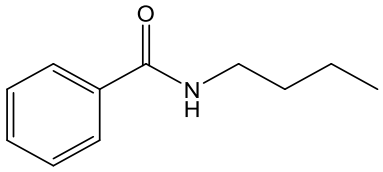

91

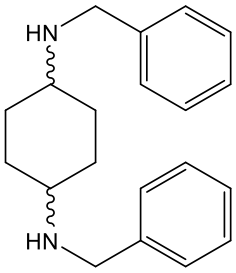

92

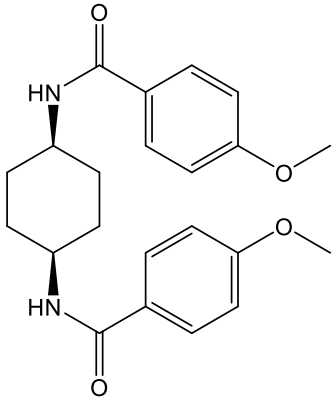

93

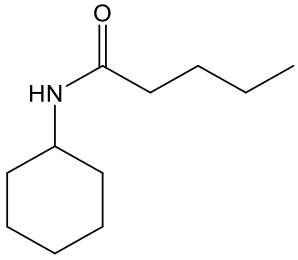

94

95) 1,3-cyclohexanediol
96) 1,4-cyclohexanedione
97) 1,4-cyclohexanedimethanol
98) Cis and trans-1,4-cyclohexanediamine
99) EDA
100) 4-fluorophenyl hydrazine
101) 3- fluorophenyl hydrazine
102) 2,3,6-trifluorobenzylamine
103) 1,4-cyclohexanediol
104) 2-methylbenzylamine
105) 4-aminophenol
106) 4-methoxybenzylamine
107) 2-bromoaniline
108) 3,4-difluoroaniline
109) 3,5-difluoroaniline
110) 5-methoxyindole
111) 3-fluorobenzyl amine
112) 4-fluoroaniline

113) Phenylethylamine
114) 4-bromo-N,N-dimethylaniline
115) m-nitroaniline
116) 2-fluoroaniline

4.2 General Experimental Conditions (Synthetic chemistry)

All anhydrous reactions were carried in flame-dried glassware under a positive pressure of dry argon. Air or moisture-sensitive reagents as well as anhydrous solvents were transferred with oven-dried syringes or cannula. Flash chromatography was performed with E. Merck silica gel (230-400 mesh). Solution-phase reactions were monitored using analytical thin layer chromatography (TLC) with E. Merck 0.2mm pre-coated silica gel aluminum plates 60 F254. Compounds were visualized by illumination with short-wavelength (254 nm) ultra-violate light and/or staining with ceric ammonium molybdate solution. Anhydrous dichloromethane (DCM) used for reactions was purified using an LC Technology Solution SPBT-1 bench top solvent purification system. Pyridine was dried over activated 4Å molecular sieves under argon. ^{1}H NMR (300, 400 or 500 MHz) and ^{13}C NMR (75, 100 or 125 MHz) spectra were recorded at ambient temperature on a Bruker Avance (300, 400 or 500), Avance II 300 or Varian Inova 500 spectrometer. Deuterated chloroform ($CDCl_3$), acetone ($(CD_3)_3CO$), methanol (CD_3OD) or water (D_2O) were used as NMR solvents, unless otherwise stated. Chemical shifts are reported in ppm using the solvent residual peak as an internal standard. Splitting patterns are designated as follows: s, singlet; d, doublet; t, triplet; q, quartet; quint, quintet; m, multiplet and br, broad. Low-resolution mass spectrometry (LRMS) was performed on a Micromass Quatro-LC Electrospray spectrometer with a pump rate of 20 μL/min using electrospray ionization (ESI).

4.3 Synthesis of PAMAM Dendrimer compounds

4.3.1 Synthesis of multiester (G-0.5) (**75**)

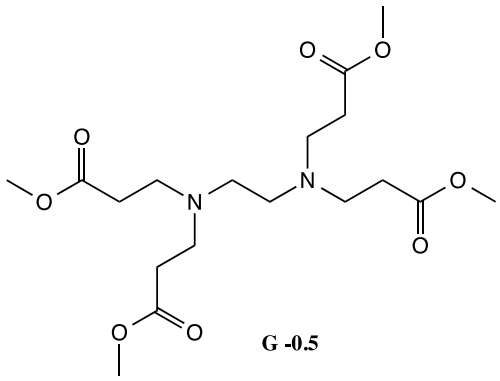

G -0.5

Ethylene diamine EDA (1.0g, 0.017mol) was dissolved in (50mL, 1.24mol) methanol. The mixture was cooled to approximately 0˚C then methyl acrylate (6.8mL, 0.075mol) was added drop wise. After the addition, the mixture was allowed to warm up to room temperature and kept at this temperature for five days and then warmed to 40˚C for an additional two days. Excess methyl acrylate and solvent were removed under vacuum and product was obtained as clear viscous syrup (7.45g). The crude product was purified by column chromatography (DCM:MeOH 10:1) to yield again a clear viscous syrup (6.94g). Some methanol and methyl ester residues may still be found in the product, as it was very difficult to remove it under high pressure evaporation.

^{1}H NMR (300 MHz, $CDCl_3$): δ 3.49 (s, 12H), 2.59 (t, J = 7.2 Hz, 8H), 2.32 (s, 4H), 2.27 (t, J = 6.9 Hz, 8H). ^{13}C NMR (76 MHz, $CDCl_3$): δ 172.9, 52.05, 49.63, 32.45.

4.3.2 Synthesis of generation 0 (G0) (**76**)

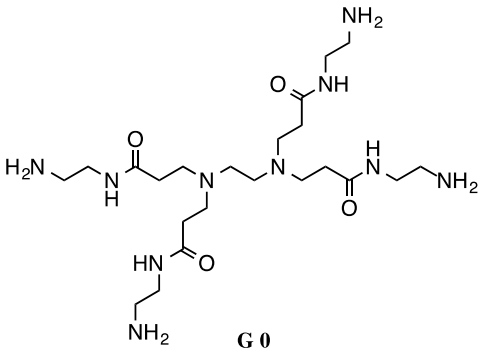

G 0

The multiester compound (G-0.5) (3.0g, 0.0074mol) was dissolved in (7.5 mL) methanol and cooled down to approximately -30˚C. In a separate RBF, EDA (60 mL, 0.89 mol) was also dissolved in (34mL) methanol. The multiester solution was gradually added to the EDA solution at a rate keeping the temperature below -25˚C. The reaction then was left to warm up to room temperature and then stirred for 168 hours. The mixture was distilled to remove any excess EDA as an azeotrope with butanol. The remaining material weighed 4.1g.

^{1}H NMR (300 MHz, CDCl3): δ 7.67 (t, J = 4.2 Hz, 4H), 3.15 (q, J = 4.5 Hz, 8H), 2.69 (t, J = 4.5 Hz, 8H), 2.55 (t, J = 4. 5 Hz, 8H), 2.31 (s, 4H), 2.24 (t, J = 4.2 Hz, 8H). ^{13}C NMR (76 MHz, CDCl3): δ 173.1, 51.92, 50.56, 42.33, 41.49, 34.30.

4.3.3 Synthesis of glycosidated ornithine

Step 1

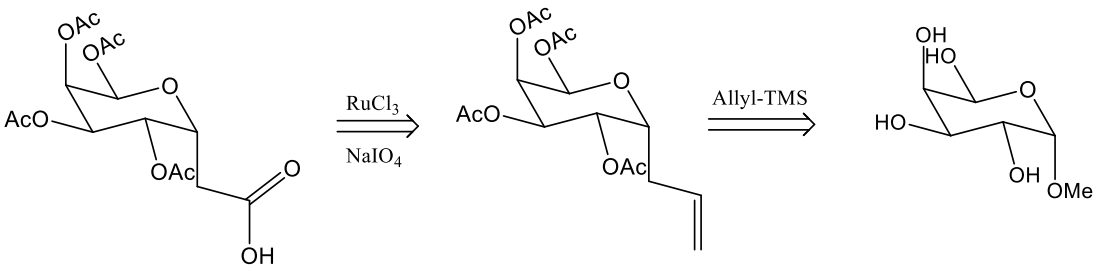

Methyl-D-galactopyranoside monohydrate (0.25g) was added to a dry reaction flask filled with argon. Then pyridine (2.5mL) was added and stirred while continuous flushing with argon. The mixture then was cooled down to 0°C and stayed for few minutes. TMS-Cl (1mL) was then added drop wise. When finished adding the TMS-Cl, the reaction was let to warm up to room temperature and kept stirring for 2 hours with continuous argon flush. Petroleum ether was then added to precipitate the product and then filtered. The product was placed under vacuum and washed with toluene. Product yield 97%.

The product (0.55g) was added to a dry flask and mixed with acetonitrile (0.5mL). The solution was cooled down to 0°C, then Allyl-TMS (0.33mL) was added. After few minutes, TMSOTf (0.12mL) was added dropwise to the mixture at 0°C. The reaction was allowed to warm up to room temperature and left to stir overnight under argon. The next day, water was added to quench the reaction, and was cooled down to 0°C. Basic Amberlite was then added to neutralize the mixture, and then was filtered. Product yield 75%.

Allyl α-D-galactopyranoside (2.4g) is mixed in pyridine at 0°C. Then acetic anhydride (6 equivalents) was added and the reaction was warmed up to room temperature and stirred overnight. The next day, the reaction was quenched by removing solvents under vacuum and washed three times with toluene to yield the acetylated allyl α-D-galactopyranoside.

Allyl α-D-galactopyranoside (0.35g) was dissolved in DCM at room temperature and then MeCN and water were added. To the mixture, $NaIO_4$ (1.2g) was added then $RuCl_3$ (0.0074g) was added. The reaction was left to stir overnight. The reaction was extracted with DCM and water (10% HCl). The aqueous layer was removed, and the organic layer was dried and evaporated to give the final product.

Step 2

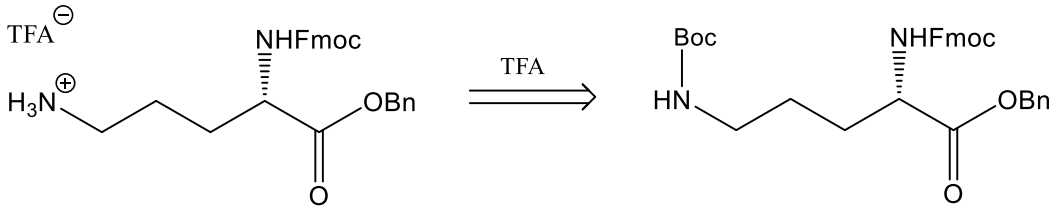

Fmoc-Orn(Boc)-OH (0.2g) was dissolved in DCM and cooled down to 0°C, then TFA was added. The reaction stirred for 2 hours then evaporated to washed with ether. The precipitate was collected to give the final product.

Step 3

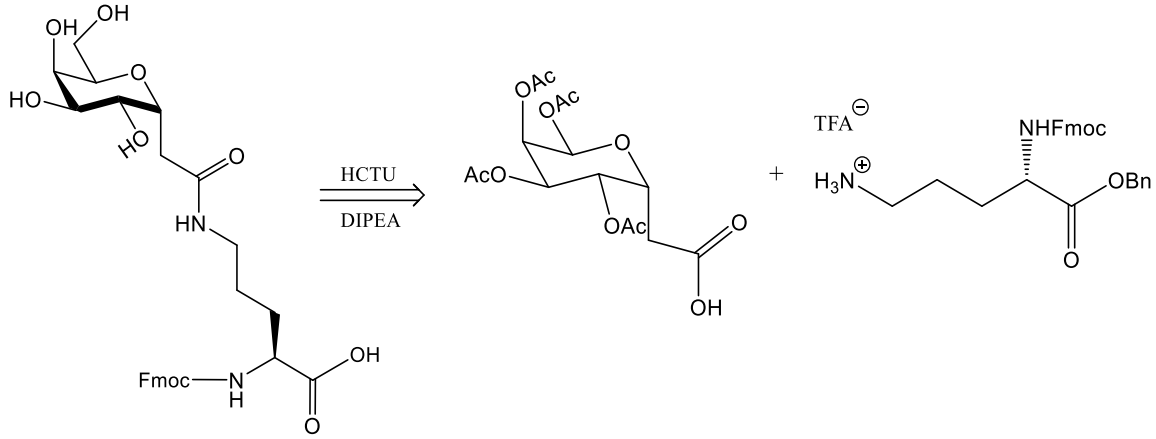

In a flame dried flask flushed with argon, the product from step 1 (0.4g) was dissolved with HCTU (0.4g) in DCM (15mL). Mixture was left to stir for few minutes, then the product from step 2 (0.55g) was added with DIPEA (0.34mL). The reaction was left to stir overnight. The product yield was 83%.

4.3.4 Coupling of PAMAM with Glycosidated Ornithine

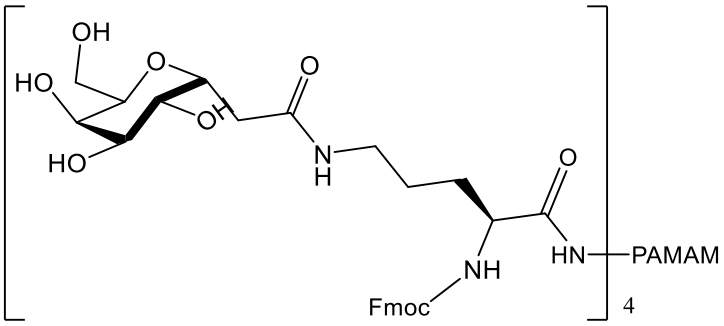

PAMAM (0.035g) was added to a dry flask and dissolved in MSDO (15mL). Glycosidated Ornithine (0.23g) was then added with HCTU (0.15g). Reaction was left to stir for few minutes. Then, DIPEA was added until pH 9 was reached. Reaction left to stir overnight.

4.3.5 Coupling of PAMAM with Gluconolactone

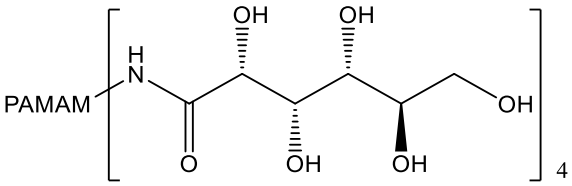

Gluconolactone (0.3g) was dissolved in refluxing MeOH (4.3mL), then PAMAM (0.2g) was added. Reaction was left to stir at reflux for 1 hour. Then, it was let to cool down to 0°C. Precipitate were collected and washed with cold methanol. Product yield was 74%.

4.3 General Synthesis procedures for small molecules

All the following compounds are known compounds. At the time they were prepared they were characterized by proton and carbon NMR and the spectral data was found to be consistent with the expected structure. Data are not available due to restrictions and personal reasons.

a) *trans*-1,4-Cyclohexanediamine (0.1g, 0.88mmol) and trimethylamine (0.266g, 2.63mmol) were added to a dry RBF and then dissolved in dry DCM (2mL). This mixture was added drop wise to a solution of benzoyl chloride (0.33g, 2.63mmol) in DCM (2mL). The reaction was left to stir for 18 hours at room temperature. The product was filtered as a precipitate and collected (0.213g). This product was not soluble in the usual NMR solvents that were available. Solid phase ^{13}C NMR (76 MHz, $CDCl_3$): δ 166.8, 136.2, 129.6, 126.5, 47.77, 31.51, and 30.24.

The extra peaks are due to misadjustment of Z2 shim, which results in loss of resolution and potential missing peak splitting. Also, it may be as simple as a poorly positioned sample causing high-order shimming problems or as perplexing as persistent out-of-phase 3 Hz sidebands.

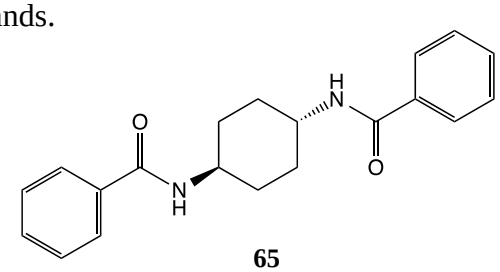

65

b) Cyclohexanediamine (0.1mL) was dissolved in DCM (5mL) under dry conditions. Then, heptanoic acid (0.27mL) was added followed by CDI (0.28g). Precipitate was collected.

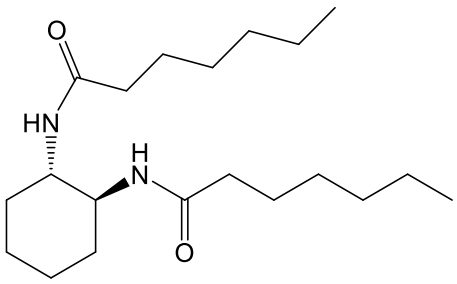

84

c) To a dry flask flushed with argon, the acetylated α-D-galactopyranoside (0.1g) was mixed with HCTU (0.42g) in DMF anhydrous. The reaction was left to stir for 45 minutes. In a separate dry flask, cyclohexanediamine • TFA (0.38g) was mixed with DIPEA (0.42g)

in DMF anhydrous. The second reaction was added to the first reaction dropwise and left to stir overnight. The solvent was removed by high pressure evaporation and was dissolved in DCM, then washed several times with $NaHCO_3$, water and brine.

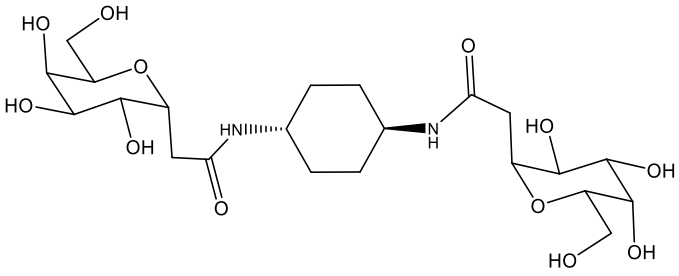

85

d) Methyl acrylate was dissolved in methanol under dry conditions. While stirring, cyclohexanediamine was added. Reaction was left to stir for 3 days.

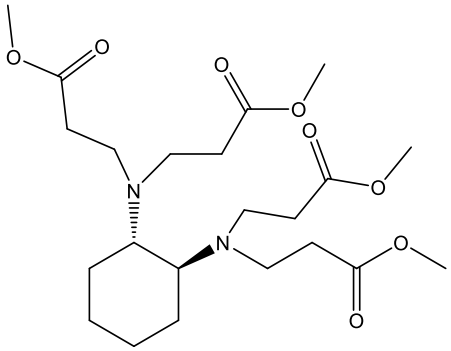

90

e) Benzaldehyde (0.32g) and aminobutane (0.1g) were dissolved in THF separately. The benzaldehyde solution was added to the amine solution and stirred for few minutes. Then, NaTABH (0.1g) and Acetic acid (0.02mL) were added and the reaction was left to stir overnight. THF was removed and the product was dissolved in methanol and stirred for 20 minutes. Then methanol was removed, and ethyl acetate was added to dissolve the product and washed with $NaHCO_3$, water and brine.

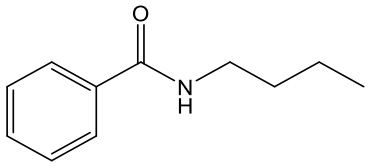

91

f) 1,4-Cyclohexanedione (0.1g) and benzylamine (0.2g) were dissolved in THF separately. The benzaldehyde solution was added to the amine solution and stirred for few minutes. Then, NaTABH (0.6g) and Acetic acid (0.02mL or few drops) were added and the reaction was left to stir overnight. THF was removed and the product was dissolved in methanol and white precipitate was formed.

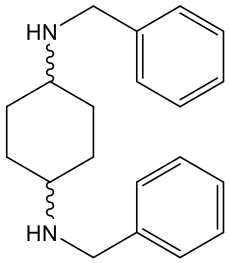

92

g) To a dry flask flushed with argon, the acetylated valeric acid (0.1g) was mixed with CDI (0.16g) in DCM. The reaction was left to stir for 45 minutes. In a separate dry flask, aminocyclohexane (0.1g) was mixed with DIPEA (0.14g) in DCM. The second reaction was added to the first reaction dropwise and left to stir overnight. The solvent was removed by high pressure evaporation and was dissolved in DCM then washed several times with $NaHCO_3$, water and brine. Evaporation afforded a 61.8% yield of the desired product.

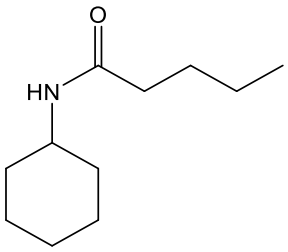

94

h) Benzoic acid was dissolved in dry DCM under dry conditions and cooled down to 0°C. When the mixture reached 0°C, triethyl amine was added followed by ethyl chloroformate, and left to stir for 15 minutes. Then Ethylene diamine was added to the mixture and left to stir. The reaction was monitored by TLC, and once it was completed, the reaction was quenched by adding 0.25M HCl, then washed with water, $NaHCO_3$ and dried.

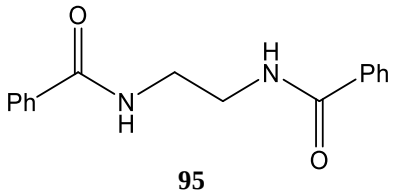

95

Conclusions

In conclusion, it has been shown that the presence of an amine group in a small molecule can have a positive effect on the ability of that molecule to inhibit ice recrystallization. Investigations in compounds like cyclohexyl amine and cyclohexane diamines can have the potential to find new compounds that can act as cryoprotectants. Also, molecules with an aryl ring are important, because the position and type of group on the ring can play a big role in determining the IRI activity. Increasing the number of amines in a molecule has been found to have little effect on the IRI activity of that compound. The lack of a consistent electronic effect and the absence of an additive effect on IRI activity, suggests that a combination of factors are at play in governing the behavior of these compounds. Further studies are necessary to evaluate the changes these functional groups have on the hydrogen-bonding abilities, hydrophobicity, and solubilities of the overall compounds in question.

References

1. Knight, C.A.; Hallett, J.; DeVries, A.L. Solute effects on ice recrystallization: an assessment technique. *Cryobiology.* **1988**, *25*, 55-60.

2. Tam, R. Y.; Ferreira, S. S.; Czechura, P.; Chaytor, J. L.; Ben, R. N., Hydration index--a better parameter for explaining small molecule hydration in inhibition of ice recrystallization. J. Am. Chem. Soc. **2008**, 130, 17494-17501.

3. Jackman, J.; Noestheden, M.; Moffat, D.; Pezacki, J.P.; Findlay, S.; Ben, R.N. Assessing antifreeze activity of AFGP 8 using domain recognition software. *Biochem. Biophys. Res. Commun.* **2007**, *354*, 340-344.

Chapter 5: 1α-Hydroxycorticosterone (1α-OH-B)

5.1 Introduction

During the late 1950s and early 1960s, corticosteroids were first identified and isolated from both teleost and elasmobranch fish[1,2]. Corticosterone and cortisol, being the dominant secretions from tissue analogous to mammalian adrenocortical tissue, were measurable in the plasma of elasmobranchs[3,4]. In 1966 Idler and Truscott isolated several corticosteroids from the plasma or two species of ray, and later found that 1α-hydroxycorticosterone (1α-OH-B) was the dominant corticosteroid produced by the internal tissue in an additional 6 species of ray, 2 dogfish and 5 sharks[5-7].

At the same time, scientists were able to synthesize 1α-OH-B (**117**), which led to the development of a radioimmunoassay (RIA) for the measurement of the steroid from significantly smaller volumes of plasma[8]. However, only limited amount of 1α-OH-B was synthesized because available supplies were exhausted in the early 1990s, despite repeated attempts to synthesize and purify the steroid commercially. In recent years, synthetic 1α-OH-B was used in steroid receptor studies to examine the evolution of the corticosteroid receptor system[9]. The same synthetic 1α- OH-B was used to develop and validate an enzyme linked immunosorbent assay (ELISA) for the measurement of this unique corticosteroid in the Atlantic stingray, *Dasyatis sabina*[10].

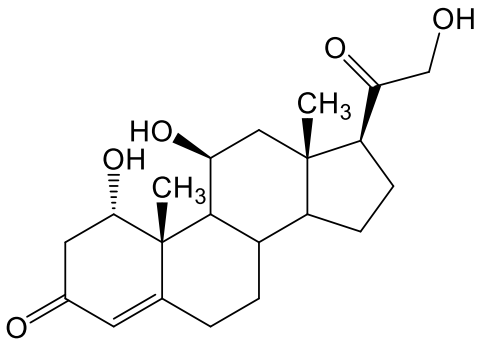

117

A recent study by W. G. Anderson concluded that that there is a need for a definitive measurement of 1α-OH-B in the plasma of elasmobranch fish following a stressful event alongside the examination of in vivo and in vitro actions of 1α-OH-B in regard to mobilization of energy reserves before we can truly describe this steroid as a "stress hormone".[11] In mammals, the principal mineralocorticoid is aldosterone. An earlier study by Brent *et. al.*, suggested the presence of aldosterone in elasmobranchs,[12] yet a newer study by Bridgham *et. al.*, recognized that fish do not synthesize and release this steroid,[13] and that corticosteroids such as cortisol and 1α-OH-B may play a dual role in regulating both mineralocorticoid and glucocorticoid responses in fish.[14]

The purpose of this project is to synthesize 1α-OH-B from corticosterone which would then be used by the Prof. Pat Walsh (Biology) lab to feed dogfish, sharks and other fish species and examine their stress level.

5.2 Synthesis of 1α-hydroxycorticosterone (1)

1α-Hydroxycorticosterone (**117**) is the major corticosteroid hormone in genus *Raja* (skate). The only synthesis of 1α-OH-B was reported by David Kime in 1975 starting from corticosterone 21-acetate (**118**).[15] He wanted to confirm the ready conversion of 1α-OH-B via its diacetate into the known 1,2-didehydrocorticosterone and to compare its NMR and chromatographic mobility with those of a number of related compounds.[15]

5.2.1 The Kimes synthesis of 1α-hydroxycorticosterone (1α-OH-B)[15,16]

The following paragraphs describe the Kimes synthesis (Scheme 5.1) of this compound beginning with corticosterone. Corticosterone (**118**) was first selectively protected at the primary hydroxyl group to yield corticosterone 21-acetate (**119**). This compound was dehydrogenated with chloranil to 1,2,6,7-tetradehydrocorticosterone acetate (21-acetoxy-11ß-hydroxypregna-1,4,6-triene-3,20-dione) (**120**). Treatment of the triene (**120**) with alkaline hydrogen peroxide gave lα,2α-epoxy-11ß,21 dihydroxypregna-4,6-diene-3,20-dione (**121**). Hydrogenation of the epoxide (**121**) in pyridine over palladium-calcium carbonate gave 1α-hydroxycorticosterone (**123**).[15]

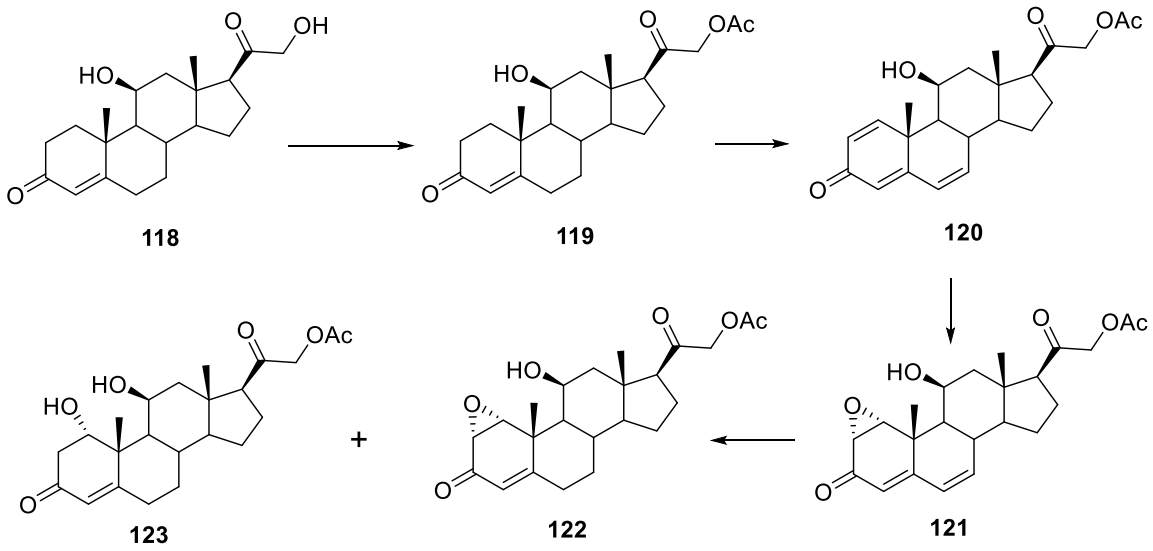

Scheme 5.1 Synthesis of 1α-hydroxycorticosterone using Kimes Synthesis.

The Kimes synthesis is short but it suffers from low yields in each of the final three steps [3➔4 (26%); 4➔5 (23%) and 5➔6 (11%)] with the overall yield in these three steps being 0.65%. The initial goal in this project was to repeat the Kimes synthesis and potentially make improvements in a variety so that sufficient amounts of material would be available for the planned biological assays.

The mechanism of the dehydrogenation reaction **119** to **120** and the alkaline peroxide induced epoxidation are shown below (Scheme 5.2 and 5.3).

Chloranil induced dehydrogenation **119➔120**:

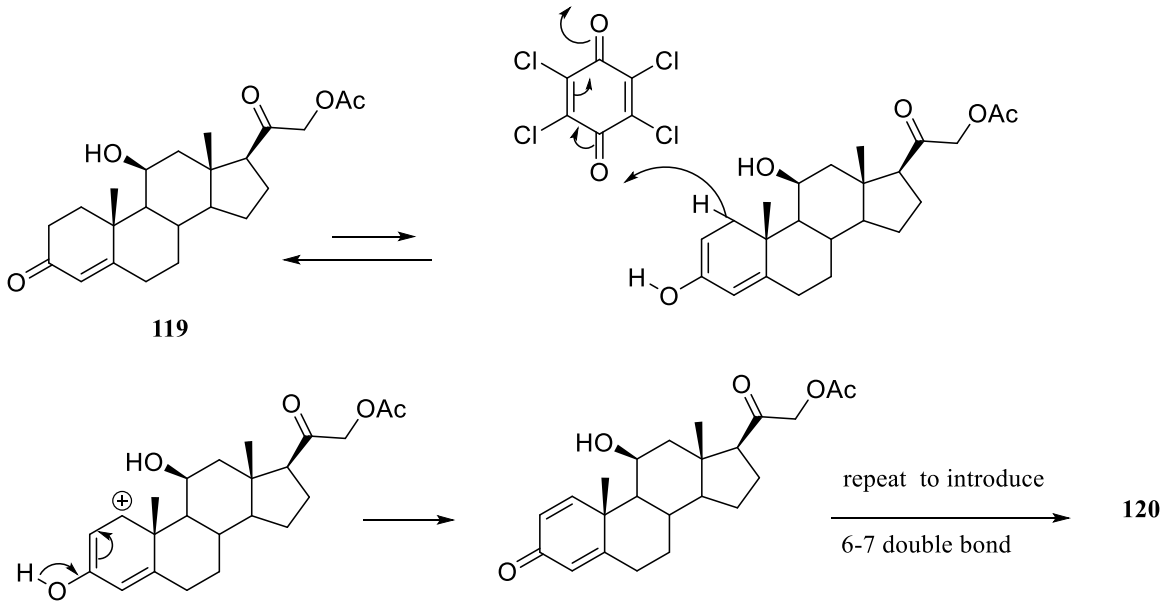

Scheme 5.2 Dehydrogenation reaction to produce double bond.

Basic peroxide induced epoxidation:

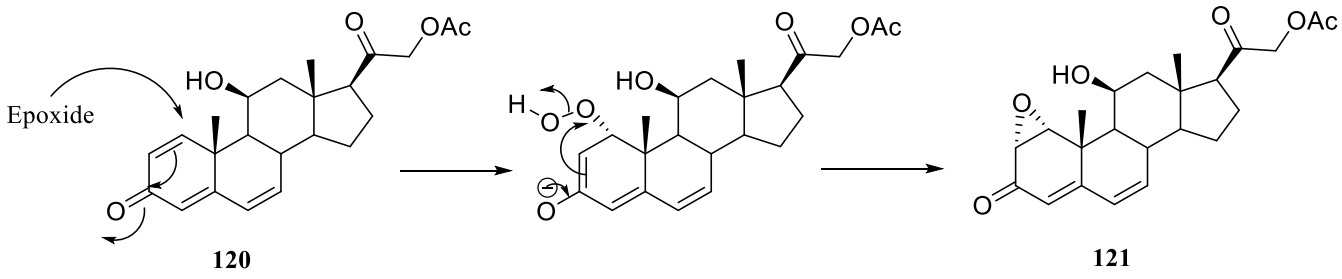

Scheme 5.3 Epoxidation reaction.

As part of this, an intensive review of considerable amount of steroid chemistry related to this project was done. These included alternate methods of introduction of the A ring diene system and the production of the α-1,2-epoxide which was necessary to generate the desired 1α-hydroxy compound **117.**

5.3 Potential alternative methods for Ring A dienone

Diao and Stahl[17] reported that 5α-cholestan-3-one (**124** was converted to the 1,4 diene-3-one **125** in 94% yield upon treatment of an acetic acid solution with a catalytic amount of Pd(TFA) in an oxygen atmosphere and in the presence of small amounts of DMSO. Surprisingly, only one double bond was introduced by this procedure. It was anticipated that the second double could be introduced using chloranil as described by Kimes.

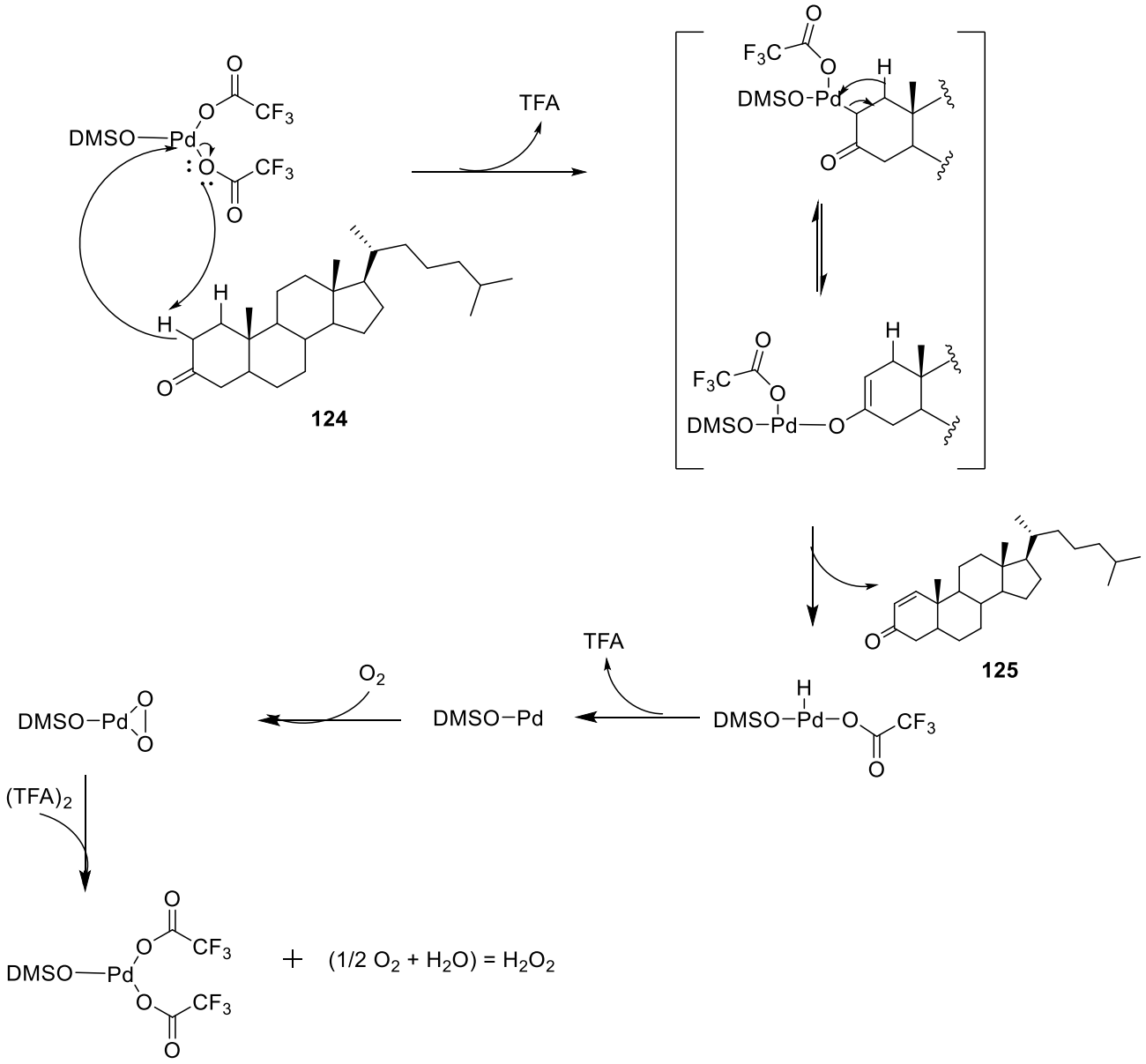

Scheme 5.4 Synthesis of the double bond on ring A.

Gao and coworkers[18] reported the conversion of dihydrocinnamyl alcohol **126** into cinnamaldehyde, **127,** upon reaction with palladium acetate in the presence of potassium carbonate.

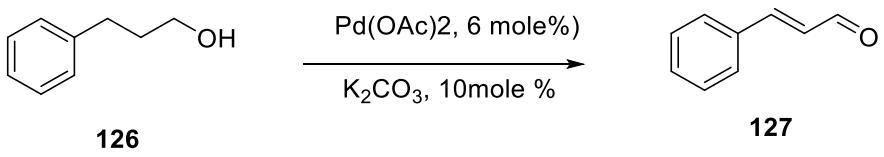

126 **127**

Scheme 5.5 Other method used to synthesis the double bond.

This conversion, while intriguing was considered problematic when applied to cortisone, **119**, or its 22-acetate since one could imagine unwanted oxidation of the 12-hydroxy group and possibly even the primary acetate to give compound **128**. This oxidation was not attempted due to the lack of sufficient starting material.

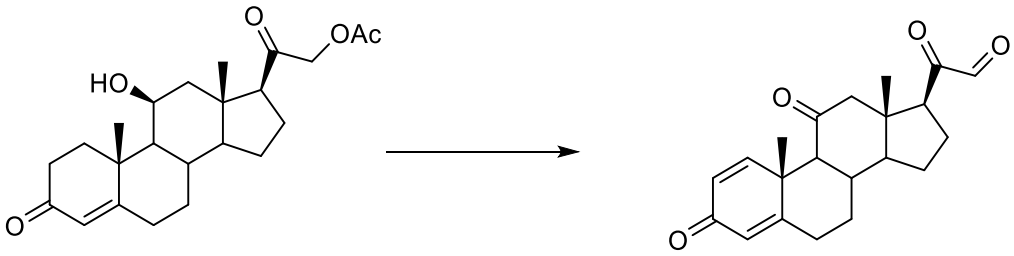

119 **128**

Scheme 5.6 Synthesis of the double bond on ring A.

5.4 Other possible methods for generating the 1,2-α-epoxide

5.4.1 Dioxirane Reaction with Steroids

Bovicelli.and Lupattelli[19] reported the epoxidation of a variety of steroids carrying one or several double bonds using the highly reactive and strongly electrophilic dimenthyldioxirane. Some of the steroids they used during their work were similar to the corticosterone derivative (**120**). This suggested a possible new method for preparing the epoxide (**121**). One would anticipate that 1,2-double bond should be more reactive due to

less steric hindrance; It is however recognized that the 4,5-double bond, being more substituted is more nucleophilic and thus more reactive towards the highly electrophilic

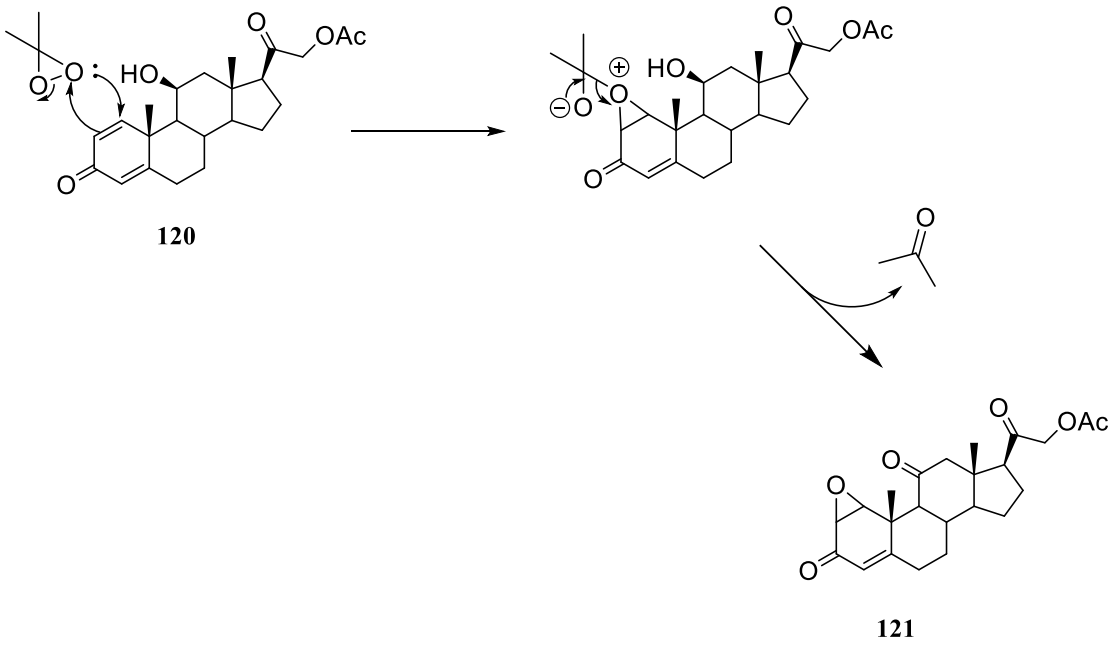

Scheme 5.7 Synthesis of the epoxide.

5.4.2 Epoxidation using DBU and t-BuO₂H

Chad Christian et al proposed a synthesis for epoxidation using DBU and *t*-BuO_2H.[20] A particularly relevant example is the formation of the epoxide (**121**) in good yield. The mechanism of this reaction is similar to that involving hydrogen peroxide and base. It involves generation of the t-butylperoxy anion followed by nucleophilic addition to the more accessible double bond. The attack by the t-butylperoxy anion occurs preferentially from the least hindered α side, opposite the 10-β-methyl group

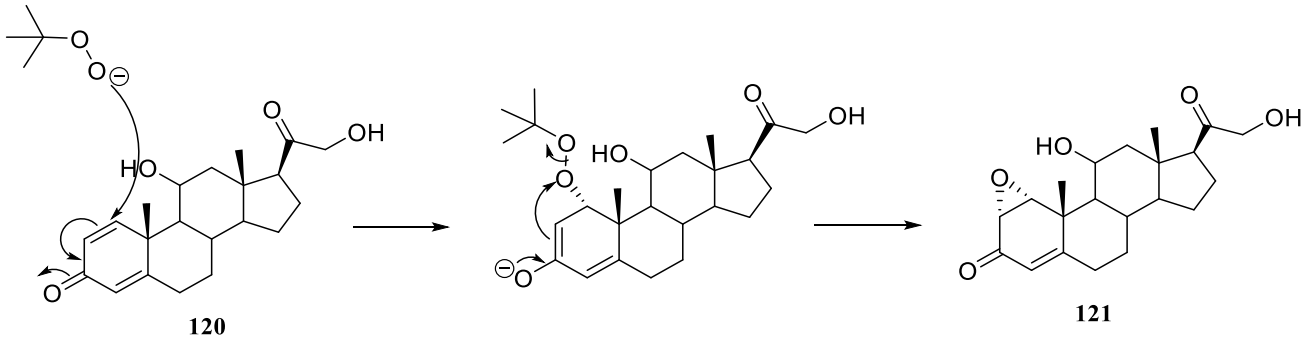

Scheme 5.8 Other method to synthesize of the epoxide.

5.5 The Authors work for this project

During the first year in the master program, an extensive amount of research about steroids was done and many ways to synthesize the required molecule were found. It was very difficult dealing with this project due to lack of experience and material. Several attempts to duplicate the Kimes synthesis of **117** were made as well as the model reactions mentioned above with significant success.

The starting material (**118**) was the only material available and since it was very expensive to purchase, only limited quantities were available at hand. This limitation made it very difficult to succeed since reactions that were not successful, were not repeated. It should be pointed out again that the Kimes reactions proceeded only in quite poor yield and thus likely left behind starting materials or many different reaction products, which would make isolation of the desired products very difficult. Being the only person working on a steroid project in the lab made it very difficult to take advantage of my fellow students' experience in this area.

Recalling from memory, some reactions were done successfully and the formation of molecule **119** from **118** was done. Most of the products of the several attempts were confirmed by NMR, GC and MS.

Unfortunately, it is not possible to give more details regarding the many experiments tried in this project. The reason for this is the missing work book and other documents related to this project. When the author returned from the leave of absence the lab note book and other relevant documents were nowhere to be found.

References

1. Chester-Johns, I., Phillips, J.G., Holmes, W.N., Comparative physiology of the adrenal cortex. In: Gorbman, A. (Ed), Comparative Endocrinology. Wiley, New York, **1959**. pp. 582-621.

2. Chester-Johns, I., Chan, D.K.O., Henderson, I.W., Ball, N.J., The adrenocorticosteroids, adrenocorticotropin and the corpuscles of Stannius. Fish Physiol. I, **1968**. 321-376.

3. Phillips, J.G., Adrenocorticosteroids in fish. J. Endocrinol. **1959**. 18, xxxviii.

4. Phillips, J.G., Chester-Johns, I., The identity of adrenocortical secretions in lower vertebrates. J. Endocrinol. **1957**. 16, iii.

5. Idler, D.R., Truscott, B., 1α-hydroxycorticosterone from cartilaginous fish: a new adrenal steroid in blood. J. Fish. Res. Bd. Canada. **1966**. 23, 615-619.

6. Idler, D.R., Truscott, B., 1a-hydroxycorticosterone: synthesis in vitro and properties of an interrenal steroid in the blood of cartilaginous fish (Genus Raja). Steroids. **1967**. 9, 457-478.

7. Truscott, B., Idler, D.R., Corticosteroids in plasma of elasmobranchs. Comp. Biochem. Physiol. A. **1972**. 42, 41-50.

8. Kime, D.E., Measurement of 1a-hydroxycorticosterone and other corticosteroids in elasmobranch plasma by radioimmunoassay. Gen. Comp. Endocrinol. **1977**. 33, 344-351.

9. Carroll, S.M., Bridgham, J.T., Thornton, J.W., Evolution of hormone signalling in elasmobranchs by exploitation of promiscuous receptors. Mol. Biol. Evol. **2008**. 25, 2643–2652.

10. Evans, A.N., Rimoldi, J.M., Gadepalli, R.S.V., Nunez, B.S., Adaptation of a corticosterone ELISA to demonstrate sequence-specific effects of angiotensin II peptides and C-type natriuretic peptide on 1 a-hydroxycorticosterone synthesis and steroidogenic mRNAs in the elasmobranch interrenal gland. J. Steroid Biochem. Mol. Biol. **2010**. 120, 149–154.

11. Anderson, W.G., The endocrinology of 1α-hydroxycorticosterone in elasmobranch fish: A review. Comp. Biochem. Physiol., Part A. **2012**. 162, 73–80.

12. Bern, H.A., deRoos, C.C., Biglieri, E.G., Aldosterone and other corticosteroids from chondrichthyean interrenal glands. Gen. Comp. Endocrinol. **1962**. 2, 490–494.

13. Bridgham, J.T., Carroll, S.M., Thornton, J.W., Evolution of hormone-receptor complexity by molecular exploitation. Science. **2006**. 312, 97–101.

14. Evans, A.N., Nunez, B.S., Regulation of mRNAs encoding the steroidogenic acute regulatory protein and cholesterol side-chain cleavage enzyme in the elasmobranch interrenal gland. Gen. Comp. Endocrinol. **2010**. 168, 121–132.

15. Kime, David. Synthesis of 1α-hydroxycorticosterone. J. Chem.Soc. Perkin Trans. **1975**. 1, 2371-2374.

16. Pelc, B. and Kodicek, E., A simple preparation of 1α,2α-epoxy-3-oxo-Δ^4-steroids. J. Chem. SOC. (C). **1971**. 1568.

17. Diao, T. and Stahl, S., Synthesis of Cyclic Enones via Direct Palladium-Catalyzed Aerobic Dehydrogenation of Ketones. J. Am. Chem. Soc., **2011**. 133, 14566–14569.

18. Gao, W., He, Z., Qian, Y., Zhao, J., and Huang, Y., General palladium-catalyzed aerobic dehydrogenation to generate double bonds. Chem. Sci., **2011**. 3, 883-886.

19. Bovicelli, P. and Lupattelli, P., Regio- and Stereoselective Epoxidation of Steroidal 1,4-Diene 3-Ones by Dimethyldioxirane: A New Access to A-Norsteroids and to a Class of Estrogen Synthetase Inhibitors. J. Org. Chem**.**, **1994**. 59 (15), 4304–4307.

20. Christian, C., Takeya, T., Szymanski, M., and Singleto, D. Isotope Effects and the Mechanism of Epoxidation of Cyclohexenone with *tert*-Butyl Hydroperoxide. J Org Chem. **2007**. 72(16), 6183–6189.

Appendix: ^{1}H and ^{13}C NMR Spectra

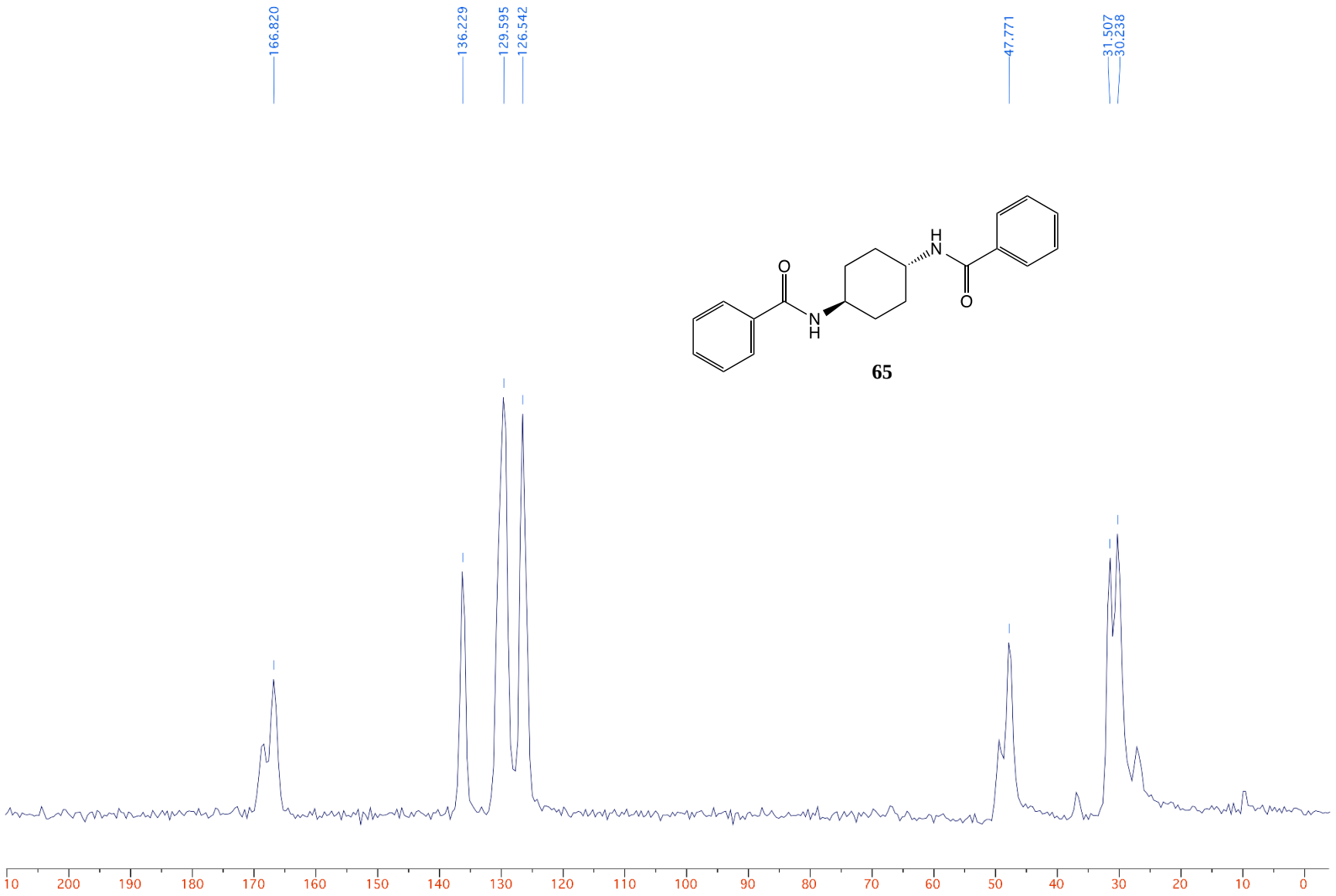
166.820
136.229
129.595
126.542
47.771
31.507
30.238
O
N
H
H
N
O
65
10
200
190
180
170
160
150
140
130
120
110
100
90
80
70
60
50
40
30
20
10
0

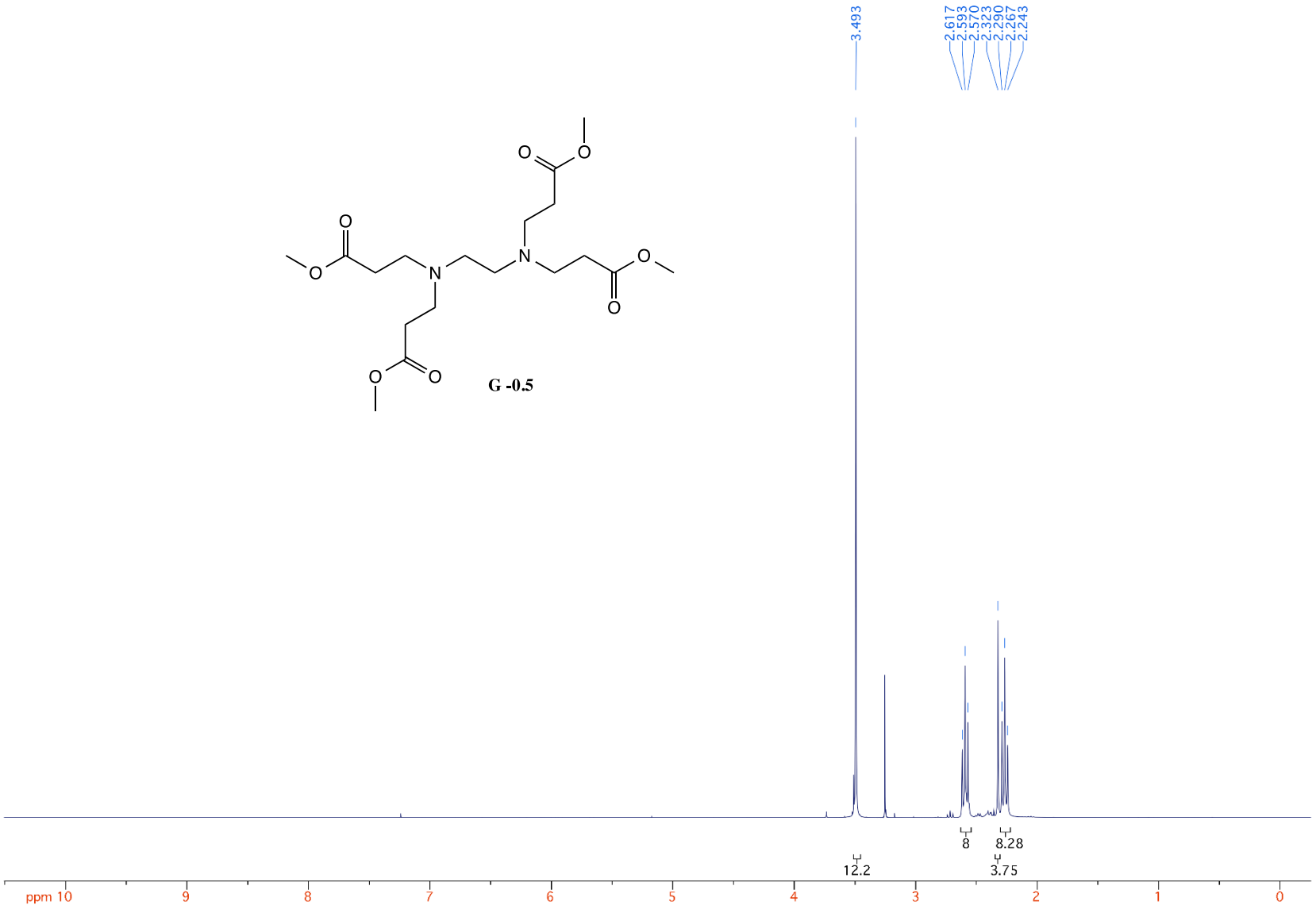
3.493
2.617
2.593
2.570
2.323
2.290
2.267
2.243
G -0.5
12.2
8
8.28
3.75
ppm 10
9
8
7
6
5
4
3
2
1
0

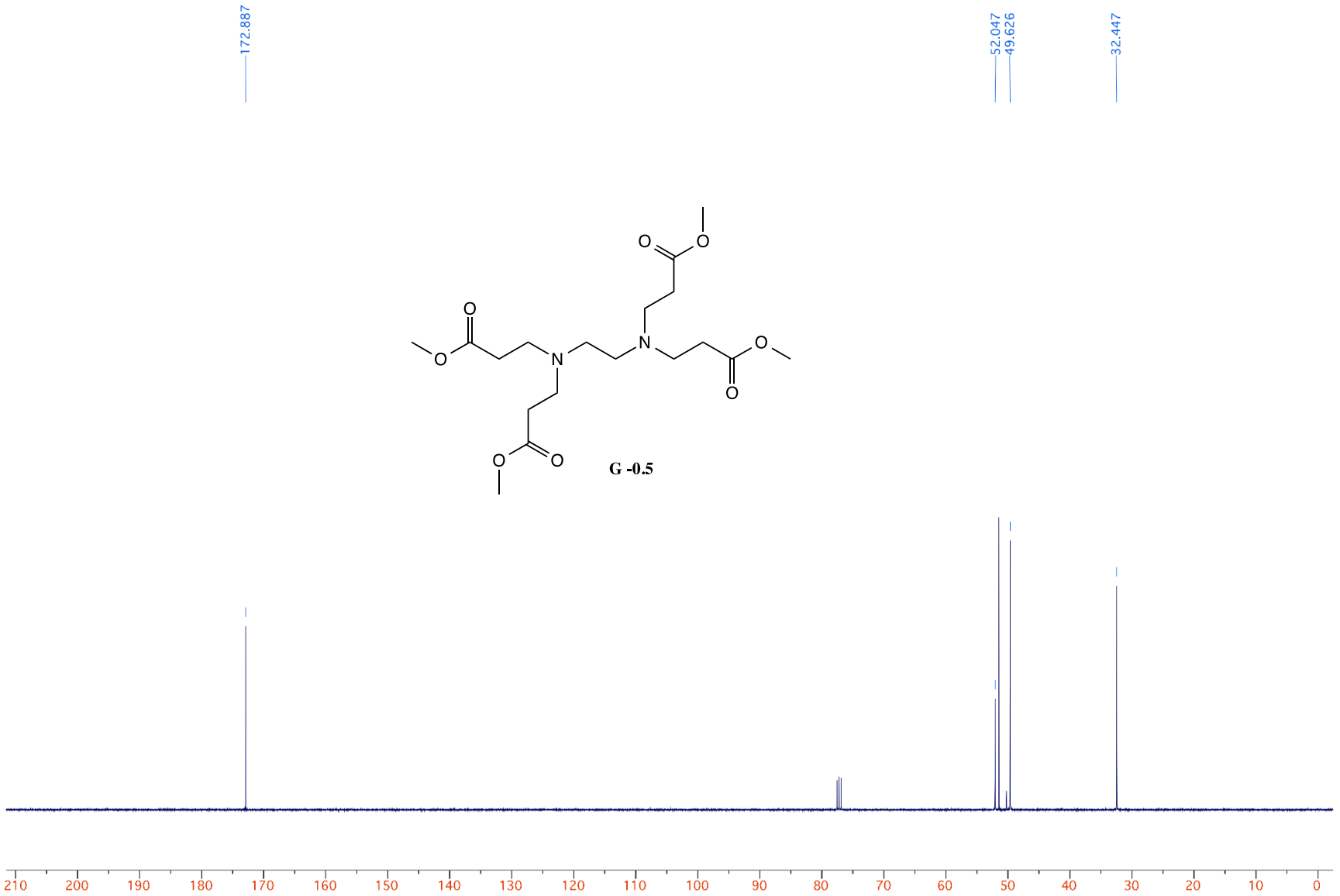
172.887
52.047
49.626
32.447
O
O
O
O
N
N
O
O
O
O
O
O
G -0.5
210
200
190
180
170
160
150
140
130
120
110
100
90
80
70
60
50
40
30
20
10
0

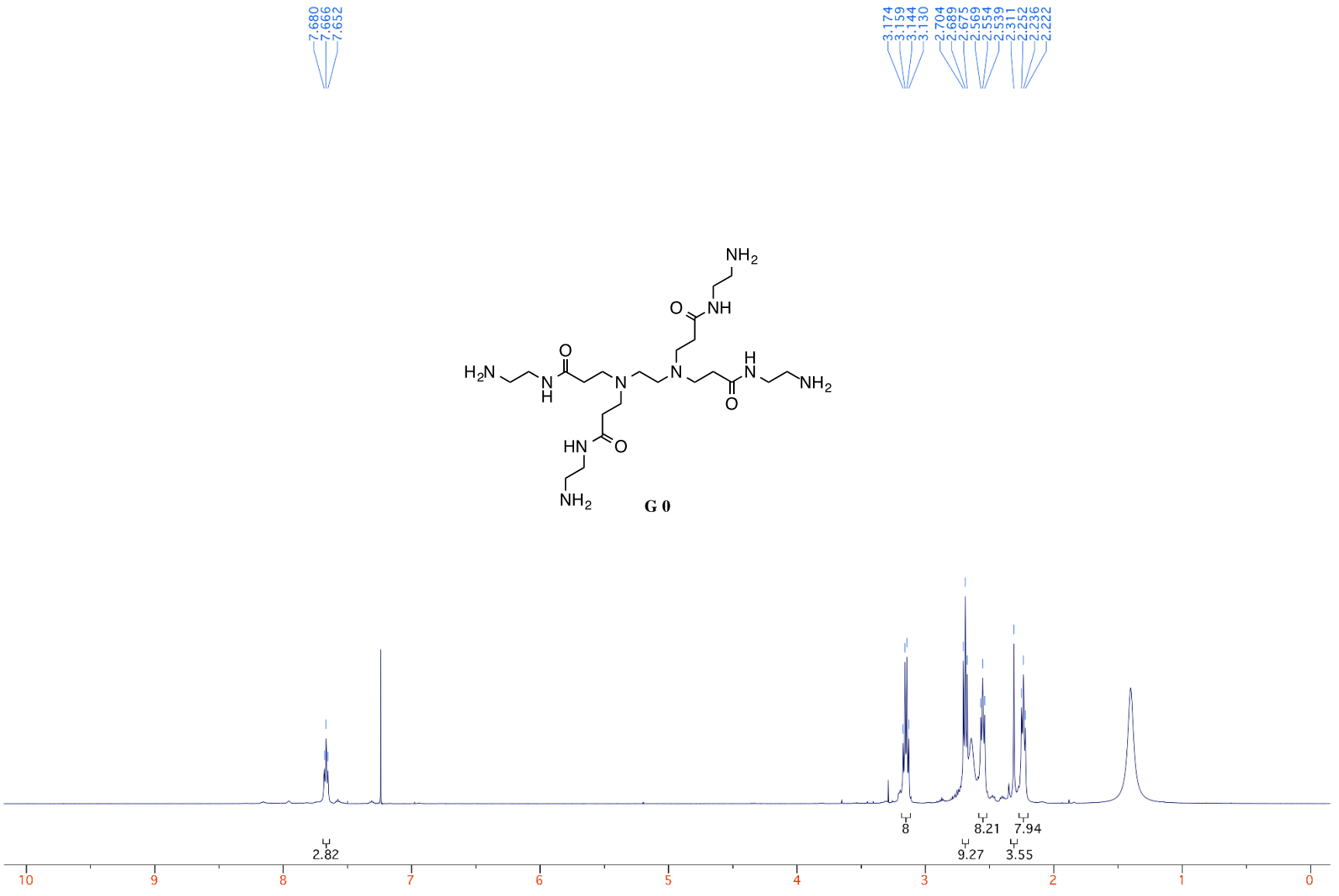
7.680
7.666
7.652
3.174
3.159
3.144
3.130
2.704
2.689
2.675
2.569
2.554
2.539
2.311
2.252
2.236
2.222
NH2
O
NH
H2N
N
H
O
N
N
H
N
NH2
O
HN
O
NH2
G 0
2.82
8
8.21
7.94
9.27
3.55
10
9
8
7
6
5
4
3
2
1
0

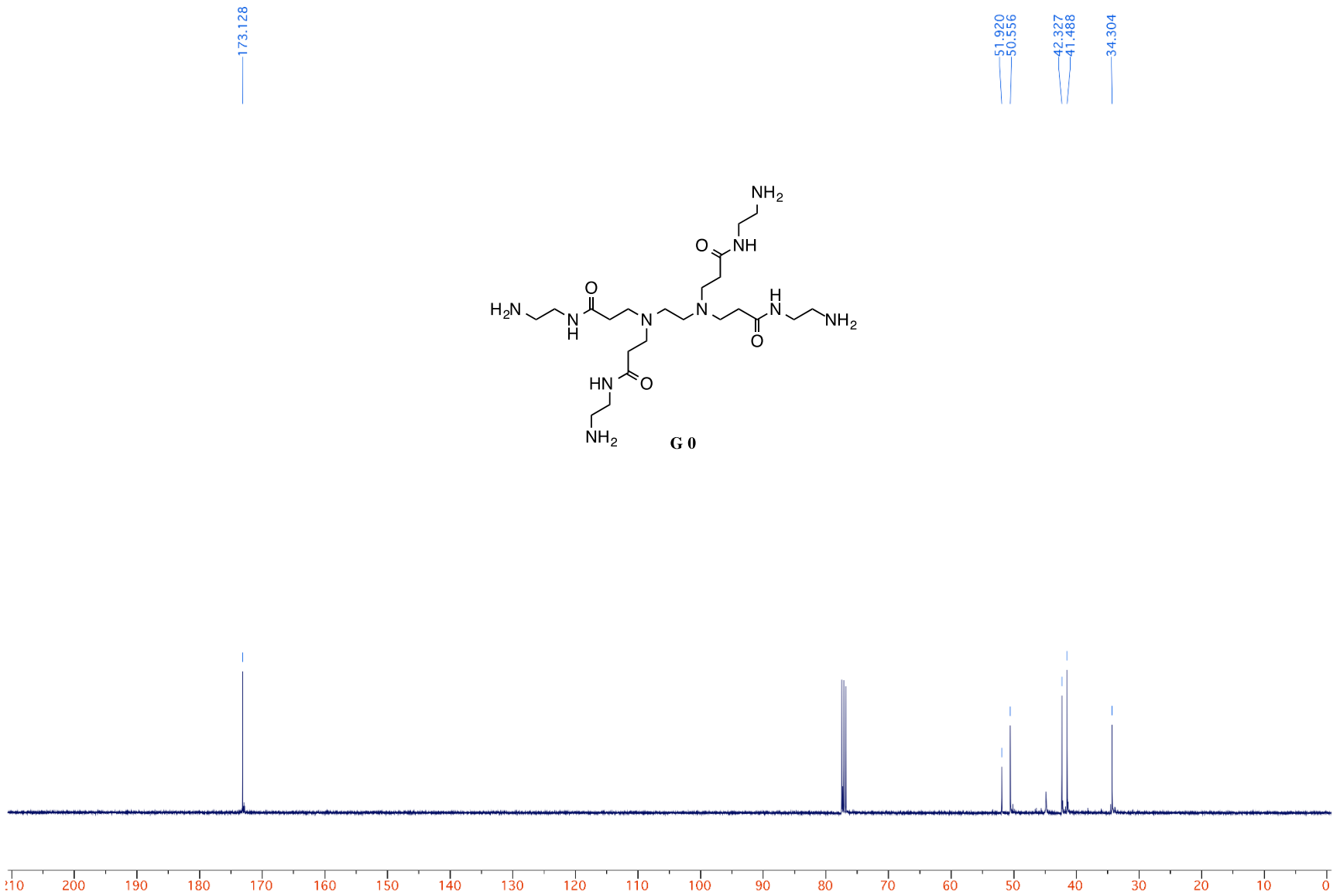
173.128
51.920
50.556
42.327
41.468
34.304
G 0
210
200
190
180
170
160
150
140
130
120
110
100
90
80
70
60
50
40
30
20
10
0